



LUND UNIVERSITY

Design of kinetic models for assessment of critical aspects in bioprocess development

A case study of biohydrogen

Björkmalm, Johanna

2019

Document Version:

Publisher's PDF, also known as Version of record

[Link to publication](#)

Citation for published version (APA):

Björkmalm, J. (2019). *Design of kinetic models for assessment of critical aspects in bioprocess development: A case study of biohydrogen.*

Total number of authors:

1

General rights

Unless other specific re-use rights are stated the following general rights apply:

Copyright and moral rights for the publications made accessible in the public portal are retained by the authors and/or other copyright owners and it is a condition of accessing publications that users recognise and abide by the legal requirements associated with these rights.

- Users may download and print one copy of any publication from the public portal for the purpose of private study or research.
- You may not further distribute the material or use it for any profit-making activity or commercial gain
- You may freely distribute the URL identifying the publication in the public portal

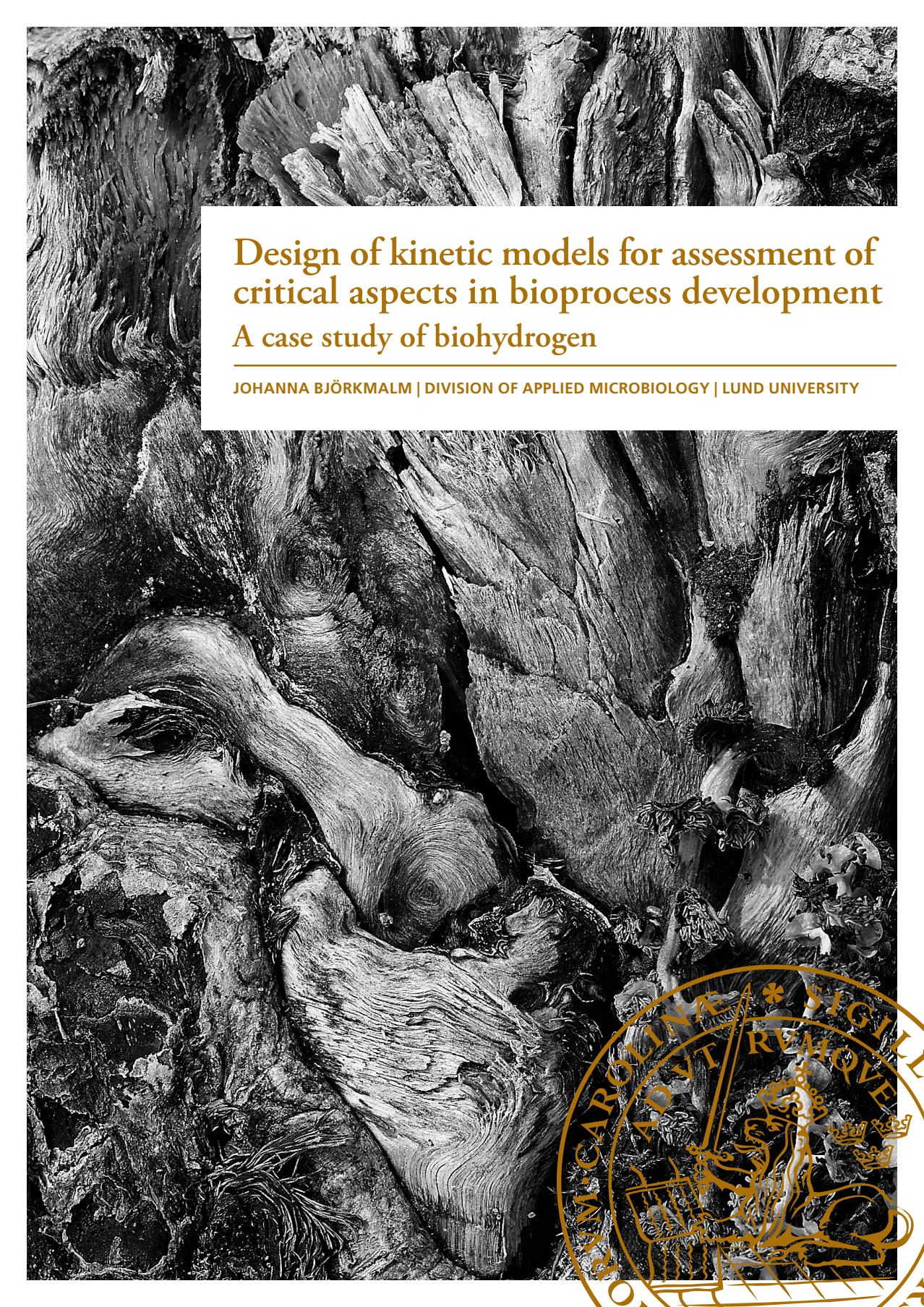
Read more about Creative commons licenses: <https://creativecommons.org/licenses/>

Take down policy

If you believe that this document breaches copyright please contact us providing details, and we will remove access to the work immediately and investigate your claim.

LUND UNIVERSITY

PO Box 117
221 00 Lund
+46 46-222 00 00



Design of kinetic models for assessment of critical aspects in bioprocess development

A case study of biohydrogen

JOHANNA BJÖRKMALM | DIVISION OF APPLIED MICROBIOLOGY | LUND UNIVERSITY



Design of kinetic models for assessment of critical aspects in bioprocess development

A case study of biohydrogen

Johanna Björkmalm



LUND
UNIVERSITY

LICENTIATE DISSERTATION

by due permission of the Faculty of Engineering, Lund University, Sweden.
To be defended in Marie Curie Room at the Center for Chemistry and Chemical
Engineering, Naturvetarvägen 14 on

27th of September 2019 at 10:00

Faculty opponent

Professor Mohammad Taherzadeh, Department of Resource Recovery and
Building Technology, University of Borås, Sweden

| | | |
|---|---|---------------------------------------|
| Organization LUND UNIVERSITY Author: Johanna Björkmalm | Document name LICENTIATE DISSERTATION | |
| | Date of issue 2019-09-27 | |
| | Sponsoring organizations Energimyndigheten, EU Horizon 2020 and Vinnova | |
| Title and subtitle: Design of kinetic models for assessment of critical aspects in bioprocess development – A case study of biohydrogen | | |
| Abstract <p>The world faces major climate challenges and extensive efforts need to be taken to combat this issue. Replacing fossil-derived fuels and chemicals with renewables are one important step on the way. Hydrogen has a great potential as a renewable energy carrier for the transport sector and as a green chemical for the industry. Today, the production of hydrogen stems primarily from fossil resources. A sustainable alternative to the current methods of hydrogen production are via biological methods using microorganisms and renewable substrates. <i>Caldicellulosiruptor</i> species are thermophilic bacteria able to produce hydrogen close to the theoretical maximum of 4mol H₂/mol hexose. Due to economic reasons, it is preferable if the microorganism can utilize different kinds of substrates containing both pentose and hexose sugars as well as to withstand high amounts of sugar in the feed. These two aspects were quantitatively evaluated in this research by using kinetic models. Modelling is an important tool in bioprocess development since it can contribute to an increased understanding of the process and function as a predictor for future process performance and hence strive towards <i>in silico</i> assessments which are more cost effective.</p> <p>When a microorganism is exposed to several sugars a phenomenon called diauxic-growth can occur. <i>Caldicellulosiruptor saccharolyticus</i> was exposed to an industrial substrate, wheat straw hydrolysate (WSH), containing glucose, xylose and arabinose, as well as to an artificial sugar mixture containing the same amount of sugars as in the WSH. It was displayed that <i>Caldicellulosiruptor saccharolyticus</i> expresses a diauxic-like behaviour; simultaneously taking up different sugars (hexose and pentose) but with a preference for the pentoses. When the pentoses are depleted, there is a short lag phase followed by the continued uptake of the hexoses, however, at an altered rate. This is displayed as a biphasic growth curve, most visible in the hydrogen and carbon dioxide productivity profile. We hypothesize that there are several enzyme systems involved in the uptake that are either upregulated or downregulated depending on which sugar that is preferred. By using cybernetic variables that describe which transport system that is active this phenomenon could be described mathematically.</p> <p><i>Caldicellulosiruptor owensensis</i>' tolerance towards high sugar and end-product concentration (i.e., high osmolarity) were evaluated and described mathematically. The kinetic growth model was appropriate to describe the behaviour of growth when exposed to 10 and 30 g/L of glucose. At higher sugar concentration, 80 g/L, the model slightly overestimated the growth. A critical osmolarity parameter was quantified and showed a fourfold increase in value with an increasing osmolarity. This means that <i>Caldicellulosiruptor</i>'s tolerance to a high osmolarity had increased in the adaptive laboratory evolution experiments conducted earlier.</p> <p>Producing biohydrogen with microorganisms such as <i>Caldicellulosiruptor</i> species has great potential in the transformation from a fossil to a bio-based economy. Further efforts in constructing and tuning kinetic models for biohydrogen production would be beneficial from a process development point of view.</p> | | |
| Key words: kinetic models, biohydrogen, <i>Caldicellulosiruptor</i> , substrate, diauxic, inhibition, osmotolerance | | |
| Classification system and/or index terms (if any) | | |
| Supplementary bibliographical information | | Language English |
| ISSN and key title | | ISBN 978-91-7422-672-0 (print) |
| Recipient's notes | Number of pages 115 | Price |
| | Security classification | |

I, the undersigned, being the copyright owner of the abstract of the above-mentioned dissertation, hereby grant to all reference sources permission to publish and disseminate the abstract of the above-mentioned dissertation.

Signature  Date 2019-08-16

Design of kinetic models for assessment of critical aspects in bioprocess development

A case study of biohydrogen

Johanna Björkmalm



LUND
UNIVERSITY

Copyright Johanna Björkmalm

Paper 1 © Biotechnology for Biofuels

Paper 2 © by the Authors (Manuscript unpublished)

Division of Applied Microbiology
Department of Chemistry
Faculty of Engineering
Lund University
P.O. Box 124
SE-221 00 Lund
Sweden

ISBN 978-91-7422-672-0 (Print)

ISBN 978-91-7422-673-7 (Electronic)

Back cover drawing by Olof Larsson

Printed in Sweden by Media-Tryck, Lund University
Lund 2019



Media-Tryck is an environmentally certified and ISO 14001:2015 certified provider of printed material. Read more about our environmental work at www.mediatryck.lu.se

MADE IN SWEDEN 

“I’ve learned that people will forget what you said, people will forget what you did, but people will never forget how you made them feel”

- Maya Angelou

Table of Contents

| | |
|---|-------------|
| Populärvetenskaplig sammanfattning | viii |
| List of papers | ix |
| My contributions to the papers | x |
| Publications not included in this thesis | xi |
| Nomenclature | xii |
| List of Figures | xv |
| List of Tables | xv |
| 1 Introduction | 1 |
| 1.1 Challenges of global warming | 2 |
| 1.2 Biofuels | 3 |
| 1.3 Feedstock | 4 |
| 1.4 Hydrogen | 5 |
| 1.4.1 Biohydrogen production | 6 |
| 1.5 Models used in bioprocess assessment | 8 |
| 1.6 Objectives of the study | 10 |
| 2 Dark fermentation: critical aspects | 11 |
| 2.1 Dark fermentation | 11 |
| 2.1.1 <i>Caldicellulosiruptor</i> as a hydrogen producer | 13 |
| 2.2 Substrate and end-product inhibition | 14 |
| 2.3 Diauxic growth | 15 |
| 2.3.1 Transport systems and diauxic growth | 17 |
| 2.3.2 “Diauxic-like” behaviour in <i>Caldicellulosiruptor</i> ? | 17 |
| 3 Modelling as a tool in bioprocess understanding and development .. | 19 |
| 3.1 Construction of a model | 19 |
| 3.2 Model selection | 20 |
| 3.2.1 Kinetic models in anaerobic bioprocesses | 20 |
| 3.2.2 Anaerobic Digestion Model No. 1 | 21 |
| 3.2.3 Modelling of dark fermentation | 21 |

| | | |
|----------|--|-----------|
| 3.2.4 | Modelling of batch and continuous processes | 22 |
| 3.3 | Model development | 22 |
| 3.3.1 | Model development for <i>Caldicellulosiruptor</i> 's hydrogen production..... | 23 |
| 3.3.2 | Substrate and end-product inhibition..... | 24 |
| 3.3.3 | Diauxic growth | 26 |
| 3.3.4 | Variables and parameters..... | 27 |
| 3.4 | Model implementation..... | 27 |
| 3.5 | Parameter sensitivity analysis..... | 28 |
| 3.6 | Parameter estimation | 30 |
| 3.7 | Validation | 31 |
| 3.7.1 | Direct validation | 31 |
| 3.7.2 | Cross validation | 32 |
| 3.8 | Interpretation of results and quantification of critical aspects..... | 33 |
| 3.8.1 | <i>C. saccharolyticus</i> displays diauxic-like behaviour | 33 |
| 3.8.2 | Osmotolerance in <i>C. owensensis</i> adapted cells..... | 34 |
| 4 | Conclusions | 37 |
| 5 | Future outlook | 39 |
| | Acknowledgement | 42 |
| | References | 45 |

Populärvetenskaplig sammanfattning

En av vår tids största utmaningar är förstå och hantera de komplexa klimatförändringarna. För att begränsa dem måste vi minska det samlade utsläppet av växthusgaser i världen. Ett steg på vägen dit är att hitta nya hållbara produktionssätt för att tillverka bränslen och kemikalier som idag produceras från ett fossilt ursprung. Vätgas besitter en stor potential som energibärare i transportsektorn och som råvara i kemisk industri. Däremot är mer än 95% av dagens vätgasproduktion icke förnybar. En alternativ metod för att tillverka vätgas är med hjälp av biologiska metoder, dvs med mikroorganismer. En sådan process är mörk fermentering där organiskt material omvandlas till bland annat vätgas. *Caldicellulosiruptor* utgör en grupp mikroorganismer som kan producera vätgas men också ättiksyra som en biprodukt i en mörk fermentering. För att denna process ska kunna bli ekonomiskt hållbar måste bland annat mikroorganismen kunna använda sig av olika typer av råvaror, s.k. substrat, och dessutom klara av höga halter av substrat. Dessa två aspekter har undersökts och kvantifierats med hjälp av kinetiska modeller.

Modellering är ett viktigt verktyg i utvecklingen av biologiska processer då det kan öka förståelsen och förutspå resultat och förändringar. Modeller kan användas som ett komplement eller en ersättning för laborativa experiment och tester samt vid processutveckling, vilket reducerar utvecklingskostnader. I denna avhandling har kinetiska modeller utvecklats för att utvärdera hur mikroorganismen *Caldicellulosiruptor* agerar vid exponering av olika typer av substrat och olika mängder av substrat i relation till dess vätgasproduktion. De utvecklade modellerna kunde väl beskriva vätgasproduktionen och upptaget av substrat. Modellerna bidrog också till en ökad förståelse för hur processen beter sig vid höga substratkoncentrationer, s.k. hög osmolaritet. Dessutom visade modellerna hur flera olika substrat kan ge upphov till en bifasisk tillväxt vilket innebär en tillväxt i två faser där ett substrat prefereras över ett annat, också kallad "diauxic" tillväxt.

Biologisk vätgasproduktion har en framtid i den biobaserade ekonomin och modellering är ett utmärkt verktyg för att vidareutveckla processen.

List of papers

This thesis is based on the following papers, which are referred to as Papers I-II in the text. The papers are attached as appendices at the end of the thesis.

Paper I **Björkmalm J.**, Byrne E., van Niel EWJ. and Willquist K. (2018). A non-linear model of hydrogen production by *Caldicellulosiruptor saccharolyticus* for diauxic-like consumption of lignocellulosic sugar mixtures. *Biotechnology for Biofuels* 11:175.

Paper II Byrne E., **Björkmalm J.**, Bostick J.P., Sreenivas K., Willquist K. and van Niel EWJ. Characterization and quantification of *Caldicellulosiruptor* strains targeting enhanced hydrogen production from lignocellulosic hydrolysates. Manuscript.

My contributions to the papers

Paper I I performed the data analysis, calculations and model development as well as most of the manuscript writing.

Paper II I performed the data analysis and calculations, model development and manuscript writing.

Publications not included in this thesis

Paper

- A. Xie Y., **Björkmalm J.**, Ma C., Willquist K., Yngvesson J., Wallberg O. and Ji. X. (2018). Techno-economic evaluation of biogas upgrading using ionic liquids in comparison with industrially used technology in Scandinavian anaerobic digestion plants. *Applied Energy* 227:742-750.

Conference proceeding

- B. Xie Y., **Björkmalm J.**, Ma C. and Ji X. (2016). Techno-economic evaluation of biogas upgrading using ionic liquids. *The 8th International Conference on Applied Energy – ICAE2016*.

Nomenclature

Acronyms

| | |
|------|---|
| AD | Anaerobic Digestion |
| ATP | Adenosine TriPhosphate |
| ADM1 | Anaerobic Digestion Model No. 1 |
| CCR | Carbon Catabolite Repression |
| DF | Dark Fermentation |
| IPCC | Intergovernmental Panel on Climate Change |
| NADH | Nicotinamide Adenine Dinucleotide |
| ODE | Ordinary Differential Equations |
| SA | Sensitivity Analysis |

State variables

| | |
|------------------|--|
| Glu | Concentration of glucose |
| Xyl | Concentration of xylose |
| Ara | Concentration of arabinose |
| Ac | Concentration of acetate |
| Lac | Concentration of lactate |
| X | Concentration of biomass |
| $H_{2,aq}$ | Dissolved concentration of hydrogen |
| $H_{2,aq,star}$ | Dissolved concentration of hydrogen at equilibrium |
| H_{2g} | Concentration of hydrogen in gas phase |
| $CO_{2,aq}$ | Dissolved concentration of carbon dioxide |
| $CO_{2,aq,star}$ | Dissolved concentration of carbon dioxide at equilibrium |

| | |
|----------------------------|---|
| $\text{CO}_{2,\text{sol}}$ | Total concentration of carbonates (HCO_3^- and CO_3^{2-}) |
| $\text{CO}_{2,\text{g}}$ | Concentration of carbon dioxide in gas phase |
| OSM | Osmolarity |
| pH | pH in the reactor, (operating variable if held constant) |
| q_{gas} | Total flow of gas |
| v_1 | Cybernetic variable controlling the activity of the first enzyme system involved in uptake |
| v_2 | Cybernetic variable controlling the activity of the second enzyme system involved in uptake |
| u | Cybernetic variable representing the fractional allocation of resources for the synthesis of the second enzyme system |

Parameters and rates

| | |
|----------------------------|---|
| μ_i | Growth rate on substrate i |
| ρ_i | Substrate uptake for substrate i |
| μ_{max} | Maximum specific growth rate |
| $k_{m,i}$ | Maximum specific uptake rate for substrate i |
| $K_{S,i}$ | Affinity constant – Half saturation constant for substrate i |
| $H_{2,\text{aq,crit}}$ | Critical dissolved concentration of hydrogen, value at which inhibition is 100% |
| OSM_{crit} | Critical osmolarity, value at which inhibition is 100% |
| $kL_{a\text{H}_2}$ | Volumetric mass transfer coefficient for hydrogen |
| $kL_{a\text{CO}_2}$ | Volumetric mass transfer coefficient for carbon dioxide |
| r_{cd} | Cell death rate |
| Y_{PS} | Yield of P (product or biomass) on substrate S |
| n_μ | Exponential parameter describing the level of inhibition |
| n_{H_2} | Exponential parameter describing the level of inhibition |

Operating variables

| | |
|------------------|-------------------------------|
| V_{liq} | Liquid volume in the reactor |
| V_{gas} | Gaseous volume in the reactor |

Constants

| | |
|--------------|--|
| pK_1 | Dissociation constant of reaction forming bicarbonate |
| pK_2 | Dissociation constant of reaction forming carbonate |
| k_{AB} | Rate constant set to a large value for infinitely fast reaction rate |
| K_{H,CO_2} | Henry's law constant for carbon dioxide |
| K_{H,H_2} | Henry's law constant for hydrogen |

List of Figures

| | |
|--|----|
| Figure 1. Global fossil CO ₂ emissions were projected to rise by 2.7% in 2018..... | 1 |
| Figure 2. Projected biomass availability in 2020, in million tonnes..... | 5 |
| Figure 3. Pathways for biohydrogen production..... | 7 |
| Figure 4. Schematic illustration of different levels of modelling..... | 9 |
| Figure 5. Schematic illustration of dark fermentation..... | 12 |
| Figure 6. Illustration of diauxic growth..... | 16 |
| Figure 7. Illustration of diauxic-like behaviour in <i>Caldicellulosiruptor</i> | 18 |
| Figure 8. The different stages of model development..... | 20 |
| Figure 9. The application of an ODE model to a bioprocess..... | 23 |
| Figure 10. Mass transfer in <i>Caldicellulosiruptor</i> | 24 |
| Figure 11. Visualisation of the modelling scripts implemented in MATLAB®..... | 28 |
| Figure 12. Model validation by R ² and curve slope values..... | 32 |
| Figure 13. Illustration of cybernetic variables in the model..... | 34 |
| Figure 14. Modelling of osmotolerance..... | 35 |
| Figure 15. Publications in Scopus in the field..... | 39 |

List of Tables

| | |
|--|----|
| Table 1. Kinetic rate equations used in anaerobic bioprocess modelling..... | 20 |
|--|----|

1 Introduction

“I think calling it climate change is rather limiting, I would rather call it the everything change” - Margaret Atwood

The critical issue of our time is climate change and we are now at a time to define the actions that need to be taken to minimize the already initialized global impacts of this issue. The average global temperature on Earth is directly linked to the concentration of greenhouse gases in the atmosphere. The concentration has been rising along with the mean global temperature since the time of the industrial revolution. Carbon dioxide (CO₂) is the most abundant greenhouse gas (Figure 1) and is largely the product of burning fossil fuels (United Nations, 2018a). Greenhouse gas emissions need to be reduced to halt this seemingly unstoppable global warming and for that, renewable fuels and chemicals are one part of the solution.

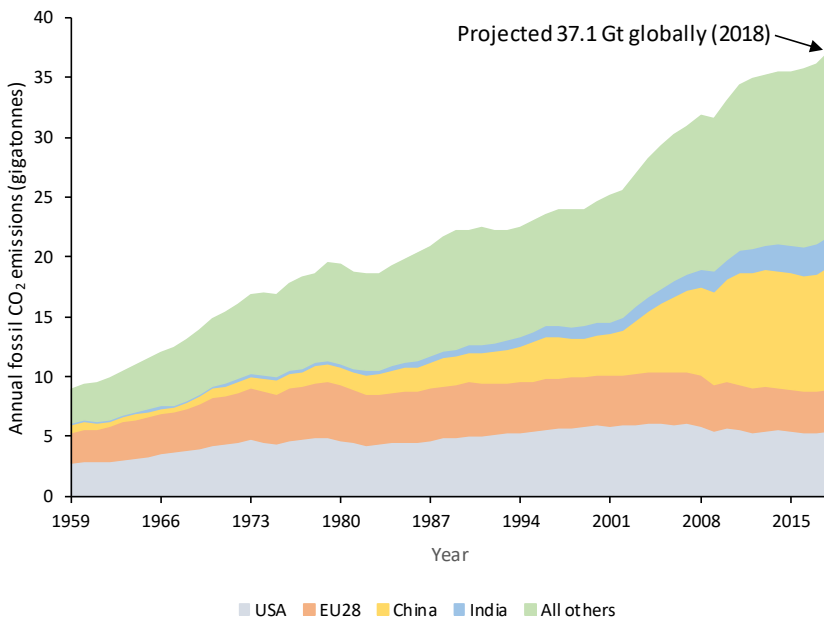


Figure 1. Global fossil CO₂ emissions were projected to rise by 2.7% in 2018. Adapted from (CDIAC; Global Carbon Project, 2018; Jackson et al., 2018; Le Quéré et al., 2018).

1.1 Challenges of global warming

Human activities have contributed to an estimated global warming of 1°C above pre-industrial levels. Between the years 2030 and 2052 the global warming is likely to reach and go beyond 1.5°C if it continues to increase at the current rate (IPCC, 2018). However, according to the Intergovernmental Panel on Climate Change (IPCC) it is possible to limit and fix the global warming to 1.5°C above pre-industrial levels if rapid and extensive changes in all parts of society are made (IPCC, 2018). International agreements such as the adopted Paris agreement and the more recent Katowice climate package will strengthen the global response to the threat of climate change and strive towards limiting the increase in temperature to 1.5°C (United Nations, 2015; United Nations, 2018b). This displays clear profits compared to reaching a global warming of 2°C or more. At 1.5°C the coral reefs would decline by 70-90%, whilst at 2°C the tropical coral reefs are predicted to vanish. The sea level rise would be 10 cm lower by 2100 if global warming is limited to 1.5°C compared to 2°C. Furthermore, by limiting the temperature rise to 1.5°C would mean that hundreds of millions of people from poor and disadvantaged populations would be exposed to less climate risks and consequently have a better chance to get out of poverty. Finally, remaining at a rise of 1.5°C could significantly reduce the part of the world population that will suffer from climate-related water shortage (IPCC, 2018).

For this to happen, extensive and rapid transitions in land, energy, industry, buildings, transport and cities are required. A reduction of the world's emissions of greenhouse gases of at least 50% would be needed by 2030. And a “net-zero” needs to be reached by 2050 meaning that remaining emissions have to be balanced by removing CO₂ from the atmosphere (IPCC, 2018). This will put pressure on our energy systems and greatly challenge the transition in the upcoming decades. Particular efforts need to be taken towards the development of renewable energy sources. The EU's 20% renewable energy target has proven an efficient driver in this development, but even more stringent targets are needed (European Commission, 2012). For 2030 the European Commission has set a renewable energy target of at least 27% of energy consumption (European Commission, 2014). The Renewable Energy Sources (RES) Directive objects to increase the share of RES in final energy consumption by 2030. This includes guiding principles of financial support schemes for RES and it seeks to strengthen mechanisms for cross-border cooperation, support the sustainability and greenhouse gas emissions-savings criteria for biofuels and normalize the use of RES in the transport sector (European Parliament, 2018).

The global energy demand is foreseen to continue to increase as improvements are made in human progress and wellbeing and with a growing population (BP, 2019). Although improvements in energy efficiency are made, the world will

crave for more energy to continue to grow and prosper. Hence, it becomes even more important to continue the development of renewable energy alternatives. In 2016, the world Total Primary Energy Supply (TPES) was 13 761 Million Tonnes of Oil Equivalent (Mtoe) of which 13.7% was produced from renewable sources (IEA, 2018a). The share of renewables is growing in the electricity, power and transport sector, however, very slow in the latter. Renewables in the transport sector is forecasted to grow only minimally from 3.4% in 2017 to 3.8% in 2023. To meet long-term goals in climate and sustainability, an acceleration in action is needed. If the renewable energy development continues at the forecasted pace, the share of renewables in TPES would be 18% by 2040 which is much lower than the IEA Sustainable Development Scenario's benchmark of 28% (IEA, 2018b).

1.2 Biofuels

Biofuels are liquid or gaseous fuels, such as ethanol, methanol, methane and hydrogen, derived from organic matter, e.g. from energy crops or commercial, domestic, agricultural and industrial waste. Biofuels have a great potential in mitigating climate change and addressing the problem of energy insecurity. However, it is important to realise that there are different kinds of biofuels and they all possess benefits and drawbacks (Acheampong et al., 2017). There is a distinction between first- and second-generation biofuels, and in addition also third- and fourth-generation biofuels are defined. First-generation biofuels are produced from food crops such as sugarcane, sugar beet and corn (van der Laak et al., 2007). The feedstock used are previously destined for human consumption which is a downside of the first-generation biofuels. In addition, in the production of first-generation biofuels, only a small part of the crop or plant is used, leaving the remainder as waste, at least for the purpose of fuel production, making it inefficient (Bomb et al., 2007). Second-generation biofuels are derived from feedstock which is not intended for human consumption, e.g. lignocellulosic biomass (Charles et al., 2007). There is great potential in the second-generation biofuels, and they are considered more environmentally friendly and produce less greenhouse gases compared to first-generation biofuels. The challenges lie within the cost-effectiveness and the difficulty to extract the fuel since there is a need for pretreatment of the biomass (Naik et al., 2010). The third- and fourth-generation biofuels involves algae-to-biofuels where microalgae and cyanobacteria are used to produce e.g. biodiesel (Chisti, 2007). The third generation is principally the production of biofuels by processing microalgae while the fourth generation makes use of metabolic engineering of the algae for enhanced biofuel production (Lü et al., 2011). Although there is an input cost for

water and energy, the microalgae are very productive and land efficient (Batan et al., 2010).

1.3 Feedstock

It is of importance to consider the type of feedstock, i.e., substrate, used for biofuel production, since it can lead to both direct and indirect land use change (DLUC and ILUC). DLUC is when there is a change from previous land use to produce biofuel feedstock instead. ILUC is a change in land use elsewhere, for example conversion of high carbon stock lands, such as forests or grasslands, to cropland to meet the demand for commodities displaced by the production of biofuel feedstock. This can lead to greenhouse gas emissions which reduce or cancel out the potential greenhouse gas savings mitigated by the biofuels (Plevin et al., 2010). Lignocellulosic biomass is an abundant and renewable resource. It consists of cellulose, hemicellulose and lignin (Hadar, 2013) and can be used to produce biofuels with no or minimal additional land requirements or impacts on food and fibre crop production (Sims et al., 2010). Lignocellulose is a primary structural component of plant cell wall and can be found in bioenergy crops like switchgrass, but also in unused waste streams such as crop residues and municipal solid waste (Minty & Lin, 2015). Lignocellulosic biomass has been estimated to account for approximately 50% of the biomass worldwide (Claassen et al., 1999) and a few years back the production was estimated to around 200 billion tonnes per year (Zhang, 2008). Within the agricultural sector in Europe the highest potential of biomass residue availability lies within straw, e.g. wheat straw (Figure 2). In Paper I, wheat straw is used as a feedstock to the bioprocess.

To increase the digestibility of lignocellulosic biomass, pretreatment is required and can be classified into biological, physical, chemical or a combination of these. However, consolidated bioprocessing (CBP) can reduce or eliminate the need for pretreatment. In CBP, production of saccharolytic enzymes, hydrolysis of cellulose and hemicellulose to monomeric sugars and fermentation of sugars all occur in the same process configuration. This means that the cost of the process can be lowered and the efficiency higher (Menon & Rao, 2012).

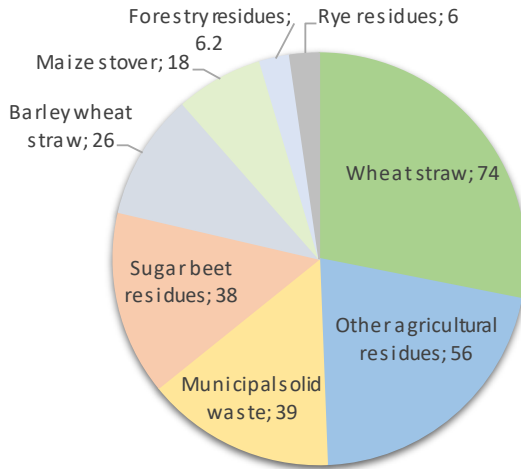


Figure 2. Projected biomass availability in 2020 in Europe, in million tonnes. Adapted from (Kretschmer, 2012).

1.4 Hydrogen

The European Commission’s Energy Roadmap 2050 points out hydrogen, fuel cells and batteries as areas where additional research and demonstration efforts are needed. These can, together with smart grids, enhance the benefits of electromobility both for decarbonisation of transport and for development of renewable fuels (European Commission, 2012). Fuel cells can transform the chemical energy in hydrogen into electricity and the process emits only water and heat. Fuel cells are more efficient than combustion engines, but expensive to build. Hydrogen fuel cells can power electric cars and large fuel cells can also be used to provide electricity in remote places with no power lines. Vehicles run on hydrogen are at the point of use, zero emitters, which has great benefits in climate change combat but also in local air quality in densely populated areas with a lot of transportation (Sharma & Ghoshal, 2015).

Around 70 million metric tons of hydrogen are used yearly (Fukui, 2018) and the largest producers are the United States and China (Bakken et al., 2016). Hydrogen is today mainly used for oil refining, in chemical production and in the food industries. However, using hydrogen as an energy carrier is of interest due to its potentially high efficiency of conversion to usable power, its low emission of pollutants and high energy density (Singh & Rathore, 2017). The most common ways of producing hydrogen have its origin in fossil-based resources

where the most frequently used technology is steam reforming of natural gas, a process which leads to large amounts of greenhouse gases (Balat & Balat, 2009). Steam reforming of methane satisfies around 50% of the international demand of hydrogen, naphtha and oil reforming in refinery or industrial off-gases constitutes close to 30% of the demand and 17% of the hydrogen is produced by coal gasification. The remaining part ~3% is produced by water electrolysis and other sources (Grand View Research Inc, 2018).

1.4.1 Biohydrogen production

A sustainable alternative to the conventional methods for producing H₂ is by biological methods, i.e. biohydrogen, using microorganisms. Biohydrogen can be produced using organic waste effluents as a nutrient source or via sunlight, CO₂, and minimal nutrients. It does not compete with food production and does not require fertile land as in comparison to first-generation biofuels. Biohydrogen can be produced by fermentation; dark fermentation or photofermentation, or via direct or indirect biophotolysis (Levin et al., 2004) (Figure 3). Biophotolysis occurs when cyanobacteria and algae break down water into hydrogen and oxygen in the presence of light. In direct biophotolysis hydrogen and oxygen are simultaneously produced which is a drawback since oxygen works as an inhibitory agent to the process. To circumvent this problem indirect biophotolysis can be applied where the biological production of hydrogen and oxygen are separated either in space or in time (Levin et al., 2004). Hydrogen can be produced under anaerobic conditions by conversion of organic acids to hydrogen and carbon dioxide by photoheterotrophic bacteria. The process is called photofermentation and occurs in the presence of light. The most promising microorganism for hydrogen production by photofermentation is the purple non-sulfur bacterium, e.g. *Rhodobacter* (Rai et al., 2012). Dark fermentation is a process where anaerobic mesophilic or thermophilic fermenting bacteria produce hydrogen from organic materials and no light is required. This include species of the genera *Enterobacter* (Nath et al., 2006), *Bacillus* (Kotay & Das, 2007), *Thermotoga* (Auria et al., 2016) and *Caldicellulosiruptor* (Willquist et al., 2010). The latter species is studied in this thesis.

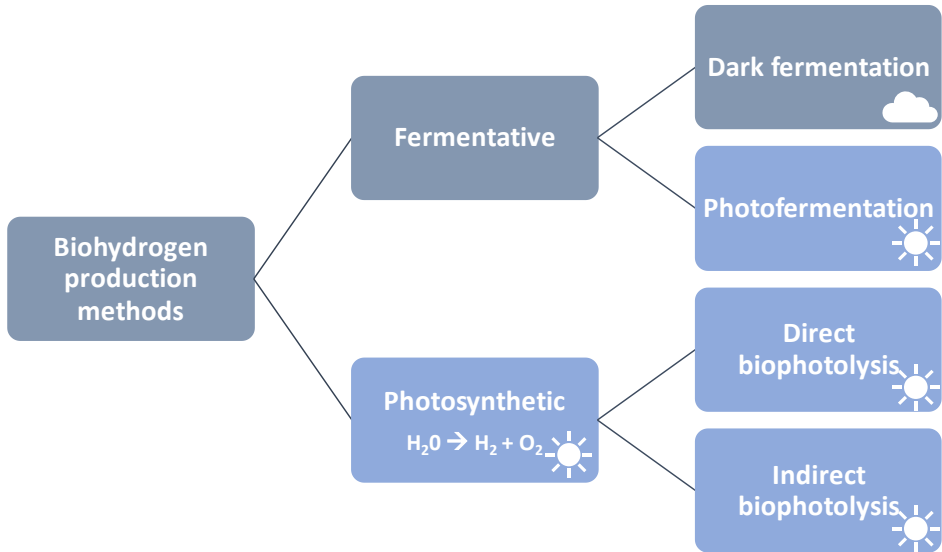


Figure 3. Pathways for biohydrogen production. The grey pathway is the focus of this study.

Caldicellulosiruptor possesses several desirable traits as a hydrogen producer, e.g. high yields of H₂ and an ability to utilize many different sources of carbon (Willquist et al., 2010). However, there are challenges towards the practical application of biohydrogen technology with *Caldicellulosiruptor* as the producer. One such challenge is its sensitivity to high osmolarity. Osmolarity is the total number of solute particles in a solution and hence this limits the maximum sugar concentration that can be fed into the process (Willquist et al., 2010). By inhibiting growth, osmolarity has a negative impact on the hydrogen productivity, and it is also a drawback when it comes to the economy of the process where a more concentrated feed, i.e., less water, is preferred (Ljunggren & Zacchi, 2010). Quantification of these factors to increase the understanding of the underlying mechanism are not widely explored and this is important for the continued development of the process. In Paper I we quantify *Caldicellulosiruptor*'s behaviour when exposed to multiple sources of carbon in the feed, both in the form of a defined solution of multiple sugars, as well as wheat straw hydrolysate. The challenge of osmolarity is addressed in Paper II, where a critical osmolarity is quantified and evaluated against an increasing sugar concentration.

1.5 Models used in bioprocess assessment

Based on the reasoning above it is clear that some aspects of the dark fermentation process need to be improved. However, before any improvements can be made, an increased understanding of the mechanisms is required. To achieve this and to quantify the success of such improvement, mathematical kinetic models can be used. Modelling can be done on several levels and with diverse aims, from the very small detailed genomic scale up to systemic analysis and environmental assessments (Figure 4).

Systems biology is the study of complex biological systems by utilising predictive mathematical models. This often includes metabolic control analysis, kinetic metabolic models and utilising data from the “omics” (e.g. genomics, proteomics) (Bruggeman & Westerhoff, 2007; Nielsen et al., 2014). In systems biology it is possible to study interactions between biological components in a system and its subsequent function or behaviour.

In contrast with the more detailed systems biology, techno-economic assessment (TEA) can provide a wider and more out-zoomed perspective of a process. TEA includes engineering-based process modelling coupled with economic estimates and assessments to quantify the product selling price. TEA requires a rigorous understanding of the process to establish mass and energy balances as a first step followed by estimations of unit operation investments and operating cost. Therefore, they are often used when assessing commercial viability of a process (Quinn & Davis, 2015). In comparison to systems biology and kinetic growth models, TEA often regards the biological process as a black box and often expresses the biological reactions in a stoichiometric manner. However, there are studies integrating growth kinetics and inhibition functions into process models (Rajendran et al., 2014).

Life cycle assessment (LCA) is a type of system analysis with an environmental impact perspective. It has become a widely used tool for assessing biofuels in regards of process energetics and environmental impact. It is of importance to clearly state the system boundaries to be able to compare the result with alternative production pathways (Quinn & Davis, 2015).

The focus of this research has been on developing mathematical kinetic models (grey, Figure 4) for assessing various aspect of biohydrogen production through dark fermentation. These models are built on kinetic rate expressions which can describe the production or consumption of molecular components. The models can for example be used to understand specific mechanisms and critical aspects of the process and to predict future performance (Almquist et al., 2014). In contrast to systems biology, the metabolic interactions within the cell are not

considered but information about ingoing concentrations, cell growth and product formation are included.

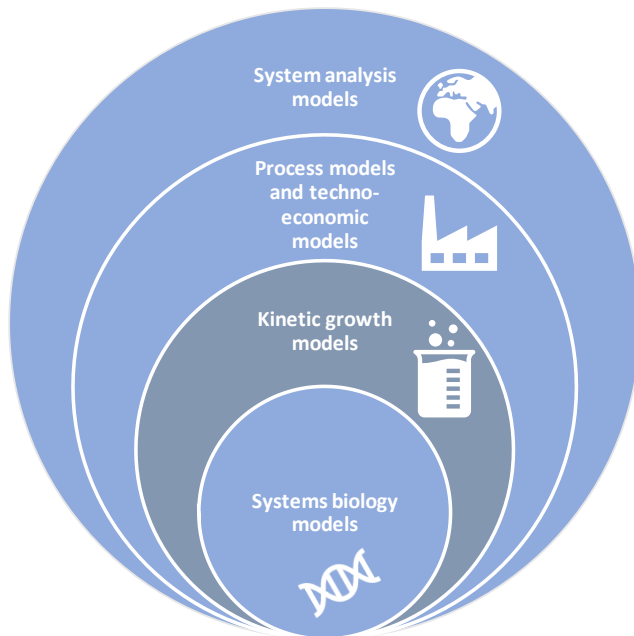


Figure 4. Schematic illustration of different levels of modelling. The focus of this thesis lies on developing kinetic growth models (grey). This representation displays how kinetic growth models are related to other quantitative tools and methods that can be used to assess bioprocesses.

1.6 Objectives of the study

This work aims to increase the **understanding** of biological hydrogen production and specific critical aspects of the process, by developing mathematical kinetic models. The long-term goal is to reach an economical and sustainable biohydrogen production process using dark fermentation that can take part in the transformation from fossil fuels to renewable fuels, and thus contributes to the combat of climate change.

The aims are summarized in the following objectives:

- To develop computational tools for increased understanding of biohydrogen produced through dark fermentation (overall objective).
- To increase the understanding of how *Caldicellulosiruptor* species behave in the presence of multiple sugars in biohydrogen production process (diauxic-like behaviour) (Paper I).
- To assess whether a higher tolerance for osmolarity can be quantitatively described in biohydrogen production by *Caldicellulosiruptor* species (Paper II).

2 Dark fermentation: critical aspects

“Fermentation and civilization are inseparable.” – John Ciardi

Dark fermentation is a process where hydrogen is produced by fermenting microorganisms. There are several critical aspects when designing the process, among which, tolerance to high substrate and end-product concentrations and the ability to utilize several different carbon sources simultaneously, are studied here.

2.1 Dark fermentation

In dark fermentation, hydrogen is produced through anaerobic breakdown of carbohydrate-rich substrates by a range of different heterotrophic microbes (Hallenbeck & Ghosh, 2009). In heterotrophic organisms, the anaerobic mode of growth poses challenges for the cell with respect to the disposition of electrons from energy-yielding oxidation reaction. The electrons need to be disposed of to maintain electrical neutrality. Various kinds of specific controls are necessary to regulate electron flow in the metabolism of anaerobes. One of these is reflected by the ability of many such organisms to dispose of “excess” electrons in the form of molecular hydrogen (H_2) through the activity of enzymes (Das & Veziroğlu, 2001). In the hydrogen fermentation process the microorganisms convert glucose to pyruvate via their glycolytic pathways, and subsequently pyruvate is oxidized to acetyl-CoA that is further converted to acetyl phosphate resulting in the generation of ATP and the formation of acetate (Figure 5). Also other products like ethanol, butanol and butyric acid can be formed depending on the microorganism (Das & Veziroglu, 2008).

Hydrogen-producing enzymes are fundamental for generation of biohydrogen. However, the enzymes themselves are quite intricate with complex metallo-clusters as active sites and synthesized through a complex process involving additional enzymes and protein maturation steps. Nitrogenase, Fe-hydrogenase and NiFe hydrogenase are currently the three known enzymes able to carry out the reaction of hydrogen production (Hallenbeck & Benemann, 2002). In dark fermentation, hydrogen can be formed in three different ways (Figure 5), either from formate via an Ech (NiFe) hydrogenase in Enterobacterial-type

fermentation (right-hand side), from reduced ferredoxin (Fd) via an FeFe hydrogenase in Clostridia-type fermentation or from NADH via an NADH-dependent FeFe hydrogenase (left-hand side) (Hallenbeck & Ghosh, 2009).

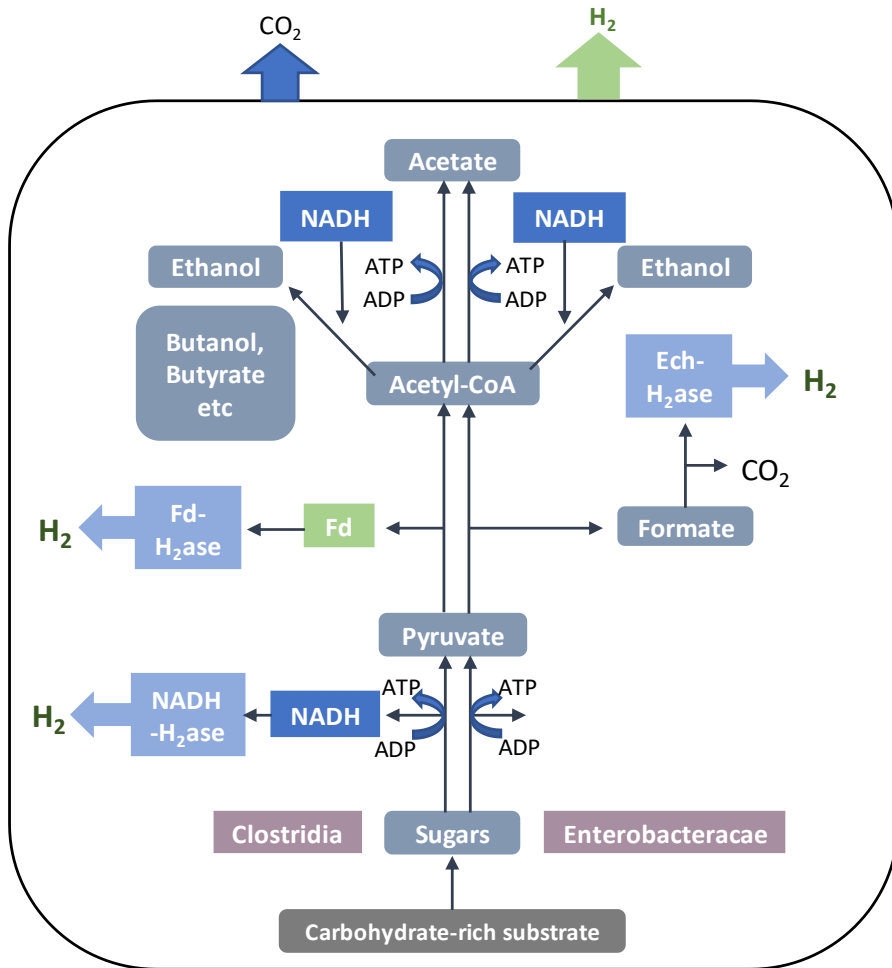


Figure 5. Schematic illustration of dark fermentation. In dark fermentation, hydrogen and various other fermentation products like acetate and ethanol are generated from carbohydrate-rich substrates. Hydrogen can be generated from i) formate via an Ech (NiFe) hydrogenase, ii) reduced ferredoxin (Fd) via a FeFe hydrogenase and iii) NADH via an NADH-dependent FeFe hydrogenase. Adapted from (Hallenbeck & Ghosh, 2009).

As mentioned previously, in addition to hydrogen, the fermenting microbes generates other products as well to satisfy their metabolic needs. These products include acetate, which permits ATP synthesis, and for example ethanol and butanol, which permit the re-oxidation of NADH, which is necessary for continuing glycolysis. Conditions like pH and the hydrogen partial pressure in the process, as well as type of organism and the oxidation state of the substrate are variables that affect the types and proportions of products formed from the fermentation (Hallenbeck & Ghosh, 2009).

There is a limitation in how much hydrogen that can be produced in dark fermentation depending on the type of microbes. Enteric bacterial type mixed acid fermentation is limited to produce 2 H₂/glucose and Clostridia-type fermentations are limited to produce 4 H₂/glucose at low hydrogen partial pressures (Hallenbeck, 2005). Consequently, the hydrogen yields are low and about two-thirds of the carbon and protons in the substrate are excreted as other products, mainly acetate (van Niel, 2016). The production of reduced compounds, other than H₂, is the main factor that limits H₂ yield in fermentative hydrogen production since their accumulation diverts electron equivalents away from H₂ (Lee et al., 2008). The low yields have been limiting when seeking industrial application since they are not competitive with other biofuels, like bioethanol or biomethane. These biofuels are derived from the same starting material but have a higher energy conversion. Also, the side products produced (acids and alcohols) need to be disposed of or used in some way. However, metabolic engineering to try and achieve a near stoichiometric conversion (Maeda et al., 2008) or various two-stage process approaches have been considered to overcome these issues (Byrne et al., 2018; Willquist et al., 2012). In the two-stage process, the dark fermentation producing hydrogen occurs in the first stage. In the second stage, there are different possibilities of converting the by-products from the dark fermentation to energy: conversion to H₂ by employing energy in the form of either light or electricity (van Niel, 2016) or reduction to CH₄ through anaerobic digestion (Pawar et al., 2013).

2.1.1 *Caldicellulosiruptor* as a hydrogen producer

Caldicellulosiruptor is a thermophilic gram-positive bacterium able to utilise lignocellulosic biomass for hydrogen production (Rainey et al., 1994; van Niel et al., 2002). It has the ability to produce hydrogen at the theoretical maximum of 4 mol H₂/mol hexose (Zeidan & van Niel, 2010) and its main fermentation products are acetate, lactate and ethanol (Rainey et al., 1994). To date, there are 14 different known species of *Caldicellulosiruptor* (Byrne, 2019). *Caldicellulosiruptor* can be cultivated with (Willquist & van Niel, 2010) or without (e.g., Paper I and Paper II) yeast extract in the supplemented medium.

In Paper I *Caldicellulosiruptor saccharolyticus* is studied for its behaviour when exposed to various different sugars both in a clean and defined substrate but also in an industrial substrate, i.e., wheat straw hydrolysate. In Paper II *Caldicellulosiruptor owensensis* is evaluated with regards to tolerance to an increasing osmolarity.

2.2 Substrate and end-product inhibition

An attractive trait for H₂-producing microorganisms is to possess an adequate tolerance to high concentrations of substrate and end-products (Pawar & van Niel, 2013). An increase in substrate concentration leads to an increase in cell mass, however, only up to a certain level where the substrate instead starts to inhibit growth, i.e., substrate inhibition (Azimian et al., 2019). Another similar phenomenon is product inhibition. This occurs when accumulation of end-products in the medium lead to a suppression of the metabolic activity (Mulchandani & Luong, 1989). Both these aspects are of importance when considering industrial application. A tolerance to high substrate and end-product concentrations can have effect on e.g. the sizing of the bioreactor and hence the economy of the process.

A high substrate load and subsequent end-products lead to increased concentrations of solutes in the medium and thus high osmolarity. In addition, this may cause substrate and end-product inhibition which implicate a repressed microbial growth, a metabolic shift towards other metabolites and an incomplete substrate conversion (Nicolaou et al., 2010). To give an example, the nonpolar undissociated form of an organic acid can enter the cell and release protons in the cytoplasm. This interferes with the proton motive force and raises the cellular maintenance energy (Jones & Woods, 1986). In contrast, the polar dissociated form leads to higher ionic strength in the solution which can affect the microbial growth and in worst case cause cell lysis (van Niel et al., 2003).

It is desirable to have a high load of substrate into the process since this can lead to high hydrogen productivities (Willquist et al., 2010). Hence *Caldicellulosiruptor* species need to be adapted to higher osmolarities. This also means lower requirement of water in the process and lower input of energy needed for heating (Ljunggren & Zacchi, 2010). In Paper II we studied the behaviour of osmotolerant strains of *Caldicellulosiruptor* species in medium with higher osmolarities and quantified a critical osmolarity parameter which alters when the microorganism is exposed to increasing sugar concentrations.

Also, hydrogen itself is inhibiting growth and its own production, and therefore, a low hydrogen partial pressure in the fermentation reactor is needed. This can be

made possible by stripping the reactor with an inert gas like N₂. However, *C. saccharolyticus* can produce hydrogen still at high hydrogen partial pressures, up to 67 kPa. A possible explanation for this is that the hydrogen-producing enzyme, (see Chapter 2.1) is still functioning at elevated hydrogen concentrations (Willquist et al., 2011). In addition, in *Thermoanaerobacter tengcongensis* the Fd-dependent hydrogenase was expressed independently of the hydrogen partial pressure (Soboh et al., 2004).

2.3 Diauxic growth

Monod coined the expression of diauxie based on the biphasic growth he observed in *Bacillus subtilis* in the early 1940s (Monod, 1941). However, this biological phenomenon was actually described much earlier. In 1900, Diénert observed how cells of *Saccharomyces cerevisiae* originally adapted to galactose lost their adaption when they were exposed to glucose or fructose (Diénert, 1900). This phenomenon became known as the “glucose effect”. Monod later explained this as diauxic growth where two carbon sources are simultaneously added but there is a preference for the one allowing a faster growth rate. Before the second carbon source is utilized there is a lag phase or a phase of adaption and then growth resumes (Figure 6). He furthermore described that each organism has a hierarchy of preferred carbon sources where glucose is usually at the top. More studies followed and it was found that, as long as the preferred carbon source was present in sufficient amounts, the enzymes needed for transport and metabolism of the second carbon source were repressed. The phenomenon was therefore named carbon catabolite repression (CCR) (Contesse et al., 1970).

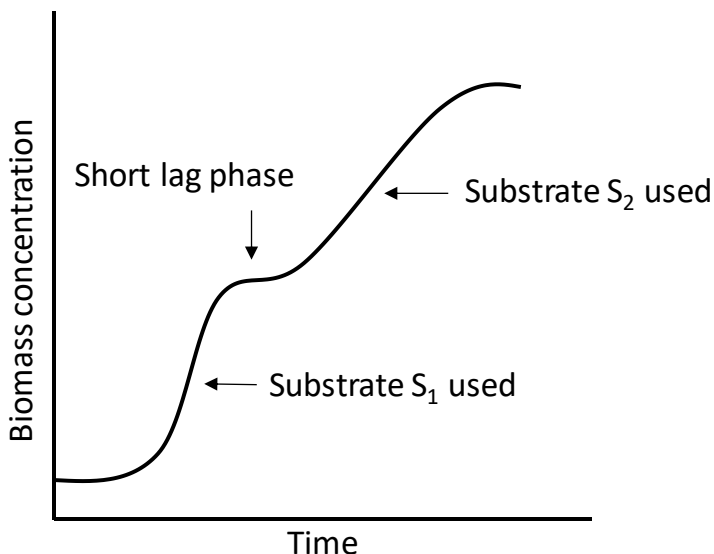


Figure 6. Illustration of diauxic growth. The preferred substrate, S_1 , is used first, then follows a lag phase before the second substrate, S_2 , is used.

For regulated sequential uptake of different substrates to occur, there are three requirements needed. First and foremost, there must be a competition between the substrates. Secondly, the uptake needs to be capacity limited. And lastly, a quality difference between the substrates is needed (Chu, 2015). Still, even when these requirements are met, regulated uptake will not always evolve. Diauxic growth can be perceived as a strategy to maximize biomass production in an environment where more than one carbon source is available. However, the growth dynamics in such an environment can be inefficient, i.e., the growth rate is increased at the expense of the yield as discussed in (Chu, 2015).

Having a broad preference for different carbon sources is an attractive trait in microorganisms considered for biofuel production from lignocellulosic substrates. According to van de Werken et al (2008) and VanFossen et al (2009), *C. saccharolyticus* is unaffected by CCR. Apparently, a xylose-specific ABC-type transporter was upregulated when growing separately on glucose and xylose as well as when growing on both. This indicated co-fermentation as these sugars seem to be taken up by the same uptake system (van de Werken et al., 2008). This was further examined by VanFossen et al (2009) which showed that *C. saccharolyticus* simultaneously consumed all monosaccharides present in the mixture, although not to the same extent; fructose > xylose/arabinose > mannose/glucose/galactose (VanFossen et al., 2009).

2.3.1 Transport systems and diauxic growth

ATP-binding cassette transporters (ABC transporters) are primary active transporters that use energy released during ATP hydrolysis to move substances against a concentration gradient without modifying them. ABC transporters are uniporters, i.e. they transport a single molecule across the membrane. ABC transporters utilize substrate-binding proteins that bind the molecule to be transported, e.g. glucose. The substrate-protein complex then interacts with the ABC transporter to move the substrate into the cell (Willey et al., 2013).

Group translocation is another type of transport system that is characterized by the chemical modification of the molecule being transported into the cell. The phosphoenolpyruvate: sugar phosphotransferase system (PTS) is an example of group translocation system. The PTS is common in many bacteria and it transports various kinds of sugars while phosphorylating them, using phosphoenolpyruvate (PEP) as the phosphate donor. PEP can be used to synthesize ATP, the cell's energy currency, however, in this case PEP is used to energize uptake and not ATP synthesis (Willey et al., 2013).

In diauxic growth, the PTS uptake system plays a major role due to its link to catabolite repression control (Deutscher, 2008). Yet, *C. saccharolyticus* to our current knowledge only has ABC transport systems for all sugars except for fructose that is transported into the cell with a PTS system (van de Werken et al., 2008). However, there are other mechanisms related to diauxic growth apart from PTS. For example a catabolite repression control (Crc) protein in *Pseudomonas putida* or via glucokinase (Glc) in *Streptomyces* (Deutscher, 2008) and hence this could also be the case in *Caldicellulosiruptor*.

2.3.2 “Diauxic-like” behaviour in *Caldicellulosiruptor*?

In Paper I we studied how lignocellulosic feedstock that contains various kinds of sugars, i.e., wheat straw hydrolysate containing hexose and pentose sugars, can affect the production process. Here we hypothesize that the uptake of the sugars occurs in two phases (Figure 7). In the first phase xylose and glucose are taken up by the same transport system, however, with a greater affinity for xylose, meaning that xylose uptake is faster. When xylose is depleted this transport system is downregulated and we enter the second phase. In phase II another transport system is upregulated and mediates the uptake of glucose but with an altered rate compared to glucose uptake in phase I. This could be described as a diauxic-like behaviour in *C. saccharolyticus* and it is clearly expressed in the hydrogen and carbon dioxide productivity profile (Figure 2 in Paper I). It should be mentioned that in all studies in Paper I, we did not add yeast extract in the

medium. This omission could be a contribution to a diauxic-like behaviour being exposed, as the presence of yeast extract could have masked this phenomenon.

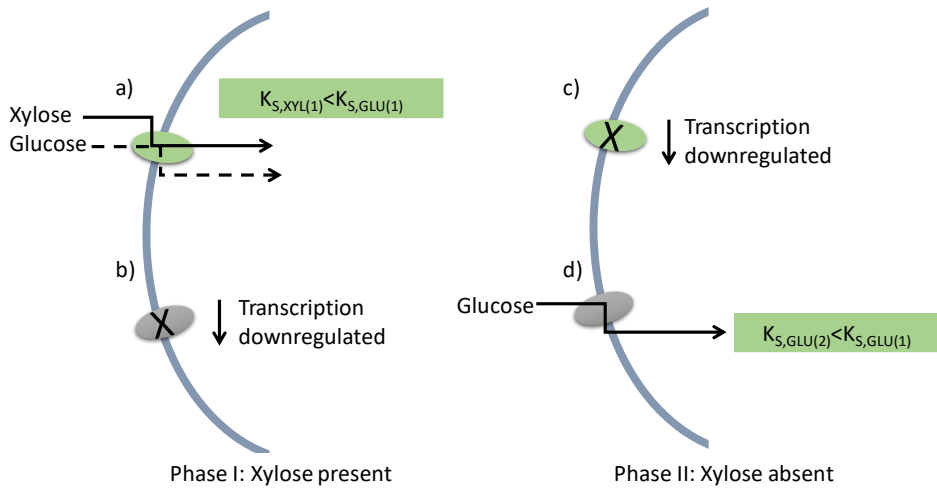


Figure 7. Illustration of diauxic-like behaviour in *Caldicellulosiruptor*. Phase I. a) The transporter is only upregulated on xylose. It can let glucose through but with a lower affinity, i.e. higher K_S value b) In the presence of xylose the transporter is repressed. Phase II. c) In the absence of xylose, the transporter is repressed. d) The transporter becomes active and is upregulated on glucose alone, with an altered affinity and hence an altered rate.

3 Modelling as a tool in bioprocess understanding and development

“Remember that all models are wrong; the practical question is how wrong they have to be to not be useful.” - George Box.

Mathematical kinetic models can be used to increase the understanding of a bioprocess, to predict future behaviour and to optimize the configuration of the bioreactor system. In addition, both time and resources can be saved if valid models are constructed and used to discover and evaluate improvement strategies *in silico*. However, there are many challenges associated with it, e.g. sufficient amount of information and data are needed for construction and validation of such models (Almquist et al., 2014). Though, in the long-term perspective, mathematical kinetic models have a great potential in acting as a driving force for reaching industrial application of bioprocesses.

3.1 Construction of a model

There are several steps to take when constructing a model (Figure 8). First and foremost, it is important to consider the objectives of the model. What problem/need does the model address? What is expected from it in terms of results? To answer these, it is vital to have sufficient knowledge about the process to be modelled, both qualitative and quantitative information. The next step is to develop the model, e.g. to choose the appropriate kinetic rate expressions and moreover to implement the model in a suitable software. Further on, the parameters of the model are evaluated and estimated. The last steps consist of validating the model and interpreting the results.

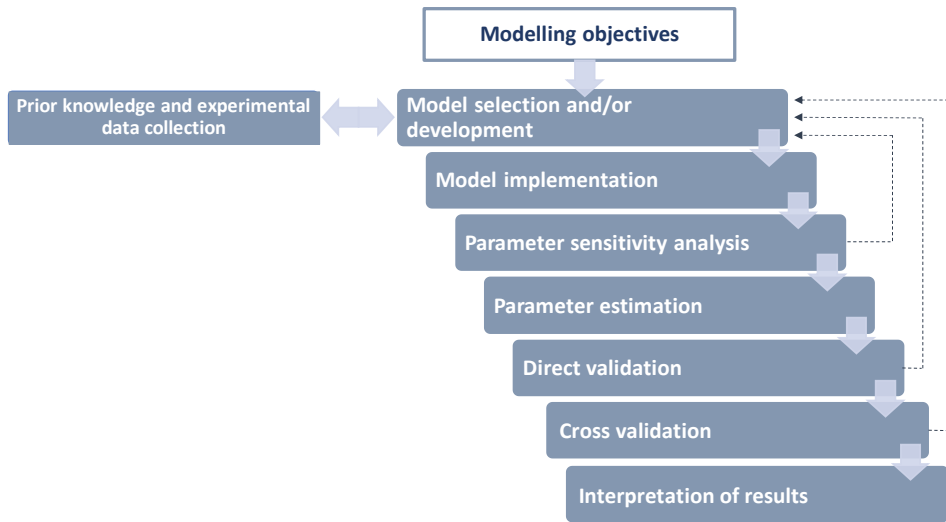


Figure 8. The different stages of model development. Figure adapted from (Donoso-Bravo et al., 2011).

3.2 Model selection

3.2.1 Kinetic models in anaerobic bioprocesses

Growth rate and substrate utilization rate are the two fundamental relationships that biological growth kinetics are based on (Pavlostathis & Giraldo-Gomez, 1991). Various mathematical models have been set up to describe the effect of the growth-limiting substrate concentration on the rate of microbial growth (Table 1).

Table 1. Kinetic rate equations used in anaerobic bioprocess modelling.

| | Kinetic model, rate equation | Ref |
|------------------|--|--------------------------------------|
| First order | $\mu = \frac{K_{S,max} \cdot S}{S_0 - S} - b$ | (Pavlostathis & Giraldo-Gomez, 1991) |
| Monod | $\mu = \mu_{max} \cdot \frac{S}{S + K_S} - b$ | (Monod, 1941) |
| Contois | $\mu = \mu_{max} \cdot \frac{S}{S + K_X \cdot X} - b$ | (Contois, 1959) |
| Grau | $\mu = \mu_{max} \cdot \frac{S}{S_0} - b$ | (Grau et al., 1975) |
| Chen & Hashimoto | $\mu = \mu_{max} \cdot \frac{S}{S(1-K) + K \cdot S_0} - b$ | (Chen & Hashimoto, 1980) |

Where μ is the growth rate (h^{-1}), μ_{max} is the maximum specific growth rate (h^{-1}), S is the substrate concentration (M), S_0 is the initial concentration of the limiting substrate (M), X is the biomass concentration (M), K_S is the affinity constant (M), K_X is a growth parameter that is constant under defined conditions ($\text{M}_{\text{substrate}} \cdot \text{M}_{\text{biomass}}^{-1}$), K is a dimensionless kinetic parameter and b is the biomass decay rate (h^{-1}).

3.2.2 Anaerobic Digestion Model No. 1

To reach a conformity among many of the anaerobic digestion models that have been developed and to be able to compare the results, the International Water Association (IWA) assigned a task group to develop a model platform for anaerobic digestion. In 2002, this resulted in the Anaerobic Digestion Model No. 1 (ADM1) (Batstone et al., 2002). The model includes disintegration and hydrolysis, acidogenesis, acetogenesis and methanogenesis steps. Disintegration and hydrolysis are described by first order kinetics while the other biochemical reactions are built on a substrate-based Monod-type kinetics. Various kinds of inhibition functions are included in the model, such as pH, free ammonia and hydrogen. In addition, acid-base reactions and liquid-to-gas mass transfer are modelled (Batstone et al., 2002). Since the ADM1 was published extensive research have been carried out in its context. Both by utilizing the model for various applications as well as to extend and develop it further (Bornhöft et al., 2013; Fezzani & Cheikh, 2009; Nordlander et al., 2017) and many more. The ADM1 is a broad and extensive model which can, if implemented correctly, give good predictions of performance. However, one of the challenges with the model is the large number of parameters, of which the implications are further discussed in Chapter 3.3.4.

3.2.3 Modelling of dark fermentation

Modelling of dark fermentation has been conducted by several research groups (Alexandropoulou et al., 2018; Lin et al., 2007; Trad et al., 2016). *Thermotoga maritima* was evaluated as a hydrogen producer through model development. The model was able to predict the hydrogen productivity profile, however, it was limited and only valid under certain process conditions (Auria et al., 2016) as many models tend to be. Ljunggren et al (2011) developed a kinetic growth model for *Caldicellulosiruptor saccharolyticus* to be used to assess substrate concentration and stripping rate for determining optimal operating conditions for H_2 production (Ljunggren et al., 2011). This model is further developed in Paper I in this thesis where the substrate is divided into its specific sugar concentrations to understand the different uptake rates of pentose and hexose sugars. The model

is also further developed in Paper II where the critical osmolarity parameter is assessed.

3.2.4 Modelling of batch and continuous processes

In batch processes there is no change in mass to the system, everything is added in the beginning, and hence no input or output to the system with time (Eq. 1), except for the gas stream.

$$\frac{dS}{dt} = \underbrace{\frac{q_{in}}{V_{liq}} \cdot (S_{in} - S)}_{= 0 \text{ if batch process}} - \rho_S \quad (1)$$

Equation 1 describes the change in substrate concentration over time, where q_{in} is the inflow to the reactor, S_{in} and S is the inflow concentration of substrate and the substrate concentration in the reactor respectively. ρ_S is the kinetic rate equation of substrate uptake. In a batch process, q_{in} and S_{in} are both 0.

Batch experiments are quite quick in time compared to continuous experiments. However, the lack of input excitation to a batch system can result in a lack of parameter sensitivity. This needs to be considered when modelling batch experiments and can be alleviated by varying the initial conditions (Flotats et al., 2003). This was done in Paper I by doing separate experiments with individual sugars, a mixture of sugars and a mixture of sugars in an industrial substrate, i.e., wheat straw hydrolysate. In Paper II, several experiments with different initial sugar concentration, 10, 30 and 80 g/L respectively, were conducted.

In continuous operation spent medium or digestate is replaced with fresh medium (substrate). Continuous experiments are in general more time consuming than batch experiments and there is also a risk of wash-out of the microbial population. However, continuous experiments can serve as a platform for kinetic analysis as long as a series of experiments at different dilution rates can be carried out (Donoso-Bravo et al., 2011).

3.3 Model development

Many bioprocesses, for example the batch processes studied herein, are dynamic (non-stationary) and these systems are characterized by their dependence on time. Dynamic systems like this are often described by mathematical expressions for the biochemical reaction rates. Mass balance equations are then formed using the reaction kinetics (Almquist et al., 2014). The mass balances describe the time-

based behaviour of all biochemical species present in the modelled system. Ordinary differential equations (ODE) are used to describe the rates of change of a specific state variable in the modelled system but do not describe the actual value of the variable. Instead, numerical integration is used to solve the ODEs. The solutions typically consist of the predicted profiles of each state variable plotted against time (Mata-Alvarez & Mitchell, 2009) (Figure 9).

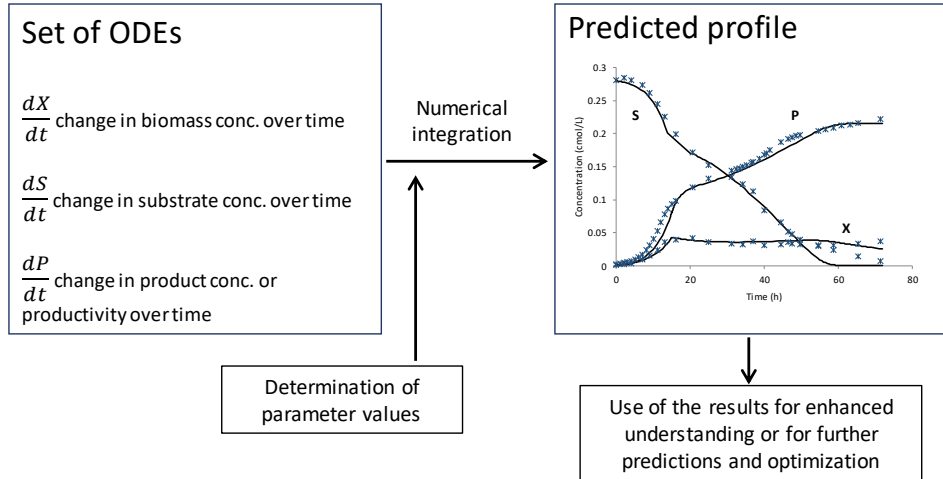


Figure 9. The application of an ODE model to a bioprocess. Figure adapted from (Mata-Alvarez & Mitchell, 2009)

The level of detail in which the biological mechanisms of the cell are described in models can vary. In unstructured models the cell is considered a black box where substrates are utilised, and products are formed, whilst in structured models the cell is considered a multicomponent chemical system (Mata-Alvarez & Mitchell, 2009). The models in both Paper I and Paper II are unstructured according to this classification.

3.3.1 Model development for *Caldicellulosiruptor*'s hydrogen production

The model in Paper I is based on Monod-type kinetics (Eq. 2), using a substrate-uptake instead of a growth-based approach, similar to the ADM1 model as described in chapter 3.2.2 (Batstone et al., 2002).

$$\rho = k_m \cdot \frac{S}{S+K_S} \quad (2)$$

where k_m is the maximum specific substrate uptake rate (h^{-1}), K_S the affinity constant (M), S the substrate concentration (M) and ρ is the substrate uptake rate (h^{-1}).

In *Caldicellulosiruptor*, the substrate, i.e., sugars are transported into the cell with a specific rate ρ and products like acetate, aqueous hydrogen and aqueous carbon dioxide are produced (Figure 10). The products are transported out of the cell and via gas-liquid mass transfer and with consideration to thermodynamic properties hydrogen and carbon dioxide enters the gas phase (dark blue in Figure 10). Via sparging, the gases in the liquid phase are then transported to the gas phase in the head space.

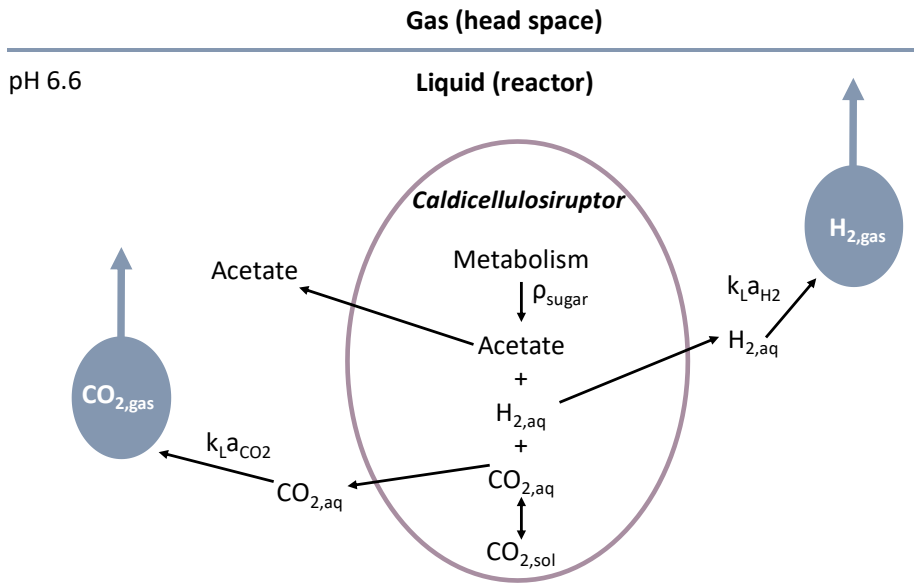


Figure 10. Mass transfer in *Caldicellulosiruptor*. The dark blue ovals represent the volume of gas in the liquid. For explanation of the state variables and parameters in this figure see the Nomenclature chapter.

3.3.2 Substrate and end-product inhibition

Competitive, non-competitive and uncompetitive inhibition (Eq. 3-5) are examples of reversible inhibition, i.e., the inhibition can be reversed if the inhibitor is removed. Competitive inhibitors compete with the substrate for the

active site on the enzyme. This type of inhibition increases the K_S -values which gives a slower uptake or growth rate and hence implies less affinity for the substrate. Non-competitive and uncompetitive inhibitors have separate binding sites on the enzyme, where the former can also bind the enzyme when substrate is not bound, which is not true for the latter. Non-competitive inhibitors decrease μ_{max} while uncompetitive inhibitors affect both μ_{max} and K_S (Saboury, 2009).

$$p_j = \frac{k_m \cdot X \cdot S}{K_S \left(1 + \frac{S_I}{K_I}\right) + S} \quad \text{competitive} \quad (3)$$

$$I = \frac{1}{1 + S_I/K_I} \quad \text{non-competitive} \quad (4)$$

$$p_j = \frac{k_m \cdot X \cdot S}{K_S + S \left(1 + \frac{K_I}{S_I}\right)} \quad \text{uncompetitive} \quad (5)$$

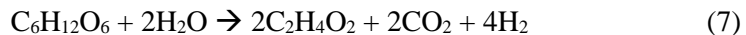
where K_I is the inhibition constant and S_I is the substrate or product that causes the inhibition.

A substrate-enzyme binding complex can also be described with the Hill equation (Eq. 6). The Hill equation has a different graphical appearance compared to the Monod equation where the former gives an S-shaped curve, i.e., for lower substrate values the Hill equation appears with logarithmic and not a linear pattern (Frank, 2013).

$$\mu = \mu_{max} \cdot \frac{S^k}{S^k + K_S^k} \quad (6)$$

where k is the Hill coefficient which is a measure of how steep the response curve is. Hill coefficients can be used to express the level of inhibition.

As described in Chapter 2.2, osmolarity is a cause of inhibition. Stoichiometrically, in hydrogen production by *Caldicellulosiruptor*, for every molecule of glucose, two molecules of acetate and carbon dioxide are produced, contributing to an increase in solute concentration. A metabolic shift towards lactate can also occur in *Caldicellulosiruptor* (Eq. 7-8).



This contributes to an osmolarity that can be calculated as follows (Eq. 9):

$$OSM = Glu + 2 \cdot Ac + 2 \cdot CO_{2,sol} + 2 \cdot Lac + 0.1 \quad (9)$$

The stoichiometric factor 2 indicates that for every mole acid produced, one mole of NaOH is added to maintain the pH, which leads to an increase in osmolarity (Ljunggren et al., 2011). In Paper II, CO_{2,sol} was excluded from the calculation since it was not measured experimentally, and according to the model CO_{2,sol} was less than 2% of the total osmolarity.

Non-competitive inhibition with a Hill coefficient is applied in the growth inhibition equation in Paper II. Inhibition due to osmolarity and aqueous hydrogen are included and expressed (Eq. 10-11):

$$I_{osm} = 1 - \left(\frac{OSM}{OSM_{crit}} \right)^{n_{\mu}} \quad (10)$$

$$I_{H_{2,aq}} = 1 - \left(\frac{H_{2,aq}}{H_{2,aq,crit}} \right)^{n_{H_2}} \quad (11)$$

where OSM_{crit} and H_{2,aq,crit} are the critical concentration of osmolarity and aqueous hydrogen, respectively. n_μ and n_{H₂} are parameters describing the level of inhibition. As displayed in Figure 6 in Paper II, I_{osm} is the most significant inhibition factor of the two, since I_{H_{2,aq}} was close to or equal to 1, i.e., no or minimal inhibition.

There are several other kinetic inhibition expressions developed for substrate and end-product inhibition (Aiba et al., 2000; Andrews, 1968; Edwards, 1970) but are not further elaborated herein.

3.3.3 Diauxic growth

To quantitatively describe the phenomenon of diauxic growth a framework for modelling of this microbial regulatory process was constructed by Kompala et al (1986) and called cybernetic models (Kompala et al., 1984; Ramkrishna, 1983). The models include specific cybernetic variables that indicate an upregulation of a specific enzyme (Eq. 12) and a fractional allocation of resources for the synthesis of the enzyme (Eq. 13) (Kompala et al., 1986).

$$v_i = \frac{\rho_i}{\max_j(r_j)} \quad (12)$$

$$u_i = \frac{\rho_i}{\sum_j r_j} \quad (13)$$

where ρ_i is the kinetic rate equation for substrate i . u_i describes the fractional allocation of a critical resource for the synthesis of specific enzymes (E_i) required for the utilization of the substrate S_i . v_i controls the activity of the enzymes (E_i), $0 < v_i < 1$, and maximum substrate uptake and subsequent biomass growth will occur when v_i is equal to 1 (Kompala et al., 1986).

3.3.4 Variables and parameters

All the entities that give a description of the system at a specific instant are called *state variables*. These include for example substrate, product and biomass concentration. Time, on the other hand, is an *independent variable* of the system. *Operating variables* can represent inputs to the system, e.g. stirrer speed or rate of feed to the system if the process is continuous. *Parameters* are inherent properties of the systems, e.g. rate and affinity values and mass transfer coefficients. A parameter is a numerical value that defines a system or sets the conditions for its operation. Parameters can be determined from knowledge acquired in laboratory experiments specifically designed for determination of the parameter or from literature. Another approach is to use estimation, i.e., to use data from experimental trials of the system under investigation, see Chapter 3.6. This is done by tuning the model parameters so that the model behaves similar to the experimental observations. When setting up a model there is a trade-off between constructing a minimal, simpler, model with fewer parameters and a more extensive model with many parameters. The ADM1, described in Chapter 3.2.2, is an example of the latter. The choice between a minimal and more extensive model is of course dependent on the purpose of usage, i.e., a simpler model could be used as a first estimate and point in one direction or another. A model with many parameters could potentially give more accurate results if the parameters can be correctly estimated. However, determining parameter values can be a challenge. And even if the parameters are determined experimentally, when pieced together, the model predictions can differ from the *in vivo* experiments due to e.g. accumulated uncertainty (Almquist et al., 2014).

3.4 Model implementation

When a model structure has been set up, which often consists of a system of non-linear differential equations including several unknown parameters, the model can be implemented in a suitable software. The models developed in Paper I and II are both constructed in the simulation software MATLAB® and consist of several different scripts connected to each other (Figure 11). This includes, a model function with ODEs, input and parameter values, a parameter estimation

script (*lsqcurvefit* further described in Chapter 3.6), numerical integration in a solver script containing an ODE solver (e.g., *ode15s*) and output result often in the form of graphical plots.

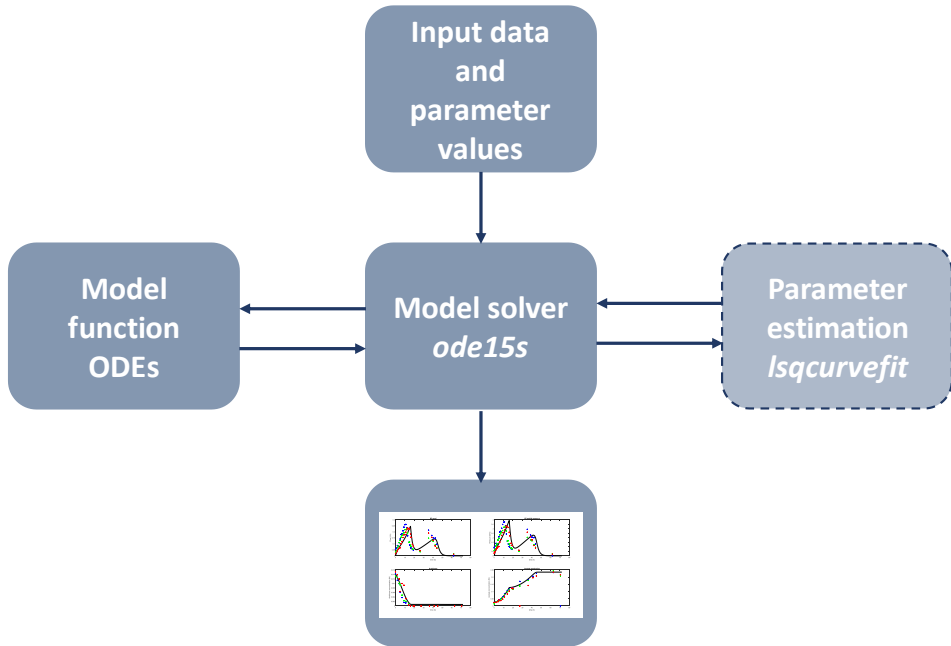


Figure 11. Visualisation of the modelling scripts implemented in MATLAB®. The parameter estimation script is depicted in dotted line since it is not needed for running the model.

When the values of the state variables were close to zero, I encountered problems with imaginary numbers in the model solution. Mostly in the modelling in Paper I. The measure taken to counteract this was to include if-statements that gave the state variable a specific value if its original value was too small.

3.5 Parameter sensitivity analysis

The purpose of a parameter sensitivity analysis is to see how a change in model parameters, initial conditions or stoichiometry can affect the model output. There are both *local* and *global methods* for this purpose, but the most common ones applied on anaerobic bioprocesses so far, are local methods (Donoso-Bravo et al., 2011). Sensitivity analysis can also be used to reduce model complexity, i.e., by eliminating insignificant parameters from the model and to identify dominant

parameters, highly correlated to the output (Hamby, 1994). There are two ways in which a model can be sensitive to the parameters i) the variability or uncertainty of a parameter can be propagated through the model leading to a large overall output variability ii) a specific parameter can be tightly correlated to the model result which means that small changes in the parameter can have significant impact on the output (Hamby, 1994).

One very fundamental way of conducting sensitivity analysis is by varying one parameter at a time, by a given percentage (Eq. 14), and see the effect on the output.

$$\Gamma_{i,j} = \frac{(y_i(\theta_j) - y_i(\theta_j + \delta \cdot \theta_j)) / y_i(\theta_j)}{\delta} \quad (14)$$

where $\Gamma_{i,j}$ is the sensitivity value with respect to state variable i and model parameter j . And $y_i(\theta_j)$ is the value of state variable i in regard to parameter j and $y_i(\theta_j + \delta \cdot \theta_j)$ is the new value of the state variable when the parameter has been altered with a factor δ (Barrera et al., 2015). This is a local sensitivity method and can quite easily give a sensitivity ranking of the parameters and can also be useful for understanding reaction paths and to select parameters that require additional research (Saltelli et al., 2005). In Paper I, the one factor at a time method was applied. The parameters were changed 1% and the effect on the result was observed. The sensitivity analysis pointed in the direction towards which parameters had an impact on the output result of the state variables and hence are important to have a good estimated value of. Therefore, the sensitivity analysis served as a basis for the subsequent parameter estimation.

However, the one factor at a time method, only addresses sensitivity relative to a specific point in the parameter space and hence does not explore the entire parameter space and the complete view of the relationship between the parameters could be missing. In contrast, *global methods* explore the parameter space or the subspace where the real parameter value is contained, e.g., variance-based methods. In addition, a third class of sensitivity methods are *screening methods* which tries to select the most important parameters when the complexity of the models is high. When the most important parameters have been identified more computationally expensive methods can be applied, e.g., the Morris' method (Degasperis, 2007). In regards of the sensitivity analysis conducted in Paper I, more emphasis can be put on this part. There are now more advanced methods to apply apart from the standard one factor at a time which is limited in its result. For upcoming research within modelling of dark fermentation, global and/or screening methods should be applied to get more extensive information about parameter sensitivity.

3.6 Parameter estimation

To fit the proposed model to experimental data, the parameters need to be estimated. This can be done by applying a cost function, and the most common used in modelling of anaerobic bioprocesses are the sum of least squares (Donoso-Bravo et al., 2011). The real system output and the model output are compared, and the deviation is calculated. Least square minimizes the sum of the squared residuals, where the residual is the difference between the observed value and the model value (Almquist et al., 2014).

A function for this purpose in MATLAB[®] is called *lsqcurvefit* which seeks the sum of least square and finds coefficient x that solves the problem in Eq. 15.

$$\min_x \|F(x, xdata) - ydata\|_2^2 = \min_x \sum_i (F(x, xdata_i) - ydata_i)^2 \quad (15)$$

where $F(x, xdata)$ represents the model and $xdata$ being the model input and $ydata$ the experimental data. *lsqcurvefit* starts at an initial parameter value x_0 and then finds a coefficient x (i.e., the parameter value) which best fit the nonlinear function F in the least square sense (Eq. 16).

$$x = lsqcurvefit(F, x_0, xdata, ydata) \quad (16)$$

Both in Paper I and II the *lsqcurvefit* function were used to estimate the parameters of greatest importance. It was discovered that the starting value, x_0 , in the parameter estimation needed to be chosen carefully since there is a risk to end up in local minima when choosing the starting value of the parameter wrongly. This, furthermore, gives a bad fit to the experimental data and a parameter of no significance. To counteract this, one can choose a variety of different starting values and in this way investigate a larger part of the parameter space (Donoso-Bravo et al., 2011). This method was applied in Paper I and Paper II.

In biological models, the parameters often have some physical meaning to explain observed mechanisms and default values can be found in literature, for example in (Batstone et al., 2002). Therefore, it is important not to “overcalibrate” a model. Such a model would give a good fit to the experimental data but would have lost the underlying meaning of the parameters and its predictive capability (Donoso-Bravo et al., 2011).

Confidence intervals can provide a view of the model’s uncertainty and hence also tell something about the validity of the model. The associated confidence interval quantifies how likely it is that a parameter lies within the intervals. A common confidence level is 95% and was used to estimate parameter uncertainty both in Paper I and II. The confidence intervals in both Paper I and II for the estimated parameters were $\pm 10\%$ or less. Some of the parameters in Paper I and II were not estimated numerically, but instead graphically estimated often with a

value found in literature as a starting point for the estimation. The reason behind not estimating some parameters numerically were their dependence on each other, i.e., parameters like k_m and K_S are closely linked and estimating them simultaneously are difficult. In addition, a more extensive experimental data set and data in several different starting concentration values could potentially have allowed for all parameters to be estimated with the cost function, *lsqcurvefit*.

3.7 Validation

When the parameters have been set it is important to assess the predictability of the model and the accuracy of the parameters. There are two steps in validation, i.e., direct validation and cross validation.

3.7.1 Direct validation

Direct validation is when the model is used to reproduce the experimental data that was used to identify the parameters. This can be done by visual inspection. This is also a way to see if the model smooths off, i.e., a model that reproduce noise for example is most likely an overparametrized model and the model will probably fail in the cross-validation test later on (Donoso-Bravo et al., 2011).

Apart from visual inspection, mathematically based methods can be used for validation, for example the coefficient of determination, R^2 , used in (Flotats et al., 2006; Palatsi et al., 2010). This provides a measure on how well the model can replicate the experimental data (Figure 12), where 1 is a perfect fit. In addition, the curve slope value k in the equation $y = k \cdot x$ also indicates the fit between model and experimental data. $k < 1$ and $k > 1$ indicate that the model underestimates or overestimates the experimental data, respectively. Both the R^2 value and the curve slope value k were applied as validation methods in Paper II.

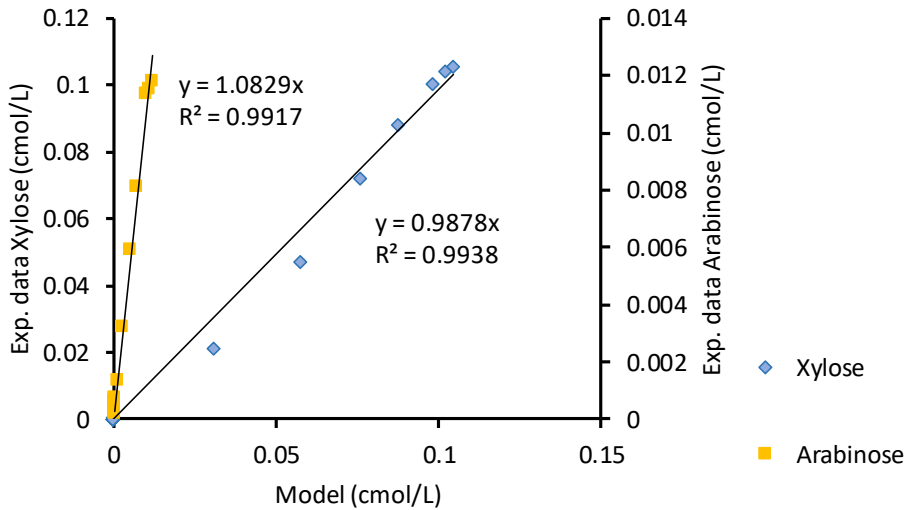


Figure 12. Model validation by R^2 and curve slope values. Example of direct validation by calculating the coefficient of determination, R^2 (0.9938 and 0.9917) and the curve slope value, k (0.9878 and 1.0829). Data and model from Paper I.

3.7.2 Cross validation

The model may very well give a good fit to the data in the direct validation, which is often the same data that was used in the parameter identification. However, to make sure that the model can reproduce the behaviour of the system a cross validation is needed. To perform a cross validation there is a requirement for enough data that can be divided into two subsets. One of the subsets are used for the parameter estimation and direct validation and the other one for the cross validation (Donoso-Bravo et al., 2011). This procedure, with two separate data sets for direct validation and cross validation, has been applied to check the validity when complex models, such as the ADM1, were used (Ozkan-Yucel & Gökçay, 2010).

Cross validation was not conducted neither in Paper I nor in Paper II. In fact, this is often a great challenge when doing modelling work. This research project has focused on modelling and hence there has been a dependence on acquiring data from elsewhere which has limited the data available for cross validation.

3.8 Interpretation of results and quantification of critical aspects

3.8.1 *C. saccharolyticus* displays diauxic-like behaviour

Cybernetic variables were applied in Paper I; the implementation can be found in Table 3 in Paper I, to describe the diauxic-like behaviour of *Caldicellulosiruptor saccharolyticus*. We also tried to simplify the model by applying *if-statements*, instead of cybernetic variables, to regulate the substrate uptake, but this meant that the physiological meaning of the model is dispersed and hence, we focused on the cybernetic approach. The cybernetic variables are used as a way to describe which transport system that is active (Figure 13), and this is connected to the preference of sugars. v_1 is associated to the first transport system when xylose is still present in phase I. v_2 is associated with the second transport system, phase II, that is activated when xylose is depleted but glucose still remains (see also Figure 7). These two variables vary between 0 and 1 depending on which transport system and consequently which substrate is preferred. When xylose is decreasing and on its way to depletion the cybernetic variable v_1 approaches 0 and vice versa for v_2 . u describes the fractional allocation of resources for the second transport system, favouring glucose, and is upregulated when xylose is depleted.

The effect of the diauxic-like behaviour is clearly visible in the hydrogen productivity profiles where a second peak in productivity is detected. This was more pronounced when using wheat straw hydrolysate as substrate (Figure 4 in Paper I). The diauxic-like model developed in Paper I was successful in describing the biphasic behaviour (Figure 3 and 4 in Paper I). The set of parameters used in the model differed between the different substrates; the mixture of sugars and the wheat straw hydrolysate respectively. The main difference could be found in the $K_{S,glu}$ -value which was substantially higher in the wheat straw case. Apart from a greater affinity for xylose in phase I, this could also be explained by unknown inhibiting compounds present in the wheat straw hydrolysate.

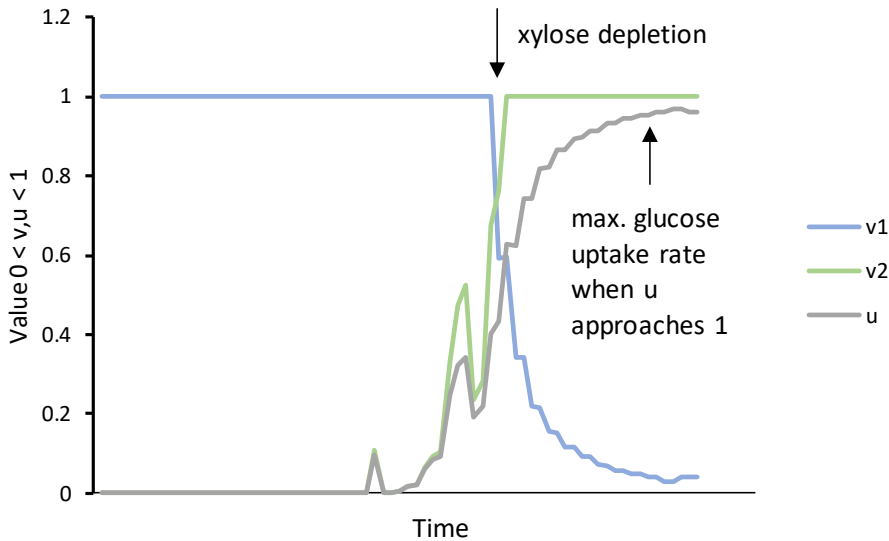


Figure 13. Illustration of cybernetic variables in the model. When xylose is present v_1 is equal to or close to 1 meaning that the enzyme related to the first transport system is very active. When xylose is depleted v_2 approaches 1 indicating that the second transport system is more active. u is related to the synthesis of the enzymes needed for uptake of glucose when xylose is depleted. This value approaches 1 as v_1 approaches 0.

3.8.2 Osmotolerance in *C. owensensis* adapted cells

Previous results have shown that *C. saccharolyticus* is mainly inhibited by hydrogen and osmolarity (Ljunggren et al., 2011). In Paper II the adapted model was used to quantify the inhibitions factors of adapted cells of *C. owensensis* that had undergone adaptive laboratory evolution to sustain a higher tolerance to osmolarity. As displayed in Figure 6 in Paper II, I_{osm} is the most significant inhibition factor of the two, since $I_{H_{2,aq}}$ was close to or equal to 1, i.e., no or minimal inhibition at the specific conditions used. The model developed in Paper II were able to describe the behaviour of growth when *C. owensensis* was exposed to 10 and 30 g/L of glucose in the feed. The model could also fairly well describe the growth when 80 g/L of glucose where added in the feed, however, with a slight overestimation of the biomass and hydrogen production. Critical osmolarity parameters, OSM_{crit} , were determined and gave almost a fourfold increase in value with an increasing sugar concentration from 10 g/L (0.23 M) to 80 g/L (0.78 M) (green, Figure 14). The OSM_{crit} parameters were linearly related to the sugar concentrations added. And furthermore, closely related to the

maximal osmolarity achieved which was calculated from the experimental data (blue, Figure 14).

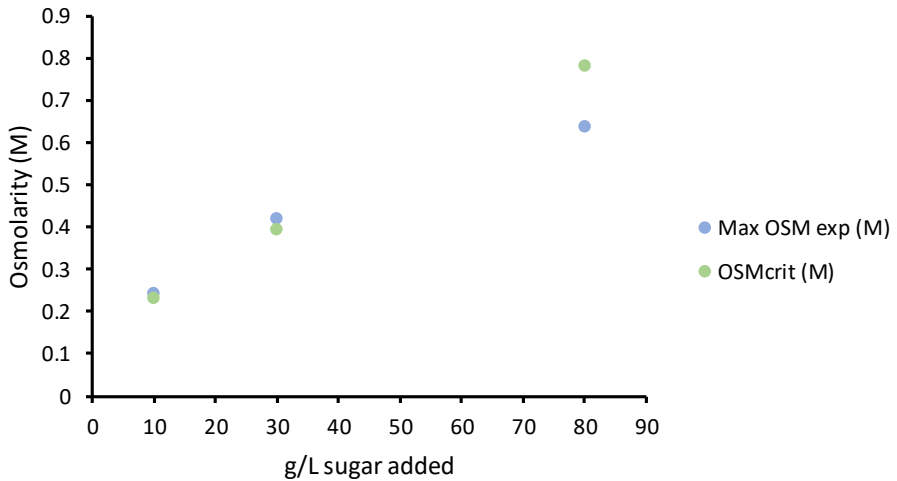


Figure 14. Modelling of osmotolerance. Maximal osmolarity achieved, calculated from the experimental data (blue; excluding $\text{CO}_{2,\text{sol}}$) and critical osmolarity parameter from the model (green).

By using the model, it was also possible to quantify how well the laboratory evolutionary engineering strategy worked in respect to robust fermentation pattern. At 30 g/L two of three replicates could be described by one model while the fitting of the model to the third replicate required an alteration in some of the parameters. This indicated that although the strategy was successful in increasing the critical osmolarity there is a possibility that the population was not completely homogenous.

4 Conclusions

Hydrogen as a future energy carrier has many desirable traits and biological production routes have great potential. *Caldicellulosiruptor* is potentially up for the task and the research has already showed its capabilities. However, further research is needed and *in silico* quantification is one suitable tool to facilitate this.

It was previously known that *Caldicellulosiruptor saccharolyticus* co-consumes different sugars but with a preference for some sugars. Here we show that xylose is preferred over glucose and this is displayed in a diauxic-like behaviour where xylose is first consumed together with glucose. When xylose is depleted glucose is further consumed but with an altered rate. This might suggest different transport systems being involved. This observation was quantitatively described in a mathematical model using cybernetic variables.

The ability to cope with a high substrate concentration is crucial for the future development of biohydrogen production by *Caldicellulosiruptor*. This research showed that quantification of a critical osmolarity parameter is possible and we were able to replicate the process *in silico*, displaying the behaviour of growth when exposed to increasing sugar concentrations.

Modelling can and is very suitable to be used as a tool in bioprocess assessment and development. In this research the emphasis has been on understanding the process with specific focus on substrate, i.e. utilization of multiple sugars and the subsequent diauxic-like behaviour and increasing sugar concentration in the feed and quantification of the behaviour. The next step should be to further develop the models to reach a stage where they can be used as predictors for further progress of the process. As an example, more extensive data sets for conducting a non-dependent cross-validation of the models would be desirable.

5 Future outlook

“If we knew what it was we were doing, it would not be called research, would it?”
- Albert Einstein

The global concerns associated with the use of fossil-based fuels and chemicals incentivises accelerated research on alternative renewable fuels and chemicals. Hydrogen produced by biological means, especially through fermentation, is an interesting future biofuel and green chemical for the industry. There are still many challenges to address, and the status of biological hydrogen production is still far from its full potential.

The last two decades there has been a substantial increase in research in the biohydrogen and dark fermentation area (Figure 15). A continuation on this path would benefit the development of the process.

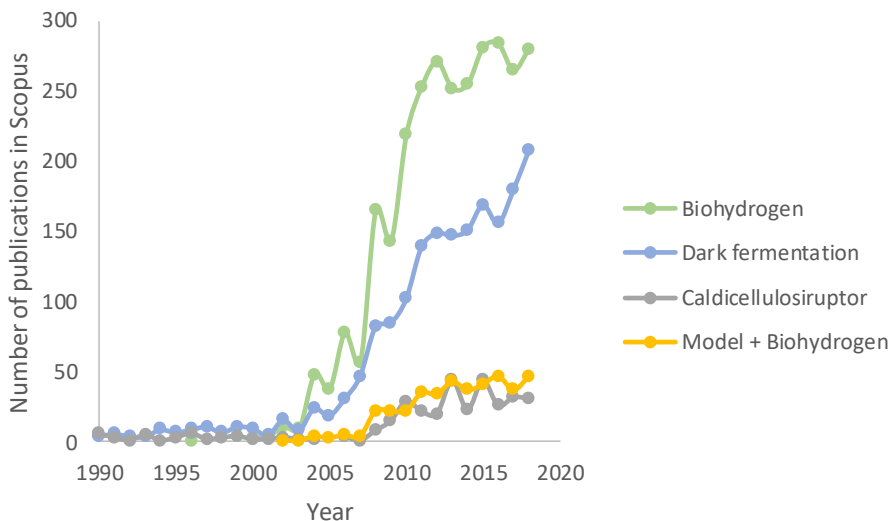


Figure 15. Publications in Scopus in the field. Key words dark fermentation, biohydrogen, *Caldicellulosiruptor* and model + biohydrogen.

Dark fermentation has reached some maturity on small scale although there are areas that still need to be addressed. Larger scale trials, i.e. pilot and demonstration scale, are to my knowledge scarce. In comparison to other ways of generating energy, e.g., solar, wind etc., biohydrogen is, as of today, not economically competitive enough (Bastidas-Oyanedel et al., 2019). Sharma et al (2015) points out several technological barriers to be resolved before moving from a carbon-based energy system to a hydrogen-based economy. The most critical point is towards the cost of sustainable hydrogen production and delivery which needs to be reduced (Sharma & Ghoshal, 2015). The cost of the feedstock can be a limiting factor in getting economy in the process. Lignocellulosic biohydrogen production using e.g., agricultural waste streams like wheat straw (Paper I) as a feedstock is a more low-cost option. Optimistic projections state that hydrogen production will rise from 4.6 EJ in 2030 to 43.8 EJ in 2050. Compared to the projected total primary energy production in 2050, hydrogen constitutes 5% of it (Moriarty & Honnery, 2009). For hydrogen to become widely available for merchant consumption efforts need to be directed towards cost efficiency of the hydrogen production technologies (Bakkenne et al., 2016).

In dark fermentation, products, like hydrogen, acetic acid and butyric acid, are produced. Hence, the focus does not solely lie on applying hydrogen as a biofuel or green chemical but considering dark fermentation as a core bioprocess in the biorefinery concept where also various biochemicals are valued products.

Hydrogen is also interesting in new applications. The steel industry contributes substantially to CO₂ emissions to the atmosphere, still there are actions taken in the fossil-free direction. In Sweden, a project called HYBRIT, which is a joint effort involving SSAB, LKAB and Vattenfall, aims to replace coking coal, which traditionally is needed for ore-based steel making, with hydrogen. If this succeed, it will reduce Sweden's CO₂ emissions by 10% (HYBRIT, 2019).

Constructing models for bioprocess assessment and hence conducting *in silico* experiments is of great importance. Being able to test different conditions in a process and predict future performance with the help of modelling could relieve the cost for developing novel bioprocesses. In the future, design of industrial processes might be dependent on a model-driven approach, where in particular kinetic models can be a strong driving force for advancement of bioprocesses. *In silico* experiments do not require as extensive resources as experiments in the laboratory and this is in alignment with the strive towards a less resource intense society.

In relation to stoichiometric models that focus on proportions of reactants and products, kinetic models can tell you when and to what extent reactions take place. However, there are several challenges to overcome. One is the need for an extensive amount of information to setup up high-quality kinetic models that can

be used for predictive purposes. Another is insecurity in parameter values and a lack of data for validation. Both quantitative and qualitative information are very important, and this needs further consideration. Another aspect is the ability to utilize the model as a support for deciding which additional experimental data is needed rather than settling with the data that is available and utilize it for model development. In regards of the studied process herein this could merit from further reflection.

As mentioned in Chapter 1, the forecasts indicate that the demand for energy will continue to increase, which means that sustainable ways of producing it is desirable. However, I would like to conclude by highlighting the very important issue of consumption. In many cases it does not matter how efficient we can make a process because that efficiency is eaten up by an increase in consumption instead. In my point of view more efforts should be made striving towards a lowered overall consumption whether it comes to fuels, materials or any resources.

Acknowledgement

This licentiate thesis is the result of a research project carried out as a joint co-operation between RISE Research Institutes of Sweden and the Division of Applied Microbiology at Lund University. I would like to acknowledge the financial support of the Swedish Energy Agency (Project No. 31090-2), the European Union (Grant Agreement number 690088) and Vinnova (2017-03286).

I have had the opportunity to conduct this research surrounded by many inspiring and helpful people and I would like to acknowledge them:

First and foremost, Karin Willquist my supervisor at RISE. You have, by far, been the most important person in my research journey. I greatly appreciate all our conversations, your endless support, all the laughs, our trips together and our friendship. No matter what turns life takes further on, you will never stop inspiring me.

A special thanks also to Ed van Niel, my main supervisor at Lund University for your scientific guidance, your eagerness to help and for bringing clarity and support.

A big thanks to everyone at the division of Applied Microbiology, who always made me feel welcome when I was there. Thank you Anette Ahlberg for answering all my administrative questions. And thanks to Jenny Schelin for all your wise thoughts and for being a great support.

A special recognition to Eoin Byrne, my fellow PhD-student, who answered all my questions regarding the experimental data and always encouraged me in my work.

I would like to acknowledge **all the past and present colleagues** in the Resources from Waste group at RISE. You have made this journey so much more fun and interesting.

- ♥ Karin, Sudha, Erika, Lina and Kristina thank you for constantly inspiring me and for being the best colleagues one could ever wish for.
- ♥ Inge, thank you for all the helpful conversations and for listening to me when I needed it the most.

- ♥ Jelena, thank you for being such an inspiring mentor and for sharing your experiences with me.
- ♥ Bo, thank you for making me see things differently and for being a great support.
- ♥ Johan, thank you for seeing something in me that I didn't quite see in myself during my first time at SP.
- ♥ Anders, Calle, Christina, Evalena, Johanna and Jonas, thank you for cheering me on and supporting me in all possible ways.
- ♥ And to Mar, I really can't remember what the office was like before you entered ;) During the past year you have helped me in so many ways and you have given me the courage to push through, thank you for that.

Thank you to all my colleagues in Hus 14 at RISE in Borås for all the fun times we have shared. All the lunch breaks, fika talks and husfester have made this a great working place and I have made many friends here. For that I will always be grateful. A special thanks to Olof for your drawing skills and for always making us smile.

My family and friends, thank you for the support you have given me on my quest on this long and winding road. Without you, nothing would have any purpose.

- ♥ To my friends Amanda, Julia, Sara, Erika, Sutina, Emelie, Matilda and Sandra thank you for being there throughout life.
- ♥ To the fantastic four: Mar, Therése, Huijuan and Lorena, I am already looking forward to our next food workshop!
- ♥ To my dearest friend Carolin, thank you for your constant encouragement. I have appreciated our endless discussions about nothing and everything. Our friendship has and will always mean a lot to me.
- ♥ To my sister Josefine, David and little Isabelle for supporting me in so many ways and always believing in me.
- ♥ And lastly and most importantly, to my parents, Ingegärd and Kjell, who gave me everything and asked for nothing.

...Thank you!

References

- Acheampong, M., Ertem, F.C., Kappler, B., Neubauer, P. 2017. In pursuit of Sustainable Development Goal (SDG) number 7: Will biofuels be reliable? *Renewable and Sustainable Energy Reviews*, **75**, 927-937.
- Aiba, S., Shoda, M., Nagatani, M. 2000. Kinetics of product inhibition in alcohol fermentation. *Biotechnology and Bioengineering*, **67**(6), 671-690.
- Alexandropoulou, M., Antonopoulou, G., Lyberatos, G. 2018. A novel approach of modeling continuous dark hydrogen fermentation. *Bioresource Technology*, **250**, 784-792.
- Almquist, J., Cvijovic, M., Hatzimanikatis, V., Nielsen, J., Jirstrand, M. 2014. Kinetic models in industrial biotechnology – Improving cell factory performance. *Metabolic Engineering*, **24**, 38-60.
- Andrews, J.F. 1968. A mathematical model for the continuous culture of microorganisms utilizing inhibitory substrates. *Biotechnology and Bioengineering*, **10**(6), 707-723.
- Auria, R., Boileau, C., Davidson, S., Casalot, L., Christen, P., Liebgott, P.P., Combet-Blanc, Y. 2016. Hydrogen production by the hyperthermophilic bacterium *Thermotoga maritima* Part II: modeling and experimental approaches for hydrogen production. *Biotechnology for Biofuels*, **9**(1), 268.
- Azimian, L., Bassi, A., Mercer, S.M. 2019. Investigation of growth kinetics of *Debaryomyces hansenii* (LAF-3 10 U) in petroleum refinery desalter effluent. *The Canadian Journal of Chemical Engineering*, **97**(1), 27-31.
- Bakenne, A., Nuttall, W., Kazantzis, N. 2016. Sankey-Diagram-based insights into the hydrogen economy of today. *International Journal of Hydrogen Energy*, **41**(19), 7744-7753.
- Balat, M., Balat, M. 2009. Political, economic and environmental impacts of biomass-based hydrogen. *International Journal of Hydrogen Energy*, **34**(9), 3589-3603.
- Barrera, E.L., Spanjers, H., Solon, K., Amerlinck, Y., Nopens, I., Dewulf, J. 2015. Modeling the anaerobic digestion of cane-molasses vinasse: Extension of the Anaerobic Digestion Model No. 1 (ADM1) with sulfate reduction for a very high strength and sulfate rich wastewater. *Water Research*, **71**, 42-54.
- Bastidas-Oyanedel, J.-R., Bonk, F., Thomsen, M.H., Schmidt, J.E. 2019. The Future Perspectives of Dark Fermentation: Moving from Only Biohydrogen to Biochemicals. in: *Biorefinery: Integrated Sustainable Processes for Biomass Conversion to Biomaterials, Biofuels, and*

- Fertilizers*, (Eds.) J.-R. Bastidas-Oyanedel, J.E. Schmidt, Springer International Publishing, Cham, pp. 375-412.
- Batan, L., Quinn, J., Willson, B., Bradley, T. 2010. Net Energy and Greenhouse Gas Emission Evaluation of Biodiesel Derived from Microalgae. *Environmental Science & Technology*, **44**(20), 7975-7980.
- Batstone, D.J., Keller, J., Angelidaki, I., Kalyuzhnyi, S.V., Pavlostathis, S.G., Rozzi, A., Sanders, W.T.M., Siegrist, H., Vavilin, V.A. 2002. Anaerobic Digestion Model No.1 IWA Task Group for Mathematical Modelling of Anaerobic Digestion Processes, IWA Publishing.
- Bomb, C., McCormick, K., Deurwaarder, E., Kåberger, T. 2007. Biofuels for transport in Europe: Lessons from Germany and the UK. *Energy Policy*, **35**(4), 2256-2267.
- Bornhöft, A., Hanke-Rauschenbach, R., Sundmacher, K. 2013. Steady-state analysis of the Anaerobic Digestion Model No. 1 (ADM1). *Nonlinear Dynamics*, **73**(1), 535-549.
- BP. 2019. BP Energy Outlook 2019 Edition.
- Bruggeman, F.J., Westerhoff, H.V. 2007. The nature of systems biology. *Trends in Microbiology*, **15**(1), 45-50.
- Byrne, E. 2019. Appraisal of strategies to improve thermophilic hydrogen production exploiting *Caldicellulosiruptor* species. in: *Department of Applied Microbiology*, Lund University. Lund, pp. 184.
- Byrne, E., Kovacs, K., van Niel, E.W.J., Willquist, K., Svensson, S.-E., Kreuger, E. 2018. Reduced use of phosphorus and water in sequential dark fermentation and anaerobic digestion of wheat straw and the application of ensiled steam-pretreated lucerne as a macronutrient provider in anaerobic digestion. *Biotechnology for Biofuels*, **11**(1), 281.
- CDIAC. Fossil-Fuel CO₂ Emissions, Carbon Dioxide Information Analysis Center.
- Charles, M.B., Ryan, R., Ryan, N., Oloruntoba, R. 2007. Public policy and biofuels: The way forward? *Energy Policy*, **35**(11), 5737-5746.
- Chen, Y.R., Hashimoto, A.G. 1980. Substrate utilization kinetic model for biological treatment process. *Biotechnology and Bioengineering*, **22**(10), 2081-2095.
- Chisti, Y. 2007. Biodiesel from microalgae. *Biotechnology Advances*, **25**(3), 294-306.
- Chu, D.F. 2015. In silico evolution of diauxic growth. *BMC evolutionary biology*, **15**, 211-211.
- Claassen, P.A.M., van Lier, J.B., Lopez Contreras, A.M., van Niel, E.W.J., Sijtsma, L., Stams, A.J.M., de Vries, S.S., Weusthuis, R.A. 1999. Utilisation of biomass for the supply of energy carriers. *Applied Microbiology and Biotechnology*, **52**(6), 741-755.
- Contesse, G., Crépin, M., Gros, F., Ullmann, A., Monod, J. 1970. *Research Article 15: On the Mechanism of Catabolite Repression*. Cold Spring Harbor Laboratory Press, Cold Spring Harbor, N.Y.

- Contois, D.E. 1959. Kinetics of Bacterial Growth: Relationship between Population Density and Specific Growth Rate of Continuous Cultures. *Microbiology*, **21**(1), 40-50.
- Das, D., Veziroglu, T.N. 2008. Advances in biological hydrogen production processes. *International Journal of Hydrogen Energy*, **33**(21), 6046-6057.
- Das, D., Veziroğlu, T.N. 2001. Hydrogen production by biological processes: a survey of literature. *International Journal of Hydrogen Energy*, **26**(1), 13-28.
- Degasperi, A. 2007. Sensitivity analysis of models of biochemical reactions. in: *Facoltà di Scienze Matematiche, Fisiche e Naturali*, University of Trento, Italy.
- Deutscher, J. 2008. The mechanisms of carbon catabolite repression in bacteria. *Current Opinion in Microbiology*, **11**(2), 87-93.
- Diénert, F. 1900. *Sur la fermentation du galactose et sur l'accoutumance des levures à ce sucre*, par M. Frédéric Diénert. Impr. de E. Charaire, Sceaux.
- Donoso-Bravo, A., Mailier, J., Martin, C., Rodríguez, J., Aceves-Lara, C.A., Wouwer, A.V. 2011. Model selection, identification and validation in anaerobic digestion: A review. *Water Research*, **45**(17), 5347-5364.
- Edwards, V.H. 1970. The influence of high substrate concentrations on microbial kinetics. *Biotechnology and Bioengineering*, **12**(5), 679-712.
- European Commission. 2012. Energy Roadmap 2050. European Commission, Publications Office of the European Union.
- European Commission. 2014. A policy framework for climate and energy in the period from 2020 to 2030. European Commission Technical Report COM (2014) 15.
- European Parliament. 2018. Promoting renewable energy sources in the EU after 2020. European Parliament EU Legislation in Progress.
- Fezzani, B., Cheikh, R.B. 2009. Extension of the anaerobic digestion model No. 1 (ADM1) to include phenolic compounds biodegradation processes for the simulation of anaerobic co-digestion of olive mill wastes at thermophilic temperature. *Journal of Hazardous Materials*, **162**(2), 1563-1570.
- Flotats, X., Ahring, B.K., Angelidaki, I. 2003. Parameter identification of thermophilic anaerobic degradation of valerate. *Applied Biochemistry and Biotechnology*, **109**(1), 47-62.
- Flotats, X., Palatsi, J., Ahring, B.K., Angelidaki, I. 2006. Identifiability study of the proteins degradation model, based on ADM1, using simultaneous batch experiments. *Water Science and Technology*, **54**(4), 31-39.
- Frank, S.A. 2013. Input-output relations in biological systems: measurement, information and the Hill equation. *Biology Direct*. 8:31
- Fukui, H. 2018. Hydrogen - Tracking Clean Energy Progress, (Ed.) I.I.E. Agency. <https://www.iea.org/tcep/energyintegration/hydrogen/>.

- Global Carbon Project. 2018. Carbon budget and trends 2018. www.globalcarbonproject.org/carbonbudget published on 5 December 2018.
- Grand View Research Inc. 2018. Hydrogen Generation Market Size, Share & Trends Analysis Report By Application (Coal Gasification, Steam Methane Reforming), By Technology, By System (Merchant, Captive), And Segment Forecasts, 2018 - 2025. Grand View Research.
- Grau, P., Dohányos, M., Chudoba, J. 1975. Kinetics of multicomponent substrate removal by activated sludge. *Water Research*, **9**(7), 637-642.
- Hadar, Y. 2013. Sources for Lignocellulosic Raw Materials for the Production of Ethanol. in: *Lignocellulose Conversion: Enzymatic and Microbial Tools for Bioethanol Production*, (Ed.) V. Faraco, Springer Berlin Heidelberg. Berlin, Heidelberg, pp. 21-38.
- Hallenbeck, P.C. 2005. Fundamentals of the fermentative production of hydrogen. *Water Science and Technology*, **52**(1-2), 21-29.
- Hallenbeck, P.C., Benemann, J.R. 2002. Biological hydrogen production; fundamentals and limiting processes. *International Journal of Hydrogen Energy*, **27**(11), 1185-1193.
- Hallenbeck, P.C., Ghosh, D. 2009. Advances in fermentative biohydrogen production: the way forward? *Trends in Biotechnology*, **27**(5), 287-297.
- Hamby, D.M. 1994. A review of techniques for parameter sensitivity analysis of environmental models. *Environmental Monitoring and Assessment*, **32**(2), 135-154.
- HYBRIT. 2019. HYBRIT - fossil-free steel. <http://www.hybritdevelopment.com/>.
- IEA. 2018b. Market analysis and forecast from 2018 to 2023. International Energy Agency.
- IEA. 2018a. Renewables information: Overview 2018. International Energy Agency.
- IPCC. 2018. Summary for Policymakers. In: Global Warming of 1.5°C. World Meteorological Organization, Geneva, Switzerland.
- Jackson, R.B., Le Quéré, C., Andrew, R.M., Canadell, J.G., Korsbakken, J.I., Liu, Z., Peters, G.P., Zheng, B. 2018. Global energy growth is outpacing decarbonization. *Environmental Research Letters*, **13**(12), 120401.
- Jones, D.T., Woods, D.R. 1986. Acetone-butanol fermentation revisited. *Microbiological Reviews*, **50**(4), 484-524.
- Kompala, D.S., Ramkrishna, D., Jansen, N.B., Tsao, G.T. 1986. Investigation of bacterial growth on mixed substrates: Experimental evaluation of cybernetic models. *Biotechnology and Bioengineering*, **28**(7), 1044-1055.
- Kompala, D.S., Ramkrishna, D., Tsao, G.T. 1984. Cybernetic modeling of microbial growth on multiple substrates. *Biotechnology and Bioengineering*, **26**(11), 1272-1281.
- Kotay, S.M., Das, D. 2007. Microbial hydrogen production with *Bacillus coagulans* IIT-BT S1 isolated from anaerobic sewage sludge. *Bioresource Technology*, **98**(6), 1183-1190.

- Kretschmer, B., Allen, B., Hart, K. 2012. Mobilising Cereal Straw in the EU to feed advanced biofuel production. Institute for European Environmental Policy.
- Le Quéré, C., Andrew, R.M., Friedlingstein, P., Sitch, S., Hauck, J., Pongratz, J., Pickers, P.A., Korsbakken, J.I., Peters, G.P., Canadell, J.G., Arneeth, A., Arora, V.K., Barbero, L., Bastos, A., Bopp, L., Chevallier, F., Chini, L.P., Ciais, P., Doney, S.C., Gkritzalis, T., Goll, D.S., Harris, I., Haverd, V., Hoffman, F.M., Hoppema, M., Houghton, R.A., Hurtt, G., Ilyina, T., Jain, A.K., Johannessen, T., Jones, C.D., Kato, E., Keeling, R.F., Goldewijk, K.K., Landschützer, P., Lefèvre, N., Lienert, S., Liu, Z., Lombardozzi, D., Metzl, N., Munro, D.R., Nabel, J.E.M.S., Nakaoka, S.I., Neill, C., Olsen, A., Ono, T., Patra, P., Peregón, A., Peters, W., Peylin, P., Pfeil, B., Pierrot, D., Poulter, B., Rehder, G., Resplandy, L., Robertson, E., Rocher, M., Rödenbeck, C., Schuster, U., Schwinger, J., Séférian, R., Skjelvan, I., Steinhoff, T., Sutton, A., Tans, P.P., Tian, H., Tilbrook, B., Tubiello, F.N., van der Laan-Luijckx, I.T., van der Werf, G.R., Viovy, N., Walker, A.P., Wiltshire, A.J., Wright, R., Zaehle, S., Zheng, B. 2018. Global Carbon Budget 2018. *Earth Syst. Sci. Data*, **10**(4), 2141-2194.
- Lee, H.-S., Salerno, M.B., Rittmann, B.E. 2008. Thermodynamic Evaluation on H₂ Production in Glucose Fermentation. *Environmental Science & Technology*, **42**(7), 2401-2407.
- Levin, D.B., Pitt, L., Love, M. 2004. Biohydrogen production: prospects and limitations to practical application. *International Journal of Hydrogen Energy*, **29**(2), 173-185.
- Lin, P.-Y., Whang, L.-M., Wu, Y.-R., Ren, W.-J., Hsiao, C.-J., Li, S.-L., Chang, J.-S. 2007. Biological hydrogen production of the genus *Clostridium*: Metabolic study and mathematical model simulation. *International Journal of Hydrogen Energy*, **32**(12), 1728-1735.
- Ljunggren, M., Willquist, K., Zacchi, G., van Niel, E.W. 2011. A kinetic model for quantitative evaluation of the effect of hydrogen and osmolarity on hydrogen production by *Caldicellulosiruptor saccharolyticus*. *Biotechnology for Biofuels*, **4**(1), 31.
- Ljunggren, M., Zacchi, G. 2010. Techno-economic analysis of a two-step biological process producing hydrogen and methane. *Bioresource Technology*, **101**(20), 7780-7788.
- Lü, J., Sheahan, C., Fu, P. 2011. Metabolic engineering of algae for fourth generation biofuels production. *Energy & Environmental Science*, **4**(7), 2451-2466.
- Maeda, T., Sanchez-Torres, V., Wood, T.K. 2008. Metabolic engineering to enhance bacterial hydrogen production. *Microbial Biotechnology*, **1**(1), 30-39.
- Mata-Alvarez, J., Mitchell, A., David, J. 2009. *Biotechnology: Methods in Biotechnology Volume II, Mathematical Modeling in Biotechnology*. Eolss Publishers Co. Ltd., Oxford, United Kingdom.

- Menon, V., Rao, M. 2012. Trends in bioconversion of lignocellulose: Biofuels, platform chemicals & biorefinery concept. *Progress in Energy and Combustion Science*, **38**(4), 522-550.
- Minty, J.J., Lin, X.N. 2015. Chapter 18 - Engineering Synthetic Microbial Consortia for Consolidated Bioprocessing of Lignocellulosic Biomass into Valuable Fuels and Chemicals. in: *Direct Microbial Conversion of Biomass to Advanced Biofuels*, (Ed.) M.E. Himmel, Elsevier. Amsterdam, pp. 365-381.
- Monod, J. 1941. Recherches sur la croissance des cultures bactériennes, Hermann. Paris.
- Moriarty, P., Honnery, D. 2009. Hydrogen's role in an uncertain energy future. *International Journal of Hydrogen Energy*, **34**(1), 31-39.
- Mulchandani, A., Luong, J.H.T. 1989. Microbial inhibition kinetics revisited. *Enzyme and Microbial Technology*, **11**(2), 66-73.
- Naik, S.N., Goud, V.V., Rout, P.K., Dalai, A.K. 2010. Production of first and second generation biofuels: A comprehensive review. *Renewable and Sustainable Energy Reviews*, **14**(2), 578-597.
- Nath, K., Kumar, A., Das, D. 2006. Effect of some environmental parameters on fermentative hydrogen production by *Enterobacter cloacae* DM11. *Canadian Journal of Microbiology*, **52**(6), 525-532.
- Nicolaou, S.A., Gaida, S.M., Papoutsakis, E.T. 2010. A comparative view of metabolite and substrate stress and tolerance in microbial bioprocessing: From biofuels and chemicals, to biocatalysis and bioremediation. *Metabolic Engineering*, **12**(4), 307-331.
- Nielsen, J., Fussenegger, M., Keasling, J.D., Lee, S.Y., Liao, J.C., Prather, K., Palsson, B. 2014. Engineering synergy in biotechnology. *Nature Chemical Biology*(5), 319.
- Nordlander, E., Thorin, E., Yan, J. 2017. Investigating the possibility of applying an ADM1 based model to a full-scale co-digestion plant. *Biochemical Engineering Journal*, **120**, 73-83.
- Ozkan-Yucel, U.G., Gökçay, C.F. 2010. Application of ADM1 model to a full-scale anaerobic digester under dynamic organic loading conditions. *Environmental Technology*, **31**(6), 633-640.
- Palatsi, J., Illa, J., Prenafeta-Boldú, F.X., Laureni, M., Fernandez, B., Angelidaki, I., Flotats, X. 2010. Long-chain fatty acids inhibition and adaptation process in anaerobic thermophilic digestion: Batch tests, microbial community structure and mathematical modelling. *Bioresource Technology*, **101**(7), 2243-2251.
- Pawar, S.S., Nkemka, V.N., Zeidan, A.A., Murto, M., van Niel, E.W.J. 2013. Biohydrogen production from wheat straw hydrolysate using *Caldicellulosiruptor saccharolyticus* followed by biogas production in a two-step uncoupled process. *International Journal of Hydrogen Energy*, **38**(22), 9121-9130.

- Pawar, S.S., van Niel, E.W.J. 2013. Thermophilic biohydrogen production: how far are we? *Applied Microbiology and Biotechnology*, **97**(18), 7999-8009.
- Pavlostathis, S.G., Giraldo-Gomez, E. 1991. Kinetics of Anaerobic Treatment. *Water Science and Technology*, **24**(8), 35-59.
- Plevin, R.J., O'Hare, M., Jones, A.D., Torn, M.S., Gibbs, H.K. 2010. Greenhouse Gas Emissions from Biofuels' Indirect Land Use Change Are Uncertain but May Be Much Greater than Previously Estimated. *Environmental Science & Technology*, **44**(21), 8015-8021.
- Quinn, J.C., Davis, R. 2015. The potentials and challenges of algae based biofuels: A review of the techno-economic, life cycle, and resource assessment modeling. *Bioresource Technology*, **184**, 444-452.
- Rai, P.K., Singh, S.P., Asthana, R.K. 2012. Biohydrogen Production from Cheese Whey Wastewater in a Two-Step Anaerobic Process. *Applied Biochemistry and Biotechnology*, **167**(6), 1540-1549.
- Rainey, F.A., Donnison, A.M., Janssen, P.H., Saul, D., Rodrigo, A., Bergquist, P.L., Daniel, R.M., Stackebrandt, E., Morgan, H.W. 1994. Description of *Caldicellulosiruptor saccharolyticus* gen. nov., sp. nov: An obligately anaerobic, extremely thermophilic, cellulolytic bacterium. *FEMS Microbiology Letters*, **120**(3), 263-266.
- Rajendran, K., Kankanala, H.R., Lundin, M., Taherzadeh, M.J. 2014. A novel process simulation model (PSM) for anaerobic digestion using Aspen Plus. *Bioresource Technology*, **168**, 7-13.
- Ramkrishna, D. 1983. A Cybernetic Perspective of Microbial Growth. in: *Foundations of Biochemical Engineering*, Vol. 207, AMERICAN CHEMICAL SOCIETY, pp. 161-178.
- Saboury, A.A. 2009. Enzyme Inhibition and Activation: A General Theory. *Journal of the Iranian Chemical Society*, **6**(2), 219-229.
- Saltelli, A., Ratto, M., Tarantola, S., Campolongo, F. 2005. Sensitivity Analysis for Chemical Models. *Chemical Reviews*, **105**(7), 2811-2828.
- Sharma, S., Ghoshal, S.K. 2015. Hydrogen the future transportation fuel: From production to applications. *Renewable and Sustainable Energy Reviews*, **43**, 1151-1158.
- Sims, R.E.H., Mabee, W., Saddler, J.N., Taylor, M. 2010. An overview of second generation biofuel technologies. *Bioresource Technology*, **101**(6), 1570-1580.
- Singh, A., Rathore, D. 2017. Biohydrogen: Next Generation Fuel. in: *Biohydrogen Production: Sustainability of Current Technology and Future Perspective*, (Eds.) A. Singh, D. Rathore, Springer. India.
- Soboh, B., Linder, D., Hedderich, R. 2004. A multisubunit membrane-bound [NiFe] hydrogenase and an NADH-dependent Fe-only hydrogenase in the fermenting bacterium *Thermoanaerobacter tengcongensis*. *Microbiology*, **150**(7), 2451-2463.

- Trad, Z., Fontaine, J.-P., Larroche, C., Vial, C. 2016. Multiscale mixing analysis and modeling of biohydrogen production by dark fermentation. *Renewable Energy*, **98**, 264-282.
- United Nations. 2015. Adoption of the Paris Agreement. United Nations.
- United Nations. 2018a. Climate Change. United Nations.
- United Nations. 2018b. Katowice climate package. United Nations.
- van de Werken, H.J.G., Verhaart, M.R.A., VanFossen, A.L., Willquist, K., Lewis, D.L., Nichols, J.D., Goorissen, H.P., Mongodin, E.F., Nelson, K.E., van Niel, E.W.J., Stams, A.J.M., Ward, D.E., de Vos, W.M., van der Oost, J., Kelly, R.M., Kengen, S.W.M. 2008. Hydrogenomics of the Extremely Thermophilic Bacterium *Caldicellulosiruptor saccharolyticus*. *Applied and Environmental Microbiology*, **74**(21), 6720-6729.
- van der Laak, W.W.M., Raven, R.P.J.M., Verbong, G.P.J. 2007. Strategic niche management for biofuels: Analysing past experiments for developing new biofuel policies. *Energy Policy*, **35**(6), 3213-3225.
- van Niel, E.W.J. 2016. Biological Processes for Hydrogen Production. in: *Anaerobes in Biotechnology*, (Eds.) R. Hatti-Kaul, G. Mamo, B. Mattiasson, Springer International Publishing. Cham, pp. 155-193.
- van Niel, E.W.J., Budde, M.A.W., de Haas, G.G., van der Wal, F.J., Claassen, P.A.M., Stams, A.J.M. 2002. Distinctive properties of high hydrogen producing extreme thermophiles, *Caldicellulosiruptor saccharolyticus* and *Thermotoga elfii*. *International Journal of Hydrogen Energy*, **27**(11), 1391-1398.
- van Niel, E.W.J., Claassen, P.A.M., Stams, A.J.M. 2003. Substrate and product inhibition of hydrogen production by the extreme thermophile, *Caldicellulosiruptor saccharolyticus*. *Biotechnology and Bioengineering*, **81**(3), 255-262.
- VanFossen, A.L., Verhaart, M.R.A., Kengen, S.M.W., Kelly, R.M. 2009. Carbohydrate Utilization Patterns for the Extremely Thermophilic Bacterium *Caldicellulosiruptor saccharolyticus* Reveal Broad Growth Substrate Preferences. *Applied and Environmental Microbiology*, **75**(24), 7718-7724.
- Willey, J., Sherwood, L., Woolverton, C. 2013. *Prescott's Microbiology: Ninth Edition*. McGraw-Hill Higher Education.
- Willquist, K., Nkemka, V.N., Svensson, H., Pawar, S., Ljunggren, M., Karlsson, H., Murto, M., Hulteberg, C., van Niel, E.W.J., Liden, G. 2012. Design of a novel biohythane process with high H₂ and CH₄ production rates. *International Journal of Hydrogen Energy*, **37**(23), 17749-17762.
- Willquist, K., Pawar, S.S., Van Niel, E.W. 2011. Reassessment of hydrogen tolerance in *Caldicellulosiruptor saccharolyticus*. *Microbial Cell Factories*, **10**(1), 111.
- Willquist, K., van Niel, E.W.J. 2010. Lactate formation in *Caldicellulosiruptor saccharolyticus* is regulated by the energy carriers pyrophosphate and ATP. *Metabolic Engineering*, **12**(3), 282-290.

- Willquist, K., Zeidan, A.A., van Niel, E.W. 2010. Physiological characteristics of the extreme thermophile *Caldicellulosiruptor saccharolyticus*: an efficient hydrogen cell factory. *Microbial Cell Factories*, **9**(1), 89.
- Zeidan, A.A., van Niel, E.W.J. 2010. A quantitative analysis of hydrogen production efficiency of the extreme thermophile *Caldicellulosiruptor owensensis* OLT. *International Journal of Hydrogen Energy*, **35**(3), 1128-1137.
- Zhang, Y.H.P. 2008. Reviving the carbohydrate economy via multi-product lignocellulose biorefineries. *Journal of Industrial Microbiology & Biotechnology*, **35**(5), 367-375.

Paper I



RESEARCH

Open Access



A non-linear model of hydrogen production by *Caldicellulosiruptor saccharolyticus* for diauxic-like consumption of lignocellulosic sugar mixtures

Johanna Björkmalm^{1,2*} , Eoin Byrne², Ed W. J. van Niel² and Karin Willquist¹

Abstract

Background: *Caldicellulosiruptor saccharolyticus* is an attractive hydrogen producer suitable for growth on various lignocellulosic substrates. The aim of this study was to quantify uptake of pentose and hexose monosaccharides in an industrial substrate and to present a kinetic growth model of *C. saccharolyticus* that includes sugar uptake on defined and industrial media. The model is based on Monod and Hill kinetics extended with gas-to-liquid mass transfer and a cybernetic approach to describe diauxic-like growth.

Results: Mathematical expressions were developed to describe hydrogen production by *C. saccharolyticus* consuming glucose, xylose, and arabinose. The model parameters were calibrated against batch fermentation data. The experimental data included four different cases: glucose, xylose, sugar mixture, and wheat straw hydrolysate (WSH) fermentations. The fermentations were performed without yeast extract. The substrate uptake rate of *C. saccharolyticus* on single sugar-defined media was higher on glucose compared to xylose. In contrast, in the defined sugar mixture and WSH, the pentoses were consumed faster than glucose. Subsequently, the cultures entered a lag phase when all pentoses were consumed after which glucose uptake rate increased. This phenomenon suggested a diauxic-like behavior as was deduced from the successive appearance of two peaks in the hydrogen and carbon dioxide productivity. The observation could be described with a modified diauxic model including a second enzyme system with a higher affinity for glucose being expressed when pentose saccharides are consumed. This behavior was more pronounced when WSH was used as substrate.

Conclusions: The previously observed co-consumption of glucose and pentoses with a preference for the latter was herein confirmed. However, once all pentoses were consumed, *C. saccharolyticus* most probably expressed another uptake system to account for the observed increased glucose uptake rate. This phenomenon could be quantitatively captured in a kinetic model of the entire diauxic-like growth process. Moreover, the observation indicates a regulation system that has fundamental research relevance, since pentose and glucose uptake in *C. saccharolyticus* has only been described with ABC transporters, whereas previously reported diauxic growth phenomena have been correlated mainly to PTS systems for sugar uptake.

Keywords: *Caldicellulosiruptor saccharolyticus*, Hydrogen, Kinetic growth model, Glucose uptake, Xylose uptake, Diauxic

*Correspondence: johanna.bjorkmalm@rise

¹ Department of Energy and Circular Economy, RISE Research Institutes of Sweden, PO Box 857, 501 15 Borås, Sweden

Full list of author information is available at the end of the article



© The Author(s) 2018. This article is distributed under the terms of the Creative Commons Attribution 4.0 International License (<http://creativecommons.org/licenses/by/4.0/>), which permits unrestricted use, distribution, and reproduction in any medium, provided you give appropriate credit to the original author(s) and the source, provide a link to the Creative Commons license, and indicate if changes were made. The Creative Commons Public Domain Dedication waiver (<http://creativecommons.org/publicdomain/zero/1.0/>) applies to the data made available in this article, unless otherwise stated.

Background

The need for renewable energy is ever increasing to tackle the major challenges of global warming, energy demand, and limited resources. According to statistics published by the International Energy Agency [1], just over 86% of the Total Primary Energy Supply (TPES) in 2014 was produced from fossil resources, leaving a modest 14% originating from renewable energy sources. When putting these numbers in relation with the adopted Paris Agreement in 2015, targeting to keep the global average temperature increase below the 2 °C above pre-industrial levels [2], it is evident that actions need to be taken. There are, however, positive trends in that the supply of renewable energy sources has grown faster, with an average annual rate of 2.0% since 1990, compared to the growth of the world TPES of 1.8% [1].

Hydrogen has the potential of becoming an important renewable energy carrier. Currently, hydrogen is widely used as a reducing agent in the chemical and food industry. However, using hydrogen as an energy carrier in sustainable applications is of great interest due to its potentially high efficiency of conversion to usable power, its low emissions of pollutants and high energy density [3]. Up to 96% of the world's hydrogen production is fossil based, i.e., natural gas, oil, and coal [4]. A sustainable alternative to the conventional methods for producing hydrogen is by biological methods, i.e., biohydrogen. There are four major categories in which production of biological hydrogen can be classified, namely: photofermentation of organic compounds by photosynthetic bacteria, biophotolysis of water using algae and cyanobacteria, bioelectrohydrogenesis, and fermentative hydrogen production, so-called dark fermentation, from organic wastes or energy crops [5, 6]. The latter is the focus of this study, where various sugars present in, e.g., agricultural waste like wheat straw, can be fermented by microorganisms for hydrogen production. This also addresses the challenge of converting lignocellulosic biomass to renewable energy.

Lignocellulosic biomass has been previously described as “the most abundant organic component of the biosphere” with an annual production of 1–5·10¹³ kg and, therefore, is an attractive substrate for biofuel production [7]. Lignocellulosic biomass primarily consists of cellulose (40–60% CDW), hemicellulose (20–40%), and lignin (10–25%) [8]. Cellulose and hemicellulose can be enzymatically hydrolyzed into smaller sugar molecules.

The thermophilic microorganism *Caldicellulosiruptor saccharolyticus* is able to produce hydrogen from lignocellulosic biomass through dark fermentation and has previously shown the potential of producing hydrogen close to the maximum theoretical yield of 4 mol hydrogen per mol hexose [9–11]. *C. saccharolyticus* is cellulolytic

and can utilize a broad range of di- and monosaccharides for hydrogen production [12]. Van de Werken et al. [13] showed that *C. saccharolyticus* coferments glucose and xylose as it lacks catabolite repression. VanFossen et al. [14] revealed that although *C. saccharolyticus* co-utilizes different sugars, it has a preference for some sugars over others. Xylose was discussed as a preferred sugar over glucose and is, therefore, utilized by the microorganism to a greater extent than glucose. However, the substrate uptake kinetics was not determined and a yeast extract (YE)-supplemented medium was used [13].

By developing a mathematical model for a biological process, it is possible to describe past and predict future performances as well as gaining a deeper understanding of the physiological mechanism behind the process. The aim of this study is to present a model that describes the growth of *C. saccharolyticus* on lignocellulosic sugar mixtures and how the uptake rate changes when the sugars are used simultaneously or individually. Similar kinds of models have been developed [15, 16]; however, these models focus on single sugar uptake. The proposed model here builds on the one presented by Ljunggren et al. [15] by adding the consumption rates for each individual sugar in the sugar mixtures. Monod [17] first described the phenomenon of diauxic growth, where a microorganism is exposed to two substrates and first consumes the substrate that supports the most efficient growth rate. Several models have been developed in this area [18, 19] describing how to capture the subsequent uptake of sugars when multiple sugars are present. This phenomenon can be modeled using a cybernetic approach to whether a particular enzyme, needed for a specific sugar to be metabolized, is upregulated or not.

This paper describes the development of a substrate-based uptake model using Monod-type kinetics including biomass growth, product formation, liquid-to-gas mass transfer, and enzyme synthesis with Hill kinetics, with *C. saccharolyticus* as model organism. The model presented in this paper takes into consideration the usage of different sugars, including hexoses, i.e., glucose, and pentoses, i.e., xylose and arabinose. The model describes the different sugar uptakes individually, exemplifying the rate at which each sugar is consumed when *C. saccharolyticus* grows on the sugar mixtures and on the individual sugars, respectively.

Methods

Strains and cultivation medium

Caldicellulosiruptor saccharolyticus DSM 8903 was obtained from the Deutsche Sammlung von Mikroorganismen und Zellkulturen (Braunschweig, Germany). Subcultivations were conducted in 250 mL serum flasks with 50 mL modified DSM 640 media [20]. The carbon source

of each cultivation corresponded to that of the subsequent fermentor cultivation. The 1000× vitamin solution and modified SL-10 solution were prepared according to [20] and [21], respectively.

All bioreactor experiments used a modified DSM 640 medium with the exclusion of yeast extract according to Willquist and van Niel [20]. To quantify the kinetics of xylose and glucose uptake and the effect of when the sugars were mixed in pure and industrial medium, the growth and hydrogen production was monitored in four different cases, where the total sugar concentration in the medium was fixed to 10 g/L. Cultivations were performed using 10 g/L glucose (Case 1), 10 g/L xylose (Case 2), a sugar mixture (Case 3), and wheat straw hydrolysate (Case 4). In Case 4, a 9% solution of wheat straw hydrolysate was used corresponding to approximately 10 g/L total sugars. In Case 3, the sugar mixture contained pure sugars with the same concentration as the wheat straw hydrolysate (6.75 g/L glucose, 3.06 g/L xylose, and 0.173 g/L arabinose). The total sugar concentrations at the start of the fermentation included the sugar added as described above and the additional sugar added from the inoculum, which varied slightly in the different conditions. The starting sugar concentration was, therefore, as follows: Case 1, 12.11 ± 0.09 g/L glucose; Case 2, 10.96 ± 0.20 g/L xylose; Case 3, 8.69 ± 0.12 g/L glucose, 3.38 ± 0.19 g/L xylose, and 0.38 ± 0.01 g/L arabinose; Case 4, 7.31 ± 0.07 g/L glucose, 3.36 ± 0.06 g/L xylose, and 0.34 ± 0.00 g/L arabinose.

Fermentor setup

Batch cultivations were performed in a jacketed, 3-L fermentor equipped with ADI 1025 Bio-Console and ADI 1010 Bio-Controller (Applikon, Schiedam, The Netherlands). A working volume of 1 L was used for cultivations and the pH was maintained at optimal conditions 6.5 ± 0.1 at 70 °C by automatic titration with 4 M NaOH. The temperature was thermostatically kept at 70 ± 1 °C. Stirring was maintained at 250 rpm and nitrogen was sparged through the medium at a rate of 6 L/h. Sparging was initiated 4 h after inoculation and was continued throughout the cultivation. A condenser cooled with water at 4 °C was utilized to prevent evaporation of the medium. Samples were collected at regular time intervals for monitoring of the optical density. The supernatant from each culture was collected and stored at -20 °C for further quantification of various sugars and organic acids. Gas samples were collected from the fermentor's headspace to quantify H₂ and CO₂. The sugar mixture and wheat straw hydrolysate experiments were done in triplicate. The individual sugar fermentations were done in biological duplicate.

A defined medium was autoclaved in each fermentor, while anoxic solutions of cysteine HCl·H₂O (1 g/L), MgCl₂·6H₂O (0.4 g/L), and carbon source(s) were prepared separately and were added to the fermentor before inoculation. Just after inoculation, the fermentor was closed for 4 h to allow buildup of CO₂ as previously described [20] necessary to initiate growth.

Analytical methods

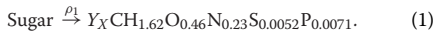
Optical density was determined using an Ultraspec 2100 pro spectrophotometer (Amersham Biosciences) at 620 nm. Sugars, organic acids, hydroxymethyl furfural (HMF), and furfural were detected using HPLC (Waters, Milford, MA, USA). For the quantification of organic acids, an HPLC equipped with an Aminex HPX-87H ion-exchange column (Bio-Rad, Hercules, USA) at 60 °C and 5 mM H₂SO₄ as mobile phase was used at a flow rate of 0.6 mL/min. Glucose, xylose, and arabinose quantification was conducted using an HPLC with a Shodex SP-0810 Column (Shodex, Japan) with water as a mobile phase at a flow rate of 0.6 mL/min. CO₂ and H₂ were quantified with a dual channel Micro-GC (CP-4900; Varian, Micro-gas chromatography, Middelburg, The Netherlands), as previously described [21].

Mathematical model description

The model developed for *C. saccharolyticus* in this study takes into account the kinetics of biomass growth, consumption of glucose, xylose and arabinose, and formation of the products acetate, hydrogen, and carbon dioxide. Furthermore, the model includes liquid-to-gas mass transfer of hydrogen and carbon dioxide as well as the equilibrium between carbon dioxide, bicarbonate (HCO₃⁻) and carbonate (CO₃²⁻). The model is developed on a cmol basis. The formation of lactate was excluded to reduce the complexity of the model, as it constituted to less than 5% of the total product in the sugar mixture fermentations. In addition, inhibition due to high aqueous H₂ concentration and high osmolarity was not included in the model to reduce the number of unknown parameters. This is motivated by the fact that the focus of this study is mainly on the consumption behavior of *C. saccharolyticus* on the different sugars.

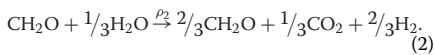
The model is constructed with a similar nomenclature and setup as in the anaerobic digestion model no 1 (ADM1) described by Batstone et al. [22] and was implemented in MATLAB R2015b (Mathworks, USA). The following biochemical degradation reactions are the basis for the model (Eqs. 1, 2).

Biomass formation from sugar [23]:



Reaction 1 is not balanced, since there were elements in the fermentation medium that were not included in the model, i.e., cysteine. The value of the yield factor Y_X is calculated from the data of the batch fermentations. It is assumed that nitrogen, sulfur, and phosphorus are in excess in the media and, therefore, are not included as separate entities in the mathematical model.

Sugar degradation to product formation by *C. saccharolyticus* in cmol:



Model inputs and initial conditions

The model requires a range of input variables. The lag time was determined by calculating the intersection point between the lag phase and the exponential phase when taking the natural logarithm of the biomass concentration over time, as illustrated by Swinnen et al. [24]. Since the lag phase is dependent on the culture status before the fermentation, which was not addressed in this study, it was excluded from the experimental data when the latter were compared to model data and for initial input values for the model. The start values of the unknown state variables are listed in Table 1. The constants used in the model are presented in Table 2.

Table 1 Start data of the unknown state variables in the model

| State variable | Description | Case 1 Glucose fermentation | Case 2 Xylose fermentation | Case 3 Sugar mix fermentation | Case 4 Wheat straw hydrolysate fermentation | Unit |
|----------------------|---|-----------------------------------|----------------------------------|-------------------------------------|--|--------|
| Glu | Glucose concentration | 0.40 | – | 0.28 | 0.26 | cmol/L |
| Xyl | Xylose concentration | – | 0.36 | 0.10 | 0.11 | cmol/L |
| Ara | Arabinose concentration | – | – | 0.012 | 0.014 | cmol/L |
| X (Biomass) | Biomass concentration | 0.0013 | 0.00071 | 0.0016 | 0.0058 | cmol/L |
| Ac | Acetate concentration | 0.0012 | 0 | 0.0039 | 0.021 | cmol/L |
| H _{2, aq} | H ₂ concentration (liquid phase) | 0 | 0 | 0 | 0 | M |
| CO _{2, aq} | CO ₂ concentration (liquid phase) | 0 | 0 | 0 | 0 | cmol/L |
| CO _{2, sol} | Concentration of all CO ₂ ionic species (HCO ₃ [–] and CO ₃ ^{2–}) | 0 | 0 | 0 | 0 | cmol/L |
| H _{2, g} | H ₂ concentration (gas phase) | 0 | 0 | 0 | 0 | M |
| CO _{2, g} | CO ₂ concentration (gas phase) | 0 | 0 | 0 | 0 | cmol/L |
| E ₂ | Enzyme concentration | – | – | 1e–7 | 1e–7 | cmol/L |

Table 2 Constants used in the model

| Constant | Value | Unit | Refs |
|---|--|-----------------|------|
| V _{liq} , liquid volume | 1 | L | |
| V _{gas} , gas volume | 0.05 | L | [15] |
| pH | 6.5 | – | |
| k _{AB} , acid base rate constant ^a | 1e4 | – | |
| T, temperature | 343.15 | K | |
| R, ideal gas constant | 0.08206 | L atm/K/mol | |
| KH _{H₂} , Henry's constant H ₂ | 7.4e–9 | mol/L/Pa | |
| KH _{CO₂} , Henry's constant CO ₂ | 2.7e–7 | mol/L/Pa | |
| k _{1, aCO₂} , volumetric mass transfer coefficient for carbon dioxide | 5.85·(N ₂ /6) ^{0.46} | h ^{–1} | [15] |
| pK ₁ , dissociation constant of reaction forming bicarbonate | 6.3 | – | |
| pK ₂ , dissociation constant of reaction forming carbonate | 10.25 | – | |
| β, enzyme decay rate | 0.05 | h ^{–1} | [18] |
| N ₂ , stripping rate | 6 | L/h | |

^a The acid–base reaction is considered to be in equilibrium at all times, which means that the reactions have infinitely fast reaction rates

Mass balances for biomass growth, substrate consumption, and product formation in the liquid phase

The stoichiometric relationships and mass balances of the reactants and products present in the model are displayed in Table 3. The model is supplemented with an enzyme, *E2*, and cybernetic variables v and u as in [18], where the former controls the activity of the enzyme and the latter is the fractional allocation of a critical resource for the synthesis of the enzyme. We hypothesize that initially, there is a first enzyme system present aiding the subsequent uptake of both hexose and pentose sugars, but with a preference for the pentoses (phase I). This transporter is only available as long as pentoses are present. After depletion of the pentoses, a second enzyme system, *E2*, is synthesized allowing for uptake of the remaining hexose sugars by a second transporter (phase II). For the sake of convenience, we simplify the enzyme system, consisting of multiple proteins, using the word enzyme and using this abstraction also in the kinetic model.

The mass balance for the biomass, X , is dependent on the rate of substrate consumption ρ , with Monod-type kinetics, and on the biomass decay rate, which is described with first-order kinetics, where r_{cd} (h^{-1}) is the cell death rate and Y_x (cmol/cmol) is the yield of biomass from total sugar (Table 3). A second glucose rate equation ($\rho_{Glu,2}$) is added to describe the diauxic-like growth appearance in the sugar mixture. The rate of the glucose consumption, when the pentose sugars are depleted, is dependent on enzyme *E2*. The rate of the enzyme synthesis, ρ_E , is based on Hill kinetics, as in [19], the decay rate of the enzyme is first-order kinetics, and the third

term, $-1 \cdot E2 \cdot \rho_{Glu,2}$, represents the dilution of the specific enzyme level as is described with kinetics similar to Hill, i.e., $E2^2$. The parameters k_m and $k_{m,2}$ (h^{-1}) are the maximal uptake rates in phase I and phase II, respectively, and $K_{s,glu}$, $K_{s,glu,2}$, $K_{s,xyl}$, $K_{s,ara}$, and $K_{s,E2}$ (cmol/L) are the affinity constants for the uptake of glucose, xylose, arabinose, and synthesis of enzyme *E2*, respectively. Finally, α is the enzyme synthesis rate (h^{-1}) and β is the enzyme decay rate (h^{-1}).

Acetate, hydrogen, and carbon dioxide are produced in the liquid phase. Y_{ac} (cmol/cmol), Y_{H_2} (mol/cmol) and Y_{CO_2} (cmol/cmol) represent the conversion yields of acetate, hydrogen, and carbon dioxide, respectively, from both hexose and pentose sugars. The conversion yields were fitted with experimental data from the batch fermentations. Y_X was determined by the slope of the curve: total sugar vs biomass; here, only phase I was considered. Y_{ac} and Y_{CO_2} were determined by first taking the slope of the curves, total sugar vs acetate, and total sugar vs carbon dioxide, and then, the actual yields were calculated according to the following equation:

$$Y_{Ac} = \frac{Y_{Ac, \text{ curve slope}}}{1 - Y_X} \quad (3)$$

When Y_{H_2} was calculated the same way as in Eq. 3, it gave a too high conversion yield. To obtain a more accurate yield, the effects of liquid-to-gas mass transport were considered and Y_{H_2} was instead determined as follows:

$$Y_{H_2} = \frac{H_{2,end} - H_{2,start}}{\text{Tot sugar}_{start} - \text{Tot sugar}_{end}} \quad (4)$$

Table 3 Description of the model setup including mass balances for the sugars (glucose, xylose, and arabinose), enzyme *E2*, biomass, acetate, aqueous hydrogen, and aqueous carbon dioxide

| Phase I | Phase II | Process ρ | | | | | | | |
|---|-------------------------------|----------------|-----|-----|--------------------------|---------------------------|----------------------------|---------------|---|
| | | Glu | Xyl | Ara | Ac | H _{2,aq} | CO _{2,aq} | E2 | X |
| Glu | | -1 | | | $(1 - Y_d) \cdot Y_{ac}$ | $(1 - Y_d) \cdot Y_{H_2}$ | $(1 - Y_d) \cdot Y_{CO_2}$ | Y_x | $\rho_{Glu} = k_m \cdot \frac{Glu}{Glu + K_{s,glu}} \cdot X \cdot V_1$ |
| | Glu | -1 | | | $(1 - Y_d) \cdot Y_{ac}$ | $(1 - Y_d) \cdot Y_{H_2}$ | $(1 - Y_d) \cdot Y_{CO_2}$ | $-1 \cdot E2$ | $\rho_{Glu,2} = k_{m,2} \cdot E2 \cdot \frac{Glu}{Glu + K_{s,glu,2}} \cdot X \cdot V_2$ |
| Xyl | | | -1 | | $(1 - Y_d) \cdot Y_{ac}$ | $(1 - Y_d) \cdot Y_{H_2}$ | $(1 - Y_d) \cdot Y_{CO_2}$ | Y_x | $\rho_{Xyl} = k_m \cdot \frac{Xyl}{Xyl + K_{s,xyl}} \cdot X \cdot V_1$ |
| Ara | | | | -1 | $(1 - Y_d) \cdot Y_{ac}$ | $(1 - Y_d) \cdot Y_{H_2}$ | $(1 - Y_d) \cdot Y_{CO_2}$ | Y_x | $\rho_{Ara} = k_m \cdot \frac{Ara}{Ara + K_{s,ara}} \cdot X \cdot V_1$ |
| | Enzyme, <i>E2</i> (synthesis) | | | | | | | 1 | $\rho_E = \alpha \cdot \frac{Glu^2}{Glu + K_{s,E2}} \cdot X \cdot u$ |
| | Enzyme, <i>E2</i> (decay) | | | | | | | -1 | $\rho_{dec,E2} = \beta \cdot E2$ |
| Biomass (decay) | Biomass (decay) | | | | | | | -1 | $\rho_{dec,X} = r_{cd} \cdot X$ |
| $V_1 = \frac{\rho_{Glu}}{\max(\rho_{Xyl}; \rho_{Glu,2})}$ $V_2 = \frac{\rho_{Glu,2}}{\max(\rho_{Xyl}; \rho_{Glu,2})}$ $u = \frac{\rho_{Glu,2}}{\text{sum}(\rho_{Xyl}; \rho_{Glu,2})}$ | | | | | | | | | |

At the bottom of the table, the cybernetic variables v and u are described

Acid–base reactions

The acid–base reaction considered in the model is that of carbon dioxide, bicarbonate, and carbonate formation. ρ_{AB,CO_2} in Table 4 describes the rate of formation of bicarbonate and carbonate.

$CO_{2,sol}$ is the sum of the ionic species, HCO_3^- and CO_3^{2-} , and Eq. 5 gives the differential equation for $CO_{2,sol}$:

$$\frac{dCO_{2,sol}}{dt} = \rho_{AB,CO_2}. \quad (5)$$

Liquid-to-gas mass transfer and mass balances for product formation

Hydrogen and carbon dioxide are produced in the liquid phase and then transferred to the gas phase via liquid-to-gas mass transport. ρ_{t,H_2} describes the mass transfer rate of hydrogen and ρ_{t,CO_2} is the mass transfer rate of carbon dioxide (Table 5). p_{gas,H_2} and p_{gas,CO_2} (in atm then converted to Pa) are the partial pressures of H_2 and CO_2 , respectively.

The expression for the mass balances describing the gaseous products can be described as in Eqs. 6, 7, where q_{gas} (L/h) is the total gas flow, and V_{liq} and V_{gas} (L) are the liquid and the gas volumes, respectively:

$$\frac{dH_{2,g}}{dt} = \frac{V_{liq}}{V_{gas}} \cdot \rho_{t,H_2} + \left(-H_{2,g} \cdot \frac{q_{gas}}{V_{gas}} \right) \quad (6)$$

$$\frac{dCO_{2,g}}{dt} = \frac{V_{liq}}{V_{gas}} \cdot \rho_{t,CO_2} + \left(-CO_{2,g} \cdot \frac{q_{gas}}{V_{gas}} \right). \quad (7)$$

Sensitivity analysis

A sensitivity analysis can identify parameters that have great effect on the model output. The sensitivity analysis

was done based on the OFAT approach, i.e., one-factor-at-at-time [25]. The chosen parameter was altered with a factor δ , as described in [26], to see the effect on the different state variable output result, as in the following equation:

$$\Gamma_{i,j} = \frac{(y_i(\theta_j) - y_i(\theta_j + \delta \cdot \theta_j)) / y_i(\theta_j)}{\delta}, \quad (8)$$

where $\Gamma_{i,j}$ is the sensitivity of state variable i with respect to model parameter j in each timepoint of the Matlab simulation. Furthermore, $y_i(\theta_j)$ is the value of state variable i in regard to parameter j and $y_i(\theta_j + \delta \cdot \theta_j)$ is the value of state variable i when parameter j has been altered with a factor δ . The parameters that were included in the sensitivity analysis were k_m , $k_{m,2}$, $K_{s,glu}$, $K_{s,glu,2}$, $K_{s,xyl}$, $K_{s,ara}$, $K_{s,E2}$, α , n , r_{cd} , and $k_{1,2,H_2}$ and the state variables that were considered were Glu, Xyl, Ara, Ac, X, and H_2 . The presented sensitivity data of one parameter in regards to a specific state variable were calculated as the average of $\Gamma_{i,j}$.

Model calibration

To get a better fit to the experimental data, the model parameters were calibrated using the knowledge that was revealed in the sensitivity analysis. This was done with the function *lsqcurvefit* in MATLAB which uses a least square method to find the right parameter value for a non-linear curve fitting by seeking to find coefficients x that solve the problem in the following equation:

$$\min_x \|F(x, xdata) - ydata\|_2^2 = \min_x \sum_i (F(x, xdata_i) - ydata_i)^2 \quad (9)$$

given the input data $xdata$ and the observed output $ydata$, where $xdata$ and $ydata$ are matrices or vectors and

Table 4 Kinetic rate equation for the acid–base reaction

| | Process↓ | | Rate ($\rho_{t,i}$, cmol/L/h) |
|------------------|--------------|-------------|--|
| | $CO_{2,sol}$ | $CO_{2,aq}$ | |
| CO_2 acid–base | 1 | –1 | $\rho_{AB,CO_2} = k_{AB} \cdot (CO_{2,aq} \cdot \left(\frac{10^{-pK_1}}{10^{-pH}} + 10^{-pK_1} \cdot \frac{10^{-pK_2}}{(10^{-pH})^2} \right)) - CO_{2,sol}$ |

Table 5 Liquid-to-gas mass transfer processes

| | Process↓ | | | | Rate ($\rho_{t,i}$, cmol/L/h) |
|-----------------|-----------|------------|------------|-------------|---|
| | $H_{2,g}$ | $CO_{2,g}$ | $H_{2,aq}$ | $CO_{2,aq}$ | |
| H_2 transfer | 1 | | –1 | | $\rho_{t,H_2} = k_L a_{H_2} \cdot (H_{2,aq} - p_{gas,H_2} \cdot KH_{H_2})$ |
| CO_2 transfer | | 1 | | –1 | $\rho_{t,CO_2} = k_L a_{CO_2} \cdot (CO_{2,aq} - p_{gas,CO_2} \cdot KH_{CO_2})$ |

$F(x, xdata)$ is a matrix-valued or vector-valued function of the same size as $ydata$.

The *lsqcurvefit* function starts at $x0$ and finds coefficient, i.e., parameter x , to best fit the non-linear function $fun(x, xdata)$ to the data $ydata$:

$$x = lsqcurvefit(fun, x0, xdata, ydata). \quad (10)$$

The uncertainties of the calibrated parameters were assessed by calculating the confidence interval. This was done with the function *nlparci* in MATLAB which computes the 95% confidence intervals for the non-linear least square parameters estimated.

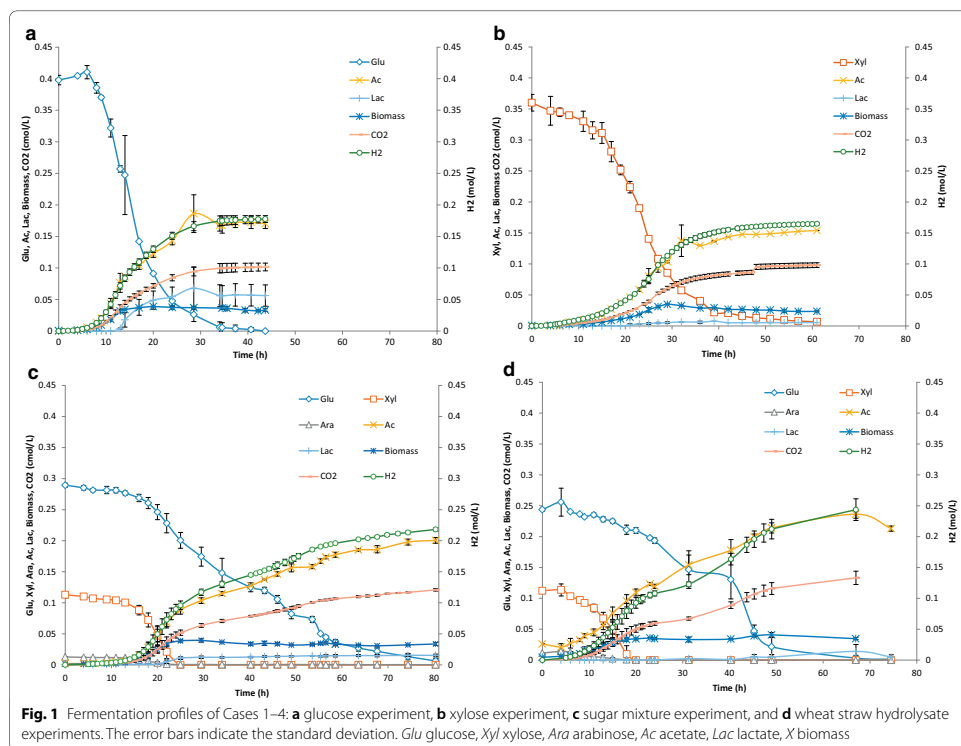
Results and discussion

Growth profiles on the various sugars

The growth profiles of the single sugar experiments (glucose; Case 1 and xylose; Case 2), sugar mixture experiments (Case 3) and wheat straw hydrolysate experiments (Case 4) are presented in Fig. 1a–d. Glucose is consumed approx. two times faster when used as sole substrate

(Case 1) than in the sugar mixtures (Cases 3 and 4). Xylose, on the other hand, is consumed approx. two times slower when used as sole substrate and is completely consumed after approx. 60 h compared to around 20 h when co-fermented with other sugars (Cases 3 and 4; Fig. 1c, d). The highest production rate of acetate and hydrogen occurred around 20 h both in the sugar mixture and in the wheat straw hydrolysate fermentations. Lactate was formed just after 20 (Case 3) and 30 h (Case 4) reaching in total 0.015 and 0.014 cmol/L, respectively.

The calculated lag phases differed for each experiment. The lag phases of the sugar mixture experiments ranged from 9 to 11 h, whereas the lag phase of the wheat straw hydrolysate experiment was 4 h. This observation could be correlated to the richer nutrient content of wheat straw than the defined sugar mixture medium. A similar observation was found by Pawar et al. [27]. The lag phase with glucose alone was 4 h, but there was no lag phase with xylose alone. It is worth noticing though that it took more effort to initiate



growth on xylose than on glucose as two out of four replicates failed, where none of the other experiments (Cases 1, 3, and 4) failed. This is due to that precautions are needed to start a culture on xylose in the absence of yeast extract, such as no sparging for several hours.

The profiles of the mixed sugars indicate a biphasic growth, where the uptake of glucose decreased after xylose was depleted, but then increased again (Fig. 1c, d). The two-phased sugar uptake was more pronounced in the wheat straw hydrolysate fermentations. The behavior can be further illustrated by the hydrogen productivity and CO₂ productivity (Fig. 2a, b). This observation has, to our knowledge, not been reported for *Caldicellulosiruptor* previously, although the transcriptomics of multiple sugar uptake have been extensively studied [13, 14]. One possible reason for this could be that many multi-sugar experimental studies on this genus have been performed on a yeast extract-supplemented medium [3]. Because yeast extract itself partly supports growth [20], it possibly masks biphasic behavior. Moreover, the initial ratio of pentose/hexose

sugars was higher in those studies [14] than in the WSH used in this study. Thus, after xylose was consumed, the culture adapted to a hexose-only medium, which initiated a second phase of growth.

The emerging pattern resembles a diauxic growth behavior, which was first described by Monod [17], and is characterized by two growth phases often separated with a lag period. This normally occurs in the presence of two carbon sources, where the preferred one is consumed first by the microorganism followed by the second after a lag period [28–30]. However, in the case of *C. saccharolyticus*, both pentose and hexose sugars are consumed simultaneously, albeit with a slight preference for the former. When the pentose sugars are depleted hexose consumption continues, but in Case 4 that happened with an increased rate (Table 8).

To quantify this behavior and investigate whether the theory of diauxic growth could be used to explain the observations, a kinetic model was developed consisting of two phases. In the phase I, glucose was consumed simultaneously with xylose and arabinose. Van de Werken et al. [13] concluded that growth on glucose and xylose mixtures as well as growth on the individual sugars all trigger transcription of the genes encoding a xylose-specific ABC transport system. This supports our hypothesis that glucose, xylose, and arabinose were initially transported by the same uptake system. However, when xylose was depleted, phase II starts with a new uptake system being expressed that had a higher affinity for glucose, transporting glucose at an altered rate. It is relevant to observe, however, that diauxic growth behavior is generally considered to be related to PTS systems [31–33]. However, according to current knowledge, *C. saccharolyticus* only possesses ABC transport systems [13, 14]. Still, it has been described that other transport systems can generate this diauxic growth profile. For example, in *Streptomyces coelicolor* and related species, the genes involved in carbon catabolite repression are PTS independent, and instead, glucose kinase is the main controlling enzyme [33].

Determination of conversion yields

The calculated conversion yields from the batch experiments differ from the stoichiometric yields (Table 6). To begin with, the single sugar fermentations the calculated yields are lower than the corresponding stoichiometric yields. This is in contrast to the yields calculated for the sugar mixture experiments, except for Y_{ac} that was slightly lower. The lower yield for acetate could be due to that part of the acetate, or rather acetyl-CoA, which is used as a building block for cell mass production [34].

The carbon balances attained in the model were 90 and 102% with start data from the sugar mixture experiments

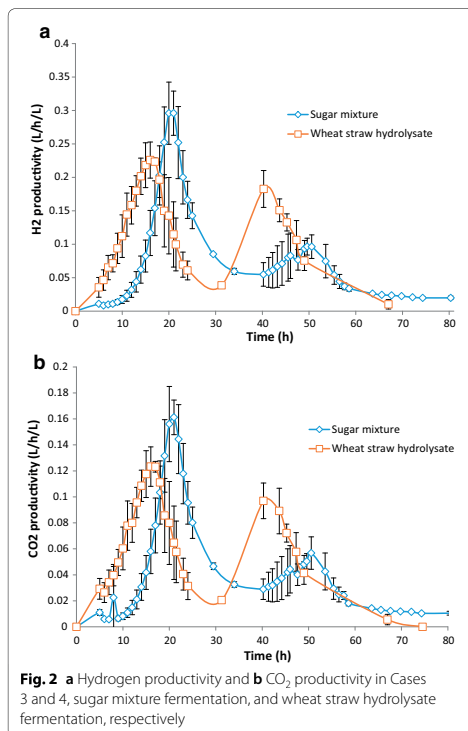


Table 6 Calculated carbon and redox balances plus the calculated yields of the four different experiments and their corresponding stoichiometric yields

| | Y_x (cmol/cmol) | Y_{ac} (cmol/cmol) | Y_{H_2} (mol/cmol) | Y_{CO_2} (cmol/cmol) | Carbon balance (%) | Redox balance (%) |
|--|-------------------------------------|-------------------------------------|--------------------------------------|--|--------------------|-------------------|
| | Yield, biomass formation from sugar | Yield, acetate formation from sugar | Yield, hydrogen formation from sugar | Yield, carbon dioxide formation from sugar | | |
| Glucose experiments (Case 1) | 0.20 | 0.51 | 0.45 | 0.30 | 82 | 87 |
| Xylose experiments (Case 2) | 0.12 | 0.50 | 0.47 | 0.31 | 80 | 81 |
| Sugar mix experiments (Case 3) | 0.21 | 0.62 | 0.53 | 0.38 | 90 | 100 |
| Wheat straw hydrolysate experiments (Case 4) | 0.18 | 0.68 | 0.67 | 0.44 | 107 | 90 |
| Stoichiometrically | – | 0.67 | 0.67 | 0.33 | – | – |

Table 7 Most sensitive parameters, i.e., sensitivity value > 1%, listed in descending order for each state variable that was evaluated

| State variable | Case 3 Sugar mixture | Case 4 Wheat straw hydrolysate |
|----------------|--|--|
| Glu | $k_{m,2}, a, k_{mv}, r_{cd}, k_{L,A_{H_2}}, K_{s,glu,2}$ | $k_{L,A_{H_2}}, a, k_{m,2}, r_{cd}, k_{mv}, K_{s,glu,2}$ |
| Xyl | $k_{L,A_{H_2}}, k_{mv}, K_{s,ara}, K_{s,xyl}$ | $k_{L,A_{H_2}}, k_{mv}, K_{s,xyl}, K_{s,ara}, K_{s,E2}$ |
| Ara | $K_{s,ara}, k_{mv}, k_{L,A_{H_2}}$ | $K_{s,ara}$ |
| Ac | – | – |
| X | – | – |
| H ₂ | – | $k_{m,2}, a$ |

and the WSH experiments, respectively, which are equal or close to the values calculated from the experimental data, 90 and 107%, respectively, Table 6. The higher values in the carbon balance, i.e., > 100%, for the WSH fermentations, could be due to that other carbon sources may be present, such as oligosaccharides, that are also converted to products giving a higher carbon and electron output.

Sensitivity analysis

Dynamic simulations using benchmark parameter values [15] showed discrepancies between the experimental results and the model predictions. To further improve the dynamic simulations, a sensitivity analysis was conducted to determine the most important parameters. This was done with start values both from the sugar mixture fermentations as well as from the wheat straw hydrolysate fermentations. The change, δ , in the parameter value was set to 1% as in [35].

The sensitivity analysis allowed ranking of the parameters, which was useful for the model calibration. The most sensitive parameters, i.e., with a sensitivity value of > 1%, in regard to each of the state variables are listed

in Table 7. The state variables that were affected the most by a change in parameter value were Glu and Xyl. The sensitivities of the other parameters for the different state variables were less than 1%.

Parameter calibration

The sensitivity analysis served as a basis for the parameter calibration. The model was calibrated with data from the four different batch experiments, Cases 1–4. Start values of the state variables were taken from the experimental data (Table 1), and initial parameter values, i.e., benchmark values, were taken from the literature [15] or guesstimated, e.g., by manually fitting the curves of the data points. The calibrated parameters together with a confidence interval of 95% are given in Table 8. Some of the parameters were graphically calibrated and, therefore, are without a confidence interval. The simulations with start data from the single glucose and xylose fermentations were carried out without the diauxic-like growth additions; thus, only phase I was applied.

The k_m values for Cases 3 and 4 describe the maximal simultaneous uptake rates of glucose, xylose, and arabinose (Table 8), and they are modeled with the same value for all the sugars in phase I. However, the K_s values for glucose in phase I, $K_{s,glu,1}$, are higher than the K_s values for xylose, $K_{s,xyl,1}$, which indicates a lower affinity for glucose in phase I, since xylose is present and preferred. Moreover, $K_{s,glu}$ in Case 4 is 18 times higher compared to $K_{s,glu,2}$ and compared to $K_{s,glu}$ in Case 3. One explanation is the greater affinity for xylose in phase I and another possible explanation is that $K_{s,glu}$ in Case 4 also includes an inhibition term due to the characteristics of the wheat straw hydrolysate media, e.g., Eq. 11:

$$K_{s,glu} = K_{s,glu,real} \cdot I, \quad (11)$$

Table 8 Parameters calibrated to experimental data

| Parameter | Benchmark value derived from [15] | Case 1 Glucose simulation | Case 2 Xylose simulation | Case 3 Sugar mixture simulation | Case 4 Wheat straw hydrolysate simulation |
|--|-----------------------------------|------------------------------|-----------------------------|------------------------------------|--|
| $k_{m,r}$, maximal uptake rate (h^{-1}) | 0.35 | – | 1.58 (± 0.042) | 0.54 (± 0.012) | 0.44 (± 0.023) |
| $k_{m,2}$, maximal uptake rate when xylose = 0 (h^{-1}) | 0.35 | 2.4 (± 0.15) | – | 0.54 (± 0.018) | 1.26 (± 0.11) |
| $K_{s,glu}$, affinity constant, glucose (cmol/L) | 0.00029 | 0.01 ^a | – | 0.01 ^a | 0.18 (± 0.043) ^b |
| $K_{s,glu,2}$, affinity constant 2, glucose (cmol/L) | – | – | – | 0.01 ^a | 0.01 ^a |
| $K_{s,xy}$, affinity constant, xylose (cmol/L) | – | – | 0.0002 ^a | 0.0002 ^a | 0.0002 ^a |
| $K_{s,ara}$, affinity constant, arabinose (cmol/L) | – | – | – | 0.026 (± 0.004) | 0.034 (± 0.0077) |
| $K_{s,E2}$, affinity constant enzyme, E2 (cmol/L) | – | – | – | 0.001 ^a | 0.001 ^a |
| a , enzyme synthesis rate (h^{-1}) | – | – | – | 0.6 ^a | 0.64 (± 0.085) |
| n , Hill coefficient | – | – | – | 2 ^a | 2 ^a |
| r_{cd} , cell death rate (h^{-1}) | 0.014 | 0.0027 ^a | 0.0027 ^a | 0.027 ^a | 0.027 (± 0.0039) |
| $k_L a_{H_2}$, volumetric mass transfer coefficient for hydrogen (h^{-1}) | 0.26 | 0.44 ^a | 0.44 ^a | 0.44 (± 0.085) | 0.44 ^a |
| Y_{H_2} , yield, hydrogen formation from sugar | – | n.c. | n.c. | 0.58 | n.c. |

Confidence interval 95% (CI, 95%) is given for those parameters which have been fitted numerically

n.c. not calibrated, but the values calculated from the experimental data were used (Table 6)

^a Graphically calibrated

^b This value possibly also includes an inhibition factor I

where I represents a competitive inhibition, Eq. 12:

$$I = 1 + \frac{S_I}{K_I} \tag{12}$$

with S_I the concentration of the inhibitor and K_I the inhibition parameter. This is possibly due to unknown inhibiting compounds in the wheat straw hydrolysate or other factors that inhibit glucose uptake in phase I in Case 4. The reason behind the competitive inhibition has not been identified, but we hypothesize the presence of oligo-saccharides that might be preferably taken up instead of glucose. However, these sugars were not quantified in the HPLC analysis of WSH.

The $k_{m,2}$ value for Case 4 is 50% lower than the corresponding value for the glucose uptake rate in Case 1. One explanation for this is that the enzymes involved in the sugar uptake in Case 4 take some time to be synthesized making glucose consumption slower in the WSH compared to the single glucose fermentation. Again, the presence of inhibiting compounds or competitive oligo-saccharides could further slow down the glucose uptake rate.

Furthermore, the results show that on single sugars and mineral medium, glucose uptake is approximately

Table 9 Maximal specific growth rates, μ_{max} , calculated from $k_{m,r}$, $k_{m,2}$, and Y_x values

| Maximal specific growth rate (μ_{max} , h^{-1}) | Phase I | Phase II |
|---|---------|----------|
| Glucose (Case 1) | 0.22 | – |
| Xylose (Case 2) | 0.13 | – |
| Sugar mixture (Case 3) | 0.33 | 0.11 |
| Wheat straw hydrolysate (Case 4) | 0.24 | 0.23 |

35% faster than xylose uptake (Table 8). Moreover, growth of *C. saccharolyticus* on glucose is approx. 40% faster than on xylose (Table 9). This outcome contradicts the previous results on these two sugars in media supplemented with yeast extract (YE), where growth is faster on xylose than on glucose [13, 14]. An explanation for this observation could be that *C. saccharolyticus* needs other sugars (present in YE) to grow optimal on xylose. Indeed, when both sugars are present the growth on xylose is stimulated by the co-uptake of glucose. The stoichiometric relationship of glucose-to-xylose uptake rate $\rho(\text{Glucose}):\rho(\text{Xylose})$ was affected by the media used and is approximately 0.7 and 0.3 in phase I for growth on defined sugar mixture and wheat

straw medium, respectively (data used from Fig. 1). Until xylose is depleted, the total glucose, xylose, and arabinose conversion rates, i.e., $0.54\text{--}3\text{ h}^{-1}$, are similar to that of xylose conversion in the absence of glucose, i.e., 1.58 h^{-1} . This observation is supported by other studies with *C. saccharolyticus* using different sugar mixtures both with and without YE, e.g. in Willquist [36]. Xylose uptake increases if a small concentration of glucose is present or if either the fermentor is sparged with CO_2 instead of N_2 gas or closed, to allow buildup of HCO_3^- in the reactor.

Model prediction

Comparison between the model and experimental results for the combined sugars is depicted in Table 10, and Figs. 3 and 4. The results show that a diauxic-like behavior model simulates well the experimental data of *C. saccharolyticus* when grown on mixtures of pentose and hexose sugars. Without the addition of a second enzyme equation as well as cybernetic variables controlling the upregulation of the enzyme, the experimental data could not be simulated.

Table 10 shows the fitting between the experimental data and the model simulation displaying the regression analysis values. It is clear that the model is well able to describe the consumption of the different sugars as well as biomass growth, acetate formation, and accumulation of hydrogen in Cases 3 and 4. The model, without the diauxic-like additions, was better at describing the individual xylose fermentations (Case 2), rather than the individual glucose fermentations (Case 1) when it comes to biomass growth and hydrogen production (Table 10).

The model only predicts a small second peak in hydrogen productivity compared to the data of the defined sugar mixture fermentations (Fig. 3g). However, the model succeeds in describing the diauxic-like behavior of the hydrogen productivity profile in the wheat straw hydrolysate fermentations (Fig. 4g). The uptake of the three sugars as well as the formation of acetate is well described by the model, both for Cases 3 and 4 (Figs. 3a–d, 4a–d).

According to the simulation, the enzyme (used to describe the diauxic behavior) concentration is very low, close to zero, in the beginning, and when phase I ends, the enzyme synthesis starts and the concentration increases up to a peak, where it begins decreasing just before $t=60\text{ h}$ in Case 3 and somewhat earlier in Case 4 (Figs. 3f, 4f). The enzyme synthesis is dependent on the biomass concentration, which is why it follows the behavior of the latter. The two biomass growth phases are clearly displayed in Case 4 and expressed by the model (Fig. 4e), where a first growth phase takes place between 0 and 20 h and a second growth phase between 20 and 45 h. The phenomenon with two growth phases is characteristic for diauxic growth behavior as described in various literatures on the topic [18, 28, 37].

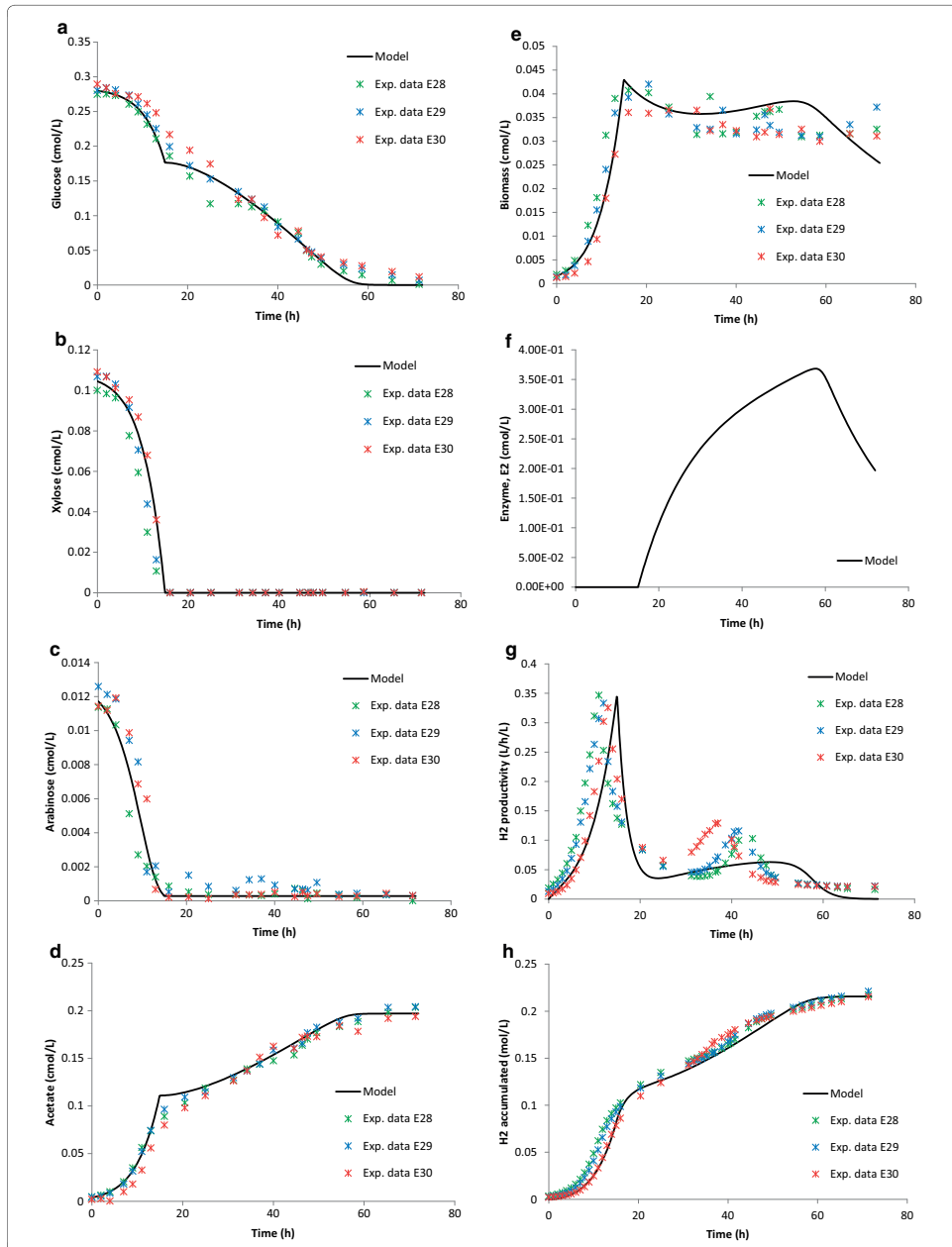
The hydrogen productivity profile, both in Cases 3 and 4, is a bit delayed in the model (Figs. 3g, 4g). This could be due to a slight underestimation of the $k_{L,A_{\text{H}_2}}$ value. The benchmark $k_{L,A_{\text{H}_2}}$ value used, from Ljunggren et al. [15], was later on calibrated against experimental data resulting in a higher value (Table 8). Still, the mass transfer seems to be less efficient in the model not being able to fully describe the experimental data.

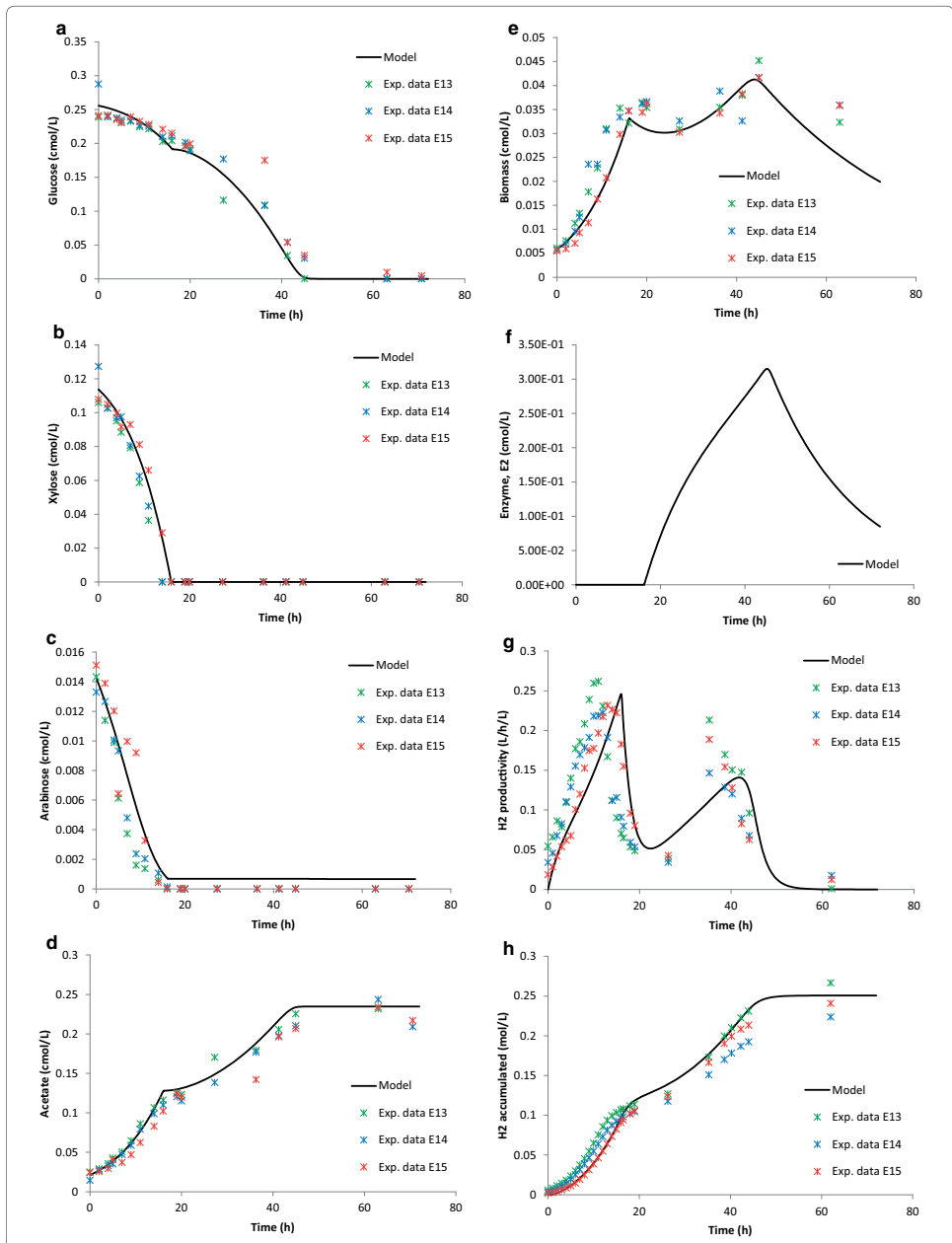
Table 10 R^2 values to describe the fit between experimental data and model simulation

| State variable | Glucose (Case 1) | Xylose (Case 2) | Sugar mixture (Case 3) | Wheat straw hydrolysate (Case 4) |
|--------------------------|------------------|-----------------|------------------------|----------------------------------|
| Glu | 0.96 | – | 0.99 | 0.97 |
| Xyl | – | 0.98 | 0.99 | 0.99 |
| Ara | – | – | 0.99 | 0.95 |
| X | 0.46 | 0.86 | 0.92 | 0.90 |
| Ac | 0.91 | 0.99 | 0.99 | 0.99 |
| H_2 accumulated | 0.74 | 0.99 | 0.99 | 0.98 |

(See figure on next page.)

Fig. 3 Sugar mixture experimental data and model simulation. **a** Glucose (cmol/L) data and model; **b** xylose data and model (cmol/L); **c** arabinose (cmol/L) data and model; **d** acetate (cmol/L) data and model; **e** biomass (cmol/L) data and model; **f** enzyme, E_2 (cmol/L) data and model; **g** hydrogen productivity (L/h/L) data and model; and **h** hydrogen accumulated (mol/L) data and model. *Exp. data E28* experimental data E28, *Exp. data E29* experimental data E29, and *Exp. data E30* experimental data E30





(See figure on previous page.)

Fig. 4 Wheat straw hydrolysate experimental data and model simulation. **a** Glucose (cmol/L) data and model; **b** xylose data and model (cmol/L); **c** arabinose (cmol/L) data and model; **d** acetate (cmol/L) data and model; **e** biomass (cmol/L) data and model; **f** enzyme, *E2* (cmol/L) data and model; **g** hydrogen productivity (L/h/L) data and model; and **h** hydrogen accumulated (mol/L) data and model. *Exp. data E13* experimental data E13, *Exp. data E14* experimental data E14 and *Exp. data E15* experimental data E15

Conclusions

The outcome of this study revealed that in batch mode, *C. saccharolyticus* ferments (un)defined sugar mixtures via different growth phases in a diauxic-like manner. This behavior could be successfully simulated with a kinetic growth model with substrate-based Monod-type kinetics and enzyme synthesis using Hill kinetics together with cybernetic variables to control the upregulation of the enzyme. The model was able to predict the behavior of growth on sugar mixtures both in a defined medium and in wheat straw hydrolysate medium. The model supported the following sequence: xylose is the preferred substrate, but glucose is taken up simultaneously, possibly with the same transporter. After xylose is depleted, glucose is further taken up with a newly induced transporter system, leading to a second hydrogen productivity peak. We further conjecture that this diauxic-like pattern might appear in defined media not containing complex nutrient mixtures, such as yeast extract, as the latter might reduce the edge of the transition point from dominant xylose uptake to dominant glucose uptake by *C. saccharolyticus*. Future studies should aim at investigating how the various uptake mechanisms in *C. saccharolyticus* act and contribute to the phenomena described in this study. In addition, a further developed model, verifying the values of several kinetic parameters, including separate maximal uptake rates for the different sugars in the sugar mixture as well as inhibition functions, would improve the applicability of this model for industrial processes.

Authors' contributions

JB: data analysis, calculations, model development, and manuscript writing. EB: planning and execution of the fermentation experiments, HPLC and GC analyses, and manuscript writing. EvN: supervision of fermentation, analysis, and manuscript writing. KW: supervision of modeling, analysis and fermentation, and manuscript writing. All authors contributed to revision of the manuscript and approved the text, figures, and tables for submission. All authors read and approved the final manuscript.

Author details

¹ Department of Energy and Circular Economy, RISE Research Institutes of Sweden, PO Box 857, 501 15 Borås, Sweden. ² Division of Applied Microbiology, Lund University, PO Box 124, 221 00 Lund, Sweden.

Acknowledgements

The authors acknowledge the Swedish Energy Agency for the financial support of this work under "Metanova" Project No. 31090-2.

Competing interests

The authors declare that they have no competing interests.

Availability of data and materials

All data generated or analyzed during this study are included in this article. If additional information is needed, please contact the corresponding author.

Consent for publication

Not applicable.

Ethics approval and consent to participate

Not applicable.

Funding

The study was funded by the Swedish Energy Agency whom did not participate in the execution of the study or in the manuscript writing.

Publisher's Note

Springer Nature remains neutral with regard to jurisdictional claims in published maps and institutional affiliations.

Received: 24 January 2018 Accepted: 12 June 2018

Published online: 22 June 2018

References

- International Energy Agency. Renewables information 2017: overview. <http://www.iea.org/publications/freepublications/publication/RenewablesInformation2017Overview.pdf>. Accessed 10 Jan 2018.
- United Nations. Adoption of the Paris Agreement. 2015. <http://unfccc.int/resource/docs/2015/cop21/eng/09r01.pdf>. Accessed 31 May 2017.
- Pawar SS, van Niel EWJ. Thermophilic biohydrogen production: how far are we? *Appl Microbiol Biotechnol*. 2013;97(18):7999–8009. <https://doi.org/10.1007/s00253-013-5141-1>.
- Press RJ, Santhanam KSV, Miri MJ, Bailey AV, Takacs GA. Introduction to hydrogen technology. 1st ed. Hoboken: Wiley; 2008.
- van Niel EWJ. Biological processes for hydrogen production. In: Hatti-Kaul R, Mamo G, Mattiasson B, editors. *Anaerobes in biotechnology*. Berlin: Springer International Publishing; 2016. p. 155–93.
- Das D, Veziroglu TN. Advances in biological hydrogen production processes. *Int J Hydrogen Energy*. 2008;33(21):6046–57. <https://doi.org/10.1016/j.ijhydene.2008.07.098>.
- Claassen PAM, van Lier JB, Contreras AML, van Niel EWJ, Sijtsma L, Stams AJM, de Vries SS, Weusthuis RA. Utilisation of biomass for the supply of energy carriers. *Appl Microbiol Biotechnol*. 1999;52(6):741–55. <https://doi.org/10.1007/s002530051586>.
- Hamelinck CN, van Hooijdonk G, Faaij APC. Ethanol from lignocellulosic biomass: techno-economic performance in short-, middle- and long-term. *Biomass Bioenergy*. 2005;28(4):384–410. <https://doi.org/10.1016/j.biombioe.2004.09.002>.
- Kengen SWM, Goorissen HP, Verhaart M, Stams AJM, van Niel EWJ, Claassen PAM. Biological hydrogen production by anaerobic microorganisms. In: Soetaert W, Vandamme EJ, editors. *Biofuels*. Chichester: Wiley; 2009. p. 197–221.
- Willquist K, Zeidan AA, van Niel EWJ. Physiological characteristics of the extreme thermophile *Caldicellulosiruptor saccharolyticus*: an efficient hydrogen cell factory. *Microb Cell Fact*. 2010;9:89. <https://doi.org/10.1186/1475-2859-9-89>.
- Thauer RK, Jungermann K, Decker K. Energy conservation in chemotrophic anaerobic bacteria. *Bacteriol Rev*. 1977;41(1):100–80.
- Rainey FA, Donnison AM, Janssen PH, Saul D, Rodrigo A, Bergquist PL, et al. Description of *Caldicellulosiruptor saccharolyticus* gen. nov.,

- sp. nov. an obligately anaerobic, extremely thermophilic, cellulolytic bacterium. *FEMS Microbiol Lett.* 1994;120(3):263–6. <https://doi.org/10.1111/j.1574-6968.1994.tb07043.x>.
13. van de Werken HJG, Verhaart MRA, VanFossen AL, Willquist K, Lewis DL, Nichols JD, Goorissen HP, Mongodin EF, Nelson KE, van Niel EWJ, et al. Hydrogenomics of the extremely thermophilic bacterium *Caldicellulosiruptor saccharolyticus*. *Appl Environ Microbiol.* 2008;74(21):6720–9. <https://doi.org/10.1128/AEM.00968-08>.
 14. VanFossen AL, Verhaart MRA, Kengen SMW, Kelly RM. Carbohydrate utilization patterns for the extremely thermophilic bacterium *Caldicellulosiruptor saccharolyticus* reveal broad growth substrate preferences. *Appl Environ Microbiol.* 2009;75(24):7718–24. <https://doi.org/10.1128/AEM.01959-09>.
 15. Ljunggren M, Willquist K, Zacchi G, van Niel EW. A kinetic model for quantitative evaluation of the effect of hydrogen and osmolarity on hydrogen production by *Caldicellulosiruptor saccharolyticus*. *Biotechnol Biofuels.* 2011;4:31. <https://doi.org/10.1186/1754-6834-4-31>.
 16. Auria R, Boileau C, Davidson S, Casalot L, Christen P, Liebgott PP, Combet-Blanc Y. Hydrogen production by the hyperthermophilic bacterium *Thermotoga maritima* Part II: modeling and experimental approaches for hydrogen production. *Biotechnol Biofuels.* 2016;9:268. <https://doi.org/10.1186/s13068-016-0681-0>.
 17. Monod J. Recherches sur la croissance des cultures bactériennes. Ph.D. thesis, Université de Paris, Hermann, Paris. 1941.
 18. Kompala DS, Ramkrishna D, Jansen NB, Tsao GT. Investigation of bacterial growth on mixed substrates: experimental evaluation of cybernetic models. *Biotechnol Bioeng.* 1986;28:1044–55. <https://doi.org/10.1002/bit.260280715>.
 19. Boianelli A, Bidossi A, Gualdi L, Mulas L, Mocenni C, Pozzi G, Vicino A, Oggioni MR. A non-linear deterministic model for regulation of diauxic lag on cellobiose by the pneumococcal multidomain transcriptional regulator CeiR. *PLoS ONE.* 2012;7:10. <https://doi.org/10.1371/journal.pone.0047393>.
 20. Willquist K, van Niel EWJ. Growth and hydrogen production characteristics of *Caldicellulosiruptor saccharolyticus* on chemically defined minimal media. *Int J Hydrogen Energy.* 2012;37(6):4925–9. <https://doi.org/10.1016/j.ijhydene.2011.12.055>.
 21. Zeidan AA, van Niel EWJ. A quantitative analysis of hydrogen production efficiency of the extreme thermophile *Caldicellulosiruptor owensensis* OL^T. *Int J Hydrogen Energy.* 2010;35(3):1128–37. <https://doi.org/10.1016/j.ijhydene.2009.11.082>.
 22. Batstone DJ, Keller J, Angelidaki I, Kalyuzhnyi SV, Pavlostathis SG, Rozzi A, Sanders WTM, Siegrist H, Vavilin VA. Anaerobic Digestion Model No. 1 IWA task group for mathematical modelling of anaerobic digestion processes. London: IWA Publishing; 2002.
 23. de Vrije T, Mars AE, Budde MA, Lai MH, Dijkema C, de Waard P, Claassen PAM. Glycolytic pathway and hydrogen yield studies of the extreme thermophile *Caldicellulosiruptor saccharolyticus*. *Appl Microbiol Biotechnol.* 2007;74(6):1358–67.
 24. Swinnen IAM, Bernaerts K, Dens EJJ, Geeraerd AH, Van Impe JF. Predictive modelling of the microbial lag phase: a review. *Int J Food Microbiol.* 2004;94(2):137–59. <https://doi.org/10.1016/j.ijfoodmicro.2004.01.006>.
 25. Hamby DM. A review of techniques for parameter sensitivity analysis of environmental models. *Environ Monit Assess.* 1994;32(2):135–54. <https://doi.org/10.1007/bf00547132>.
 26. Barrera EL, Spanjers H, Solon K, Amerlinck Y, Nopens I, Dewulf J. Modeling the anaerobic digestion of cane-molasses vinasse: extension of the Anaerobic Digestion Model No. 1 (ADM1) with sulfate reduction for a very high strength and sulfate rich wastewater. *Water Res.* 2015;71:42–54. <https://doi.org/10.1016/j.watres.2014.12.026>.
 27. Pawar SS, Nkemka VN, Zeidan AA, Murto M, van Niel EWJ. Biohydrogen production from wheat straw hydrolysate using *Caldicellulosiruptor saccharolyticus* followed by biogas production in a two-step uncoupled process. *Int J Hydrogen Energy.* 2013;38(22):9121–30. <https://doi.org/10.1016/j.ijhydene.2013.05.075>.
 28. Roop JJ, Chang KC, Brem RB. Polygenic evolution of a sugar specialization trade-off in yeast. *Nature.* 2016;530:336–49. <https://doi.org/10.1038/nature16938>.
 29. Wang J, Atolia E, Hua B, Savir Y, Escalante-Chong R, Springer M. Natural variation in preparation for nutrient depletion reveals a cost-benefit tradeoff. *PLoS Biol.* 2015;13:1. <https://doi.org/10.1371/journal.pbio.1002041>.
 30. Kremling A, Geiselmann J, Ropers D, de Jong H. Understanding carbon catabolite repression in *Escherichia coli* using quantitative models. *Trends Microbiol.* 2015;23(2):99–109. <https://doi.org/10.1016/j.tim.2014.11.002>.
 31. Deutscher J. The mechanisms of carbon catabolite repression in bacteria. *Curr Opin Microbiol.* 2008;11(2):87–93. <https://doi.org/10.1016/j.mib.2008.02.007>.
 32. Chu DF. In silico evolution of diauxic growth. *BMC Evol Biol.* 2015;15:211. <https://doi.org/10.1186/s12862-015-0492-0>.
 33. Görke B, Stülke J. Carbon catabolite repression in bacteria: many ways to make the most out of nutrients. *Nat Rev Microbiol.* 2008;6(8):613–24. <https://doi.org/10.1038/nrmicro1932>.
 34. Shen N, Zhang F, Song XN, Wang YS, Zeng RJ. Why is the ratio of H₂/acetate over 2 in glucose fermentation by *Caldicellulosiruptor saccharolyticus*? *Int J Hydrogen Energy.* 2013;38(26):11241–7. <https://doi.org/10.1016/j.ijhydene.2013.06.091>.
 35. Tartakovsky B, Mu SJ, Zeng Y, Lou SJ, Guiot SR, Wu P. Anaerobic Digestion Model No. 1-based distributed parameter model of an anaerobic reactor: II. Model validation. *Bioresour Technol.* 2008;99(9):3676–84. <https://doi.org/10.1016/j.biortech.2007.07.061>.
 36. Willquist K. Physiology of *Caldicellulosiruptor saccharolyticus*: a hydrogen cell factory. Ph.D. thesis, Lund University, Sweden. 2010.
 37. Song HS, Liu C. Dynamic metabolic modeling of denitrifying bacterial growth: the cybernetic approach. *Ind Eng Chem Res.* 2015;54(42):10221–7. <https://doi.org/10.1021/acs.iecr.5b01615>.

Ready to submit your research? Choose BMC and benefit from:

- fast, convenient online submission
- thorough peer review by experienced researchers in your field
- rapid publication on acceptance
- support for research data, including large and complex data types
- gold Open Access which fosters wider collaboration and increased citations
- maximum visibility for your research: over 100M website views per year

At BMC, research is always in progress.

Learn more biomedcentral.com/submissions



Paper II



Characterization and development of osmotolerant *Caldicellulosiruptor* strains targeting enhanced hydrogen production from lignocellulosic hydrolysates

Eoin Byrne¹, Johanna Björkmalm^{1,2}, James P. Bostick¹, Krishnan Sreenivas¹, Karin Willquist², Ed W.J. van Niel¹

¹ Division of Applied Microbiology, Lund University, PO Box 124, 221 00 Lund, Sweden

² RISE Research Institutes of Sweden, Ideon Science Park, Building Beta 2, Scheelevägen 17, 223 70 Lund, Sweden

Keywords

Osmolarity, *Caldicellulosiruptor*, biohydrogen, kinetic model, adaptive laboratory evolution

Abstract

Background

The members of the genus *Caldicellulosiruptor* have the potential for future integration into a biorefinery system due to their capacity to generate hydrogen close to the theoretical limit of 4 mol H₂/mol hexose, use a wide range of sugars and can grow on numerous lignocellulose hydrolysates. However, members of this genus are unable to survive in high osmolarity conditions, limiting their ability to grow on more concentrated hydrolysates, thereby hindering their industrial applicability. In this study five members of this genus, *C. owensensis*, *C. kronotskyensis*, *C. bescii*, *C. acetigenus* and *C. kristjanssonii*, were developed to tolerate higher osmolarities through an adaptive laboratory evolution process. The developed strain *C. owensensis* CO80 was further studied accompanied by the development of a kinetic model based on Monod kinetics.

Results

Osmotolerant strains of *Caldicellulosiruptor* were obtained with *C. owensensis* adapted to grow up to 80 g/L glucose; other strains in particular *C. kristjanssonii* demonstrated a greater limitation to adaptation. *C. owensensis* CO80 was further studied and demonstrated the ability to grow in glucose concentrations up to 80 g/L glucose but with reduced volumetric hydrogen productivities (Q_{H2}) and incomplete sugar conversion at elevated glucose concentrations. In addition, the carbon yield decreased with elevated concentrations of glucose. The ability of *C. owensensis* CO80 to grow in high glucose concentrations was further described with a kinetic growth model, which revealed that the critical osmolarity of the cells increased fourfold when cultivated at higher osmolarity.

Conclusions

The adaptation of members of the *Caldicellulosiruptor* genus to higher osmolarity established that the ability to develop improved strains via ALE is species dependent, with *C. owensensis* adapted to grow on 80 g/L, whereas *C. kristjanssonii* could only be adapted to 30 g/L glucose. Although, *C. owensensis* CO80 was adapted to a higher osmolarity medium, the strain demonstrated reduced Q_{H2} with elevated glucose concentrations. This would indicate that while ALE permits adaptation to elevated osmolarities, this approach does not result in improved fermentation performances at these higher osmolarities.

Background

The current reliance on fossil fuels as the main source of global energy production is both unsustainable and environmentally damaging. Biofuels derived from renewable sources are an extensively researched alternative for the production of energy, however, it is of great importance these fuels do not compete with food production in terms of land usage (Sims et al. 2008). Within the European Union, current legislation restricts dedicated biofuel production to 7% of total land use (European Parliament and Council 2015). Lignocellulose is a potential substrate for biofuel production due to its wide availability with 1-5 billion tonnes yielded annually (Claassen et al. 1999). Currently, over 40 million tonnes of this material is generated as a by-product of agriculture and forestry (Sanderson 2011), and is ideally suited for biofuel production as lignocellulose obtained from waste streams does not affect land usage or food production.

Biologically derived hydrogen (biohydrogen) has the potential to be an alternative energy carrier as it can be produced from renewable sources such as lignocellulose and only generates water vapour as a by-product when used as a fuel (Azwar et al. 2014). *Caldicellulosiruptor* is a genus of thermophilic hydrogen producing bacteria capable of producing hydrogen close to the maximum stoichiometric yield of 4 mol H₂/mol hexose (Rainey et al. 1994, Schleifer 2009). Notably, most members of this genus can metabolize a wide range of carbon sources including an array of mono-, oligo- and polysaccharides (Schleifer 2009). Species such as *C. saccharolyticus* and *C. owensensis* display the capacity to simultaneously consume hexoses and pentoses without catabolite repression and therefore are beneficial to an industrial process as both the cellulose and hemicellulose fractions of lignocellulose can be consumed together (Björkmalm et al. 2018, VanFossen et al. 2009, Zeidan & van Niel 2010). Additionally, *Caldicellulosiruptor* has been previously utilised to generate hydrogen from a variety of lignocellulosic material (Byrne et al. 2018, de Vrije et al. 2009, Pawar et al. 2013).

Although a promising candidate for industrial biohydrogen production, *Caldicellulosiruptor* experiences several key limitations including the ability to grow in high osmotic conditions (Byrne et al. 2018, Ljunggren et al. 2011, Pawar et al. 2013). In its natural environment *Caldicellulosiruptor* does not experience a high degree of osmotic stress and has thus adapted to low osmolalities, maximally of 0.4 to 0.425 Osmol/L, with a critical osmolarity of 0.27 to 0.29 Osmol/L (van Niel et al. 2003, Willquist et al. 2009). This osmosensitivity limits the industrial potential of *Caldicellulosiruptor* as it precludes cultivation in concentrated lignocellulose hydrolysates. Concentrated hydrolysates are essential for environmentally efficient production of thermophilic H₂ as higher substrate concentrations reduce the requirement for water addition and energy input for heating (Byrne et al. 2018, Foglia et al. 2010, Ljunggren & Zacchi 2010).

Mathematical modelling can be implemented as a powerful tool to assess how the key physical and biological phenomena in a process function. Inhibition arising from osmosensitivity can be one such phenomenon and is further addressed in this paper. This modelling of quantitative description of substrate inhibition and inhibition due to a high degree of osmotic stress have previously been studied using different types of growth kinetic equations (Azimian et al. 2019, Ciranna et al. 2014, Dötsch et al. 2008, van Niel et al. 2003). A non-competitive equation (Eq. 1) is commonly used to describe growth inhibition due to substrate or soluble end products (Ciranna et al. 2014, van Niel et al. 2003).

$$r = r_{max} \cdot (1 - C/C_{crit})^n \cdot S/(S + K_S) \quad (1)$$

where r is the specific growth rate (h^{-1}), r_{max} is the maximum specific growth rate (h^{-1}), C is the concentration of the inhibiting compound (M), C_{crit} is the critical concentration of the inhibiting compound (M), K_S is the affinity constant for the substrate (M), S is the concentration of the substrate (M) and n is the degree of inhibition.

Strain improvement can be accomplished through a process known as adaptive laboratory evolution (ALE). In this process an organism is repeatedly subcultivated under defined conditions enabling a controlled adaptation to these conditions and hence a favourable phenotype change can develop (Dragosits & Mattanovich 2013). In this study several osmotolerant strains of *Caldicellulosiruptor*, i.e., *C. owensensis*, *C. kronotsyensis*, *C. bescii*, *C. acetigenus* and *C. kristjanssonii* were developed through sequential ALE at incrementally increasing glucose concentrations. The adapted osmotolerant strain *C. owensensis* (CO80) was cultivated in controlled batch and exposed to a high concentration of glucose, up to 80 g/L. To quantify the success of strain development, this process was modelled using a growth kinetic equation based on Monod with a set of inhibition equations. Further evaluation of the co-culture of osmotolerant strains, *C. owensensis* CO80 and *C. saccharolyticus* G5, on lignocellulosic hydrolysate (Byrne et al. 2018) was also performed.

Results

Strain development

To assess the ability of different strains of the *Caldicellulosiruptor* genus to adapt to higher osmolarity and to select an osmotolerant strain for further development, ALE was undertaken on five species of *Caldicellulosiruptor*. The respective increase in viability at higher osmolarity was determined during sequential batches, whereby increased sugar concentration was used as a selective pressure.

Figure 1 illustrates the critical concentration for viability of each *Caldicellulosiruptor* strain. The ALE design replicated a previous study that achieved the selection of a *C. saccharolyticus* strain with the capacity to grow on 100 g/L glucose (Pawar 2014). Out of the five selected strains, only *C. owensensis* was successfully adapted to grow on a glucose concentration of 80 g/L over the course of approximately 250 generations. This adapted culture (CO80) was selected for further analysis. The adaptation of *C. kronotskyensis* demonstrated viability in solutions up to 60 g/L glucose but at 70 g/L it did not reach the threshold value of OD₆₂₀ 0.4 and therefore was not selected for further analysis. In contrast, the adaptation strategy of *C. kristjanssonii*, *C. bescii* and *C. acetigenus* was unsuccessful. Even with repeated cultivation at lower sugar concentrations a loss of viability occurred. *C. kristjanssonii* was particularly sensitive to adaptation and exhibited poor viability in glucose concentrations as low as 20 g/L. Overall, *C. owensensis* had a greater ability to adapt to higher osmolarity medium than any other strain. Adaptation of *C. owensensis* to 100 g/L glucose was attempted, however, strains adapted to 90 and 100 g/L displayed poor growth and a loss of viability after several rounds of cultivation.

Similar to *C. saccharolyticus* (Willquist et al. 2009), *C. owensensis* lacks key metabolic pathways for the synthesis of compatible solutes for high osmotic conditions. *C. owensensis* lacks synthetic pathways for the osmoprotectants glycine betaine, ectoine and trehalose. *C. owensensis* also lacks pathways associated with the synthesis of compatible solutes in thermophiles such as the di-myoinositol phosphate pathway (Gonçalves et al. 2012, Martins & Santos 1995) and the synthesis pathway for 2-O-(β)-mannosylglycerate in *Thermus thermophilus* (Nunes et al. 1995). In addition, no homology between the *C. owensensis* genome and 2-(O-β-d-mannosyl)-di-myoinositol-1,3'-phosphate synthase (TM0359) in *Thermotoga maritima* (Rodrigues et al. 2009) could be found. However, *C. owensensis* can produce glutamate and has the full synthetic pathway of proline.



Figure 1. Development of osmotolerant strains of *C. owensensis*, *C. kronotskyensis*, *C. bescii*, *C. acetigenus* and *C. kristjanssonii*. Values in green indicate osmotolerant adaptation steps were completed on stated concentrations of glucose. Values in yellow indicate the final osmotolerant development step and therefore the highest concentration of glucose that the strains can be grown.

Performance and quantification of CO80 at higher sugar concentrations

C. Owensensis CO80 was successfully cultivated on 10, 30 and 80 g/L using a controlled batch reactor. The trends of sugar consumption, growth and product generation in CO80 when cultivated on these different sugar concentrations, are shown in Figures 2-4.

The behaviour of CO80 at increasing glucose concentrations was quantified using dynamic simulations. In these simulations, the model and parameters derived from the wild-type strain of *C. saccharolyticus* were used as a benchmark (Ljunggren et al. 2011). However, this model was not able to describe the experimental data. One reason for this is that the benchmark value of the parameter OSM_{crit} taken from Ljunggren et al. (2011) was set too low for the higher sugar concentration. In addition, the benchmark values for parameters of maximum specific growth rate (μ_{max}), affinity constant for the sugar (K_s) and the rate of death (r_{cd}) required alteration since the growth was slower and the cell death rate was faster than predicted by the original model.

Therefore, the model was calibrated with data from the three batch experiments in duplicates or triplicates supplemented with 10 g/L, 30 g/L and 80 g/L glucose. The calibrated parameters μ_{max} , OSM_{crit} and K_s , together with additional parameters are summarized in Table 1. Comparison between the model and the experimental results are graphically shown in Figure 2-4.

Table 1. Parameters calibrated to experimental data in comparison to the benchmark parameter values from Ljunggren et al 2011. Confidence interval 95% is given for those parameters which have been fitted numerically.

| Parameter | Benchmark values Ljunggren et al. (2011) | 10 g/L | 30 g/L ¹ | 30 g/L ² | 80 g/L |
|--------------------------------|--|------------------------|--|--------------------------|--------------------|
| μ_{max} (h ⁻¹) | 0.28 | 0.33 ± 0 | 0.31 ± 0.082 | 0.31 ± 0.082 | 0.29 ± 0.02 |
| K_s (M) | 4.8 · 10 ⁻⁵ | 4.8 · 10 ⁻³ | 9.8 · 10 ⁻² ± 1.5 · 10 ⁻⁴ | 4.8 · 10 ^{-5.5} | 0.49 ± 0.064 |
| OSM_{crit} (M) | 0.28 | 0.23 ± 0.0002 | 0.39 ± 0.002 | 0.39 ± 0.002 | 0.78 ± 0.024 |
| r_{cd} (h ⁻¹) | 0.014 | 0.031 ± 0.0001 | 0.031 ± 0.0065 | 0.020 ± 0.00015 | 0.031 ³ |
| Y_{S,H_2} (mol/mol) | 4.77 | 3.5 ± 0.38 | 3.5 ± 0.12 | 3.5 ± 0.12 | 2.56 ³ |
| $Y_{S,X}$ (cmol/mol) | 4.78 | 0.79 ⁴ | 0.80 ⁴ | 0.80 ⁴ | 0.72 ³ |
| n_{H_2} | 4.5 | 5.37 ± 0.00005 | 5.37 ³ | 5.37 ³ | 4.5 ⁵ |
| n_{μ} | 4.68 | 4.68 ⁵ | 4.68 ⁵ | 4.68 ⁵ | 4.68 ⁵ |

¹First model for the 30 g/L cultures

²Second model for the 30 g/L cultures

³Graphically calibrated

⁴Calculated from experimental data

⁵Same value as in Ljunggren et al. (2011)

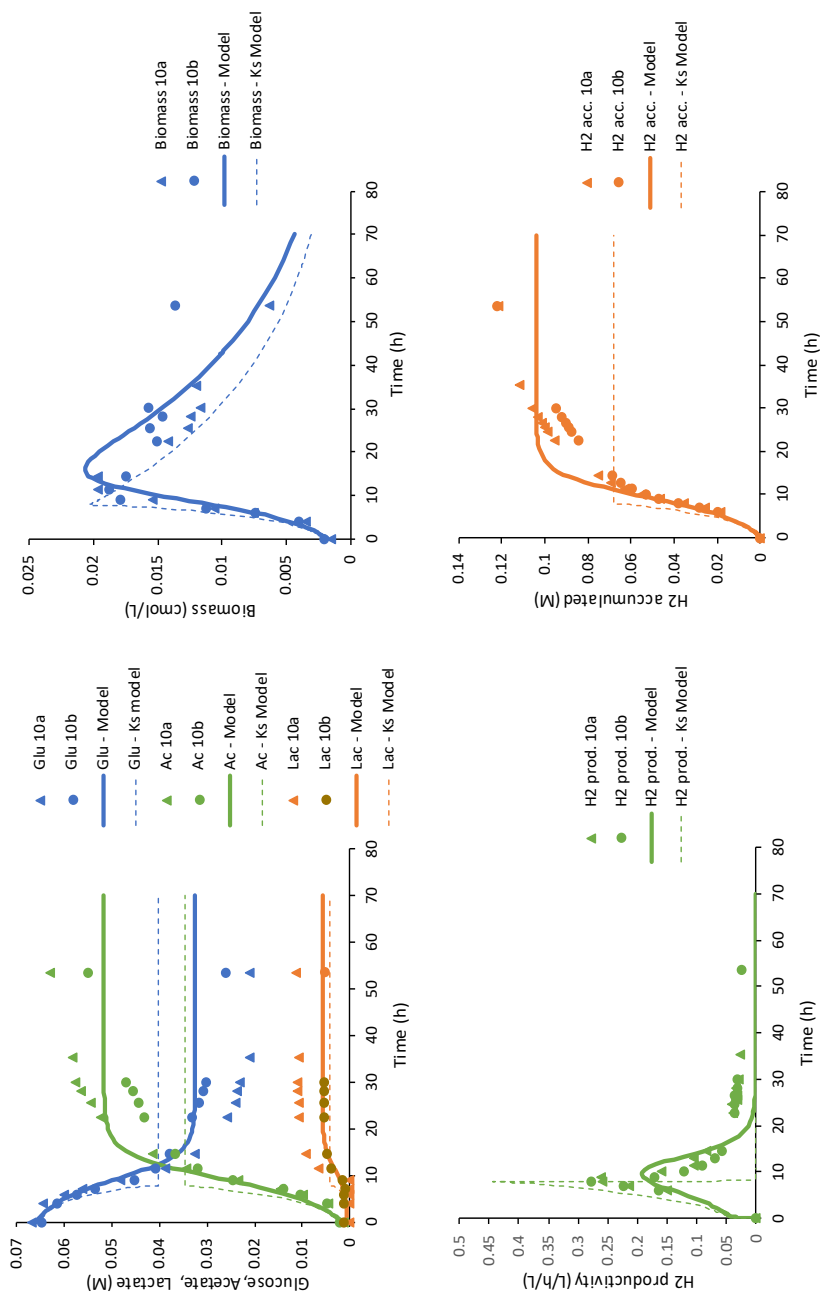


Figure 2. Experimental data and modeling results for the 10 g/L cultures. Upper left: glucose consumption, acetate and lactate production, upper right: biomass production, lower left: hydrogen productivity and lower right: accumulated hydrogen production.

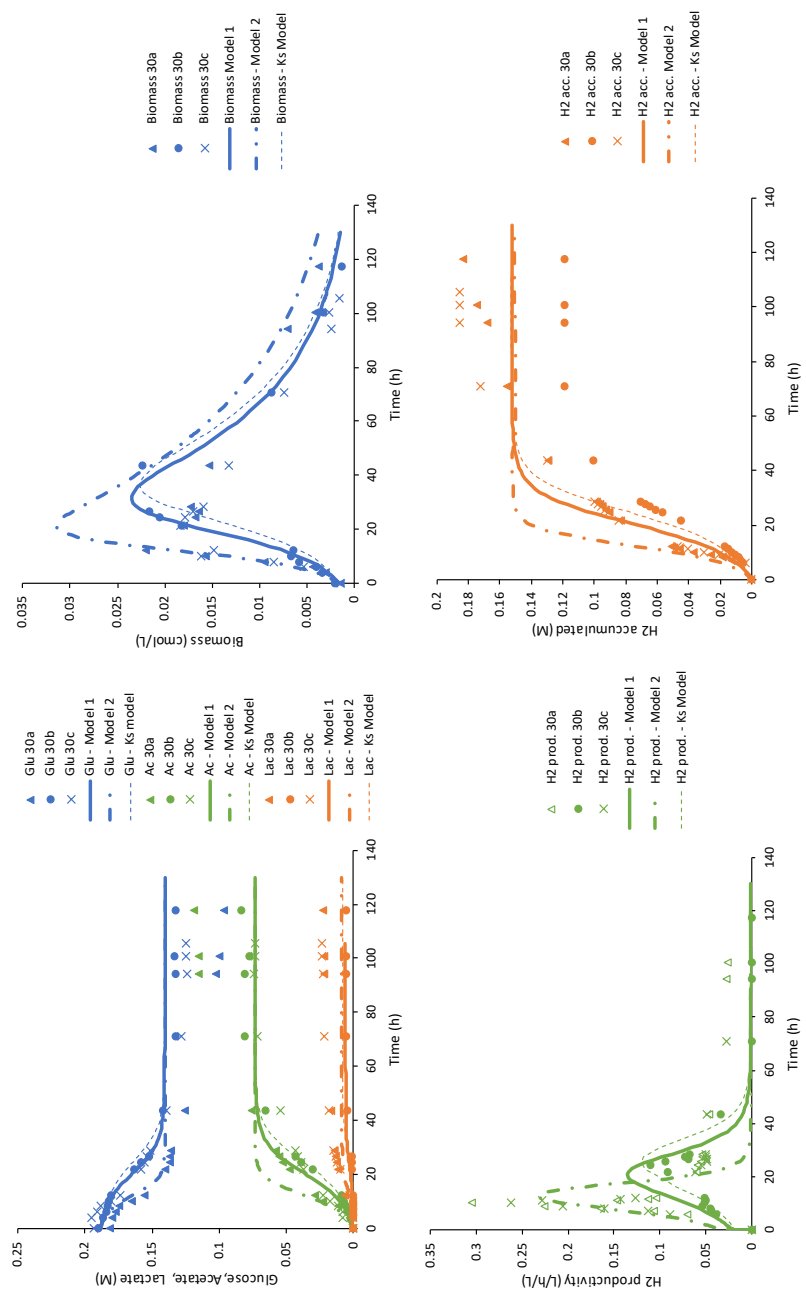


Figure 3. Experimental data and modelling results for the 30 g/L cultures. Upper left: glucose consumption, acetate and lactate production, upper right: biomass production, lower left: hydrogen productivity and lower right: accumulated hydrogen production.

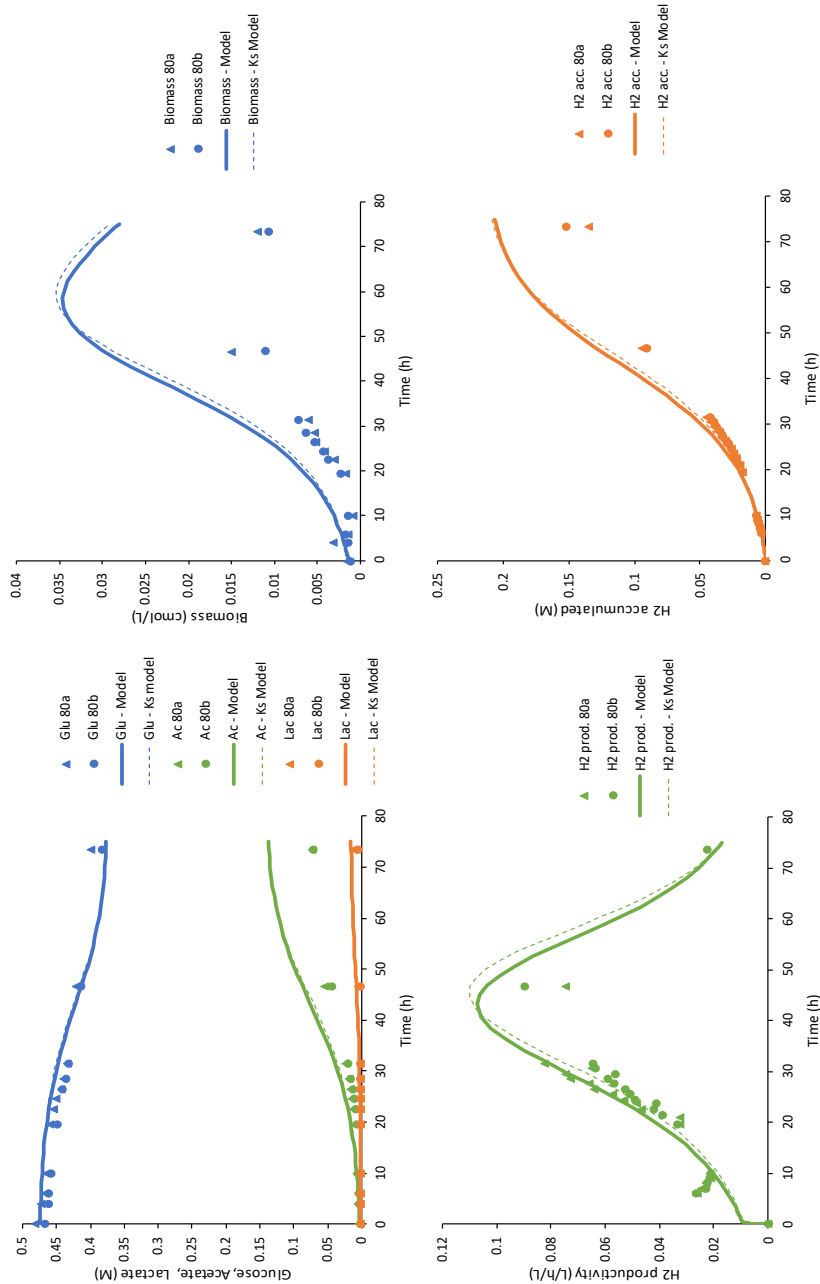


Figure 4. Experimental data and modelling results for the 80 g/L cultures. Upper left: glucose consumption, acetate and lactate production, upper right: biomass production, lower left: hydrogen productivity and lower right: accumulated hydrogen production.

The maximum hydrogen productivity from the experimental data was 10.55 ± 0.04 , 11.45 ± 0.00 and 3.35 ± 0.00 mmol/L/h for 10, 30 and 80 g/L sugar, respectively. This observation at 10 and 30 g/L is comparable to 15 mmol/L/h described in wild type *C. owensensis* grown on 10 g/L glucose supplemented with 1 g/L yeast extract (Zeidan & van Niel 2010). The model underestimated the hydrogen productivity slightly in the case of 10 and 30 g/L but overestimated productivity compared to experimental data of 80 g/L cultures. Similar overestimation was observed with respect to the cell growth on 80 g/L. Nevertheless, the model was able to predict well the experimental data.

The accuracy of the model in describing experimental data was assessed and displayed in Table 2. The R^2 values describes how well the model could predict the trend over time and the curve slope values of the linear regression (i.e. k in $y=k \cdot x$) are indicating over- or underestimations. For a perfect fit they should both be 1. With respect to most variables, the prediction error was less than 30% indicating good accuracy. The model was also able to accurately predict the trend of the assessed variables with a R^2 value close to 1 in all cases. However, analysis revealed overestimation of cell growth as well as acetate and lactate production on 30 g/L (Table 2).

Table 2. R^2 values and curve slope values to describe the fit between average experimental data and simulated data from the models at the same time points.

| R ² values/curve slope values (k) | 10 g/L | | 30 g/L | | | 80 g/L | |
|---|---------------|-------------------------|---------------|---------------|-------------------------|----------------|----------------|
| | Model | K _S model | Model 1 | Model 2 | K _S model | Model | KS model |
| Glucose | 0.94/ 0.95 | 0.67/ 0.93 | 0.91/ 0.96 | 0.89/ 0.95 | 0.83/ 1.0 | 0.87/ 0.99 | 0.85/ 0.98 |
| Biomass | 0.82/ 0.96 | 0.77/ 1.0 | 0.50/ 6.0 | 0.28/ 6.8 | 0.82/ 4.2 | 0.96/ 0.43 | 0.94/ 0.43 |
| Acetate | 0.97/ 0.97 | 0.75/ 1.2 | 0.94/ 1.1 | 0.96/ 1.1 | 0.77/ 0.85 | 0.99/ 0.54 | 0.99/ 0.55 |
| Lactate | 0.95/ 1.4 | 0.60/ 1.5 | 0.97/ 2.0 | 0.92/ 2.1 | 0.83/ 1.4 | 0.97/ 0.54 | 0.98/ 0.54 |
| H₂ accumulated | 0.94/ 0.92 | 0.51/ 1.1 | 0.94/ 0.88 | 0.96/ 0.98 | 0.76/ 0.71 | 0.99/ 0.72 | 0.98/ 0.74 |
| OSM | 0.97/ 0.98 | 0.57/ 1.0 | 0.94/ 1.0 | 0.97/ 1.0 | 0.75/ 0.96 | 0.91/ 0.40* | 0.92/ 0.40* |

*The linear regression does not intersect (0,0).

Inhibition kinetics

The effect of sugar concentration on the apparent half-saturation constant, K_S , and critical osmolarity, OSM_{crit} , is shown in Figure 5. The apparent K_S increased with an elevated sugar concentration in an almost linear fashion reaching a value four orders of magnitude higher in the 80 g/L culture. As Sivakumar et al. (1994) demonstrated, extraordinarily high K_S values can be an indicator that the growth kinetics used are insufficient in describing the process due to substrate inhibition,

hence, an extended model was constructed. In the constructed “K_S-model”, the K_S in the original model (Eq. 8 in Material and Methods) was replaced with the equation from the linear regression in Figure 5 (Eq. 2):

$$\mu = \mu_{max} \cdot \frac{Glu}{Glu+(1.32 \cdot Glu - 0.09)} \cdot I_{osm} \cdot I_{H_{2, aq}} \quad (2)$$

where μ is the specific growth rate (h⁻¹), μ_{max} the maximum specific growth rate (h⁻¹), Glu is the glucose concentration (M), I_{osm} is the inhibition due to osmolarity and I_{H_{2, aq}} is the inhibition due to aqueous hydrogen. The simulation using the “K_S-model” is illustrated in Figure 2-4 as a thin dashed line. The K_S-model was well able to describe the experimental data (Table 2) for 30 g/L and 80 g/L (Figure 3-4). However, for 10 g/L, the K_S-model could not sufficiently describe the data (Figure 2). This may be due to the greater glucose consumption at 10 g/L compared to the higher concentrations, thereby altering the K_S-model equation to a greater extent as this model is dependent on the glucose concentration.

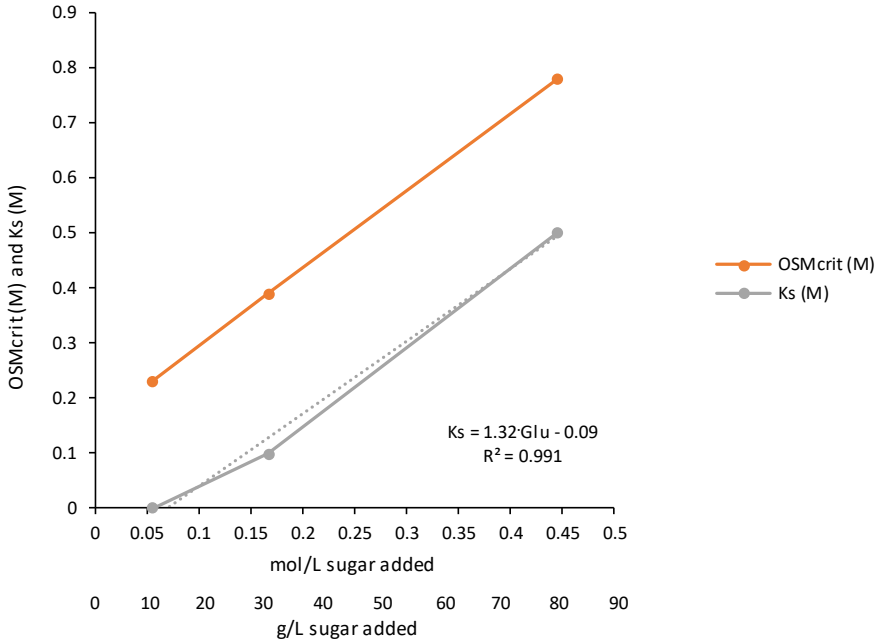


Figure 5. Comparison of the calibrated parameters OSM_{crit} (orange) and K_S (grey).

In addition to the K_S parameter, the parameter OSM_{crit} is linearly increasing at rising sugar concentration (Figure 5), which would indicate a higher tolerance of CO80 when exposed to a higher sugar concentration and higher osmolarity. This behaviour became more apparent when the inhibition kinetics of the fermentation was simulated in the different cases. The model describes two different types of

inhibition, i.e. inhibition by osmolarity (I_{osm}) and by the dissolved hydrogen concentration ($I_{H_2,aq}$) (Eq. 7 and Eq. 8 in Materials and Methods). The simulation of these are shown in Figure 6. A value around 1 means no inhibition, a lower value means that the process is inhibited. Figure 6 clearly shows that osmolarity is the crucial inhibition factor, i.e. an I_{osm} value <1 . $I_{H_2,aq}$ is of less importance since, the simulated values were $0.98 < I_{H_2,aq} < 1$, which means almost no inhibition. Though, the K_S model for 10 g/L gave values of $0.11 < I_{H_2,aq} < 1$, this rather indicates that the model is not a good fit to the experimental data, which is also shown in Figure 2. Interestingly, the simulation of I_{osm} illustrates that although all fermentations were severely affected by osmolarity, the strains grown on 80 g/L glucose reached complete inhibition after 80 h while the cultivation on 10 g/L reached complete inhibition after 20 h, although the initial osmolarity in this condition was lower. This would indicate that although *C. owensensis* CO80 is adapted to higher osmolarities it does not display the phenotype unless stressed with a medium with a high osmolarity.

It was also noted that at high levels of sugar (80 g/L), significant browning of the media occurred indicating the presence of Maillard products. This observation could not be quantified and described by the model.

Reproducibility of CO80

The model was also used to illustrate the reproducibility of growth of CO80 at increasing sugar concentrations. Three replicates were made for the 30 g/L experiments, as compared to two for the 10 g/L and 80 g/L due to a high degree of variation in one of the replicates. Several attempts at inoculating *C. owensensis* CO80 to a culture medium containing 80 g/L glucose failed, as *C. owensensis* CO80 did not grow when noticeable browning of the media due to Maillard reactions occurred. As illustrated in Figure 3, one of the three replicates (30b) from the 30 g/L experiments differ with respect to hydrogen productivity and accumulation but discrepancies could also be seen in the biomass growth. For this reason, a second model (Model 2) with a slight difference in parameter values (Table 1) was constructed for the 30 g/L experiments. However, both Model 1 and Model 2 have low R^2 values and high curve slope values for the biomass (Table 2). One of the three replicates could be simulated with respect to OSM_{crit} and apparent saturation constant (K_S ; Figure 3) whereas the other two could be fitted better with the model where the parameters were much closer to those of the 10 g/L culture. This result might indicate that the adaptation was incomplete, possibly due to the presence of subpopulations possessing different degrees of adaptation to higher osmolality (Peabody et al. 2016).

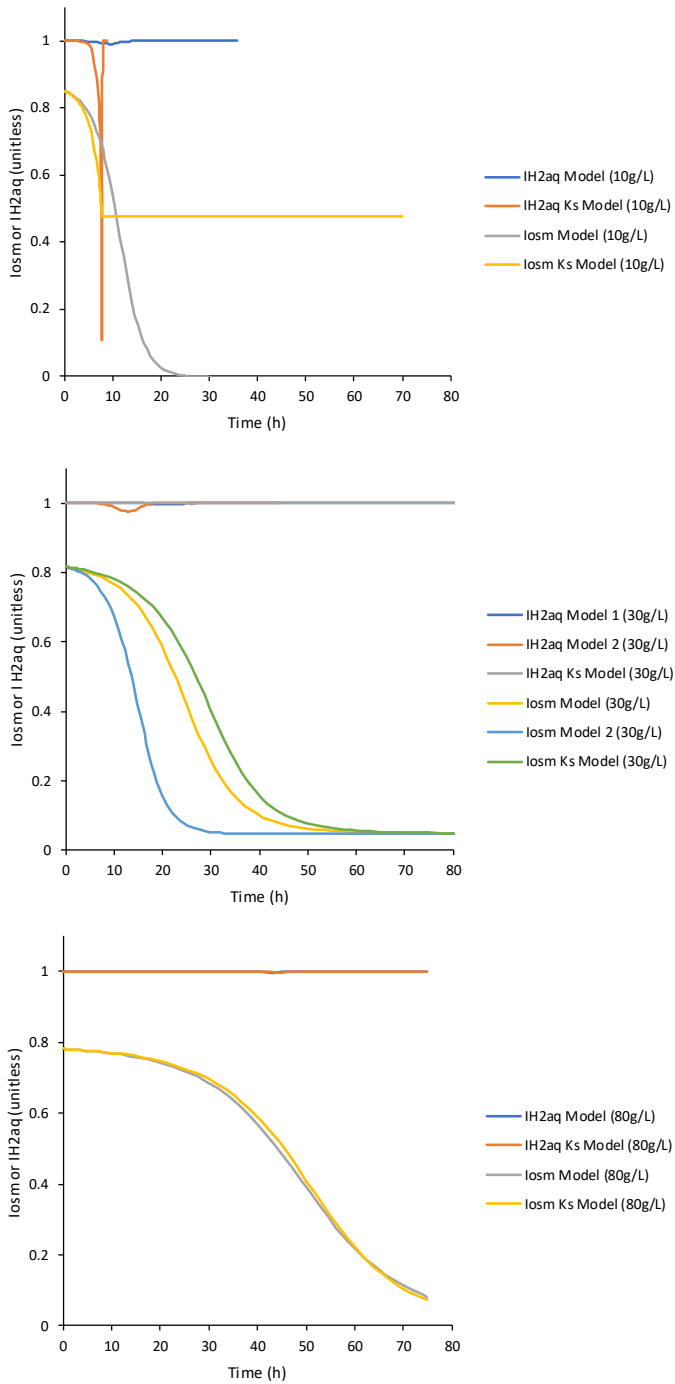


Figure 6. Simulated values of I_{osm} and $I_{H2, aq}$ for the different models.

Continuous culture of CO80 and G5

The results of the batch cultivations indicate that *C. owensensis* CO80 was adapted to increased substrate concentrations but did not grow optimally at these conditions. In an attempt to further increase the performance, a strategy involving the co-cultivation with an adapted *C. saccharolyticus* G5 culture as well as using wheat straw hydrolysis was evaluated (Byrne et al. 2018). Indeed, co-cultivations on wheat straw hydrolysate displayed higher hydrogen productivity and sugar consumption rates than the base medium with a sugar concentration corresponding to the wheat straw hydrolysate (Table 3).

Table 3. Volumetric productivity of of co-cultures of *C. owensensis* CO80 and *C. saccharolyticus* G5 (data adapted from Byrne et al. (2018))

| | Wheat straw hydrolysate with EB-1 | Defined medium with EB-1 | Defined medium Modified DSM 640 |
|------------------------|-----------------------------------|--------------------------|---------------------------------|
| Q_{glucose} | 1.88 ± 0.02 | 0.18 ± 0.16 | 0.09 ± 0.13 |
| Q_{xylose} | 2.64 ± 0.39 | 1.26 ± 0.07 | 1.49 ± 0.25 |
| $Q_{\text{arabinose}}$ | 0.18 ± 0.00 | 0.20 ± 0.00 | 0.16 ± 0.00 |
| Q_{acetate} | 4.74 ± 0.00 | 2.37 ± 0.37 | 2.63 ± 0.38 |
| Q_{H_2} | 6.71 ± 0.06 | 2.47 ± 0.55 | 3.71 ± 0.42 |

Population dynamics

Population dynamics of co-cultures presented in Byrne et al. (2018) were analysed to determine the stability of the co-cultures of *C. saccharolyticus* G5 and *C. owensensis* CO80. As illustrated in Table 4, only a minute proportion of the co-culture consisted of *C. owensensis* CO80 in each case, thus *C. saccharolyticus* G5 dominated by far in the co-culture. However, a brief interruption of pH control during the co-culture on modified DSM 640 resulted in the population of CO80 exceeding 85% of the total population before returning to less than 1% after 2 volume changes. Although, low population numbers of CO80 were observed, a large quantity of biofilm occurred in all continuous cultivations particularly at the gas-liquid interface.

Table 4. Population of C80 and G5 in continuous cultures

| | Proportion CO80 | Proportion G5 |
|-------------------------|-----------------|---------------|
| Wheat straw hydrolysate | 99.76 ± 0.43% | 0.24 ± 0.43% |
| Defined medium EB-1 | 99.91 ± 0.01 % | 0.09 ± 0.01% |
| Defined medium DSM 640 | 98.45 ± 3.06 % | 1.58 ± 3.17% |

Discussion

In this study we successfully implemented ALE as a way to improve the survival of *C. owensensis* in osmostress conditions. Next to *C. saccharolyticus* (Pawar, 2014), this is the second *Caldicellulosiruptor* strain we have improved with ALE. *C. owensensis* was successfully adapted to survive in 80 g/L glucose. However, not all *Caldicellulosiruptor* strains were as easily adaptable in our study. There were significant limitations in the adaptation of *C. bescii*, *C. acetigenus* and *C. kristjanssonii* to higher sugar concentrations. *C. kristjanssonii* displayed a particular limitation to adaptation to higher osmolarities in glucose concentrations as low as 20 g/L. Previously, a transcriptional analysis demonstrated that adaptation in *C. saccharolyticus* was a result of increased transposon activity as well as upregulation of proteins related to sugar transport (Pawar et al, unpublished results).

Although ALE increased osmotolerance, *C. owensensis* CO80 exhibits incomplete sugar consumption at elevated sugar concentrations. This phenomenon has been previously observed in wild-type *C. saccharolyticus*. In addition, when cultivated on 80 g/L glucose, a significantly reduced volumetric hydrogen productivity was obtained compared to 10 and 30 g/L. Additionally, the substrate uptake capacity was negatively affected, indicating that although *C. owensensis* is capable of surviving at 80 g/L, a significant loss of growth and hydrogen productivity is observed.

The model was shown to be a useful tool to quantify the experimental observations. A high value of the OSM_{crit} parameter in the model would indicate a higher tolerance to osmolarity. However, the sugar uptake, mainly in 30 g/L and 80 g/L batches is not complete, which is possibly due to inhibition of sugar uptake. According to the model for the 80 g/L case, the K_S is four orders of magnitude higher compared to the K_S of the cells in the 10 g/L culture. The growth kinetic equation with inhibition terms used in the model (Eq. 8 in Material and Methods) has previously been used (Ciranna et al. 2014, Ljunggren et al. 2011, van Niel et al. 2003) but in this case it might not be sufficient to describe a process with such a high sugar input. The calibrated K_S for the 80 g/L case is an “apparent K_S ” which most probably constitutes of the “real K_S ” multiplied by an inhibition factor. To counteract such a high K_S value, a second model, where K_S was a function of glucose, was used instead (Eq. 2). This model gave a similar fit to the data for the 30 g/L and 80 g/L cultures. Furthermore, the inhibition due to osmolarity had a higher significance than inhibition due to aqueous hydrogen. This viewpoint is also strengthened in Figure 6 where it can be seen that I_{osm} rather than $I_{H_2,aq}$ are the cause of the inhibitions.

When calibrating the parameters in the model to get a good fit to the experimental data, an initial guess value of the parameter needs to be given as an input. These values are of great importance for the end result as a poorly chosen initial value could result in a local minimum in the parameter estimation procedure, leading to a bad fit of the model to the experimental data and a faulty estimated parameter. To counteract this, the guess values were initially chosen in proximity to the benchmark value from Ljunggren et al. (2011). When these values did not give the right fit to the experimental data, several new initial guess values were tested as input in the *lsqcurvefit* function in MATLAB.

The reduction in Q_{H_2} observed in batch fermentations is consistent with the data derived from Byrne et al. (2018) establishing that utilizing osmotolerant strains facilitated use of more concentrated hydrolysates albeit at the expense of Q_{H_2} . In that study the Q_{H_2} of the co-culture (6.71 ± 0.06 mmol/L/h) was lower than that observed for the wild-type *C. saccharolyticus* grown on an approximately 3-fold less concentrated WSH containing 11 g/L monosaccharides (8.69 mmol/L/h) (Pawar et al. 2013). However, the Q_{H_2} obtained with the defined DSM 640 medium was similar to that of wild-type *C. saccharolyticus* (4.2 mmol/L/h) (de Vrije et al. 2007). Furthermore, the co-culture grown on WSH displayed a higher Q_{H_2} when cultivated on wheat straw hydrolysate compared to a defined medium. This confirms previous observations that *Caldicellulosiruptor* possesses a higher Q_{H_2} when cultivated on wheat straw hydrolysate than on pure sugar (Pawar et al. 2013). This may be due to the presence of additional nutrients found in the wheat straw compared to that of the defined medium. The reduction of Q_{H_2} compared to the wild-type *C. saccharolyticus* could be due to the presence of higher concentrations of inhibitory compounds that may reduce hydrogen productivity. *C. saccharolyticus* strain is sensitive to HMF and furfural concentrations above 1 and 2 g/L, respectively (de Vrije et al. 2009, Panagiotopoulos et al. 2010). Even though higher hydrolysate concentrations were used in the present study, only trace amounts of HMF and furfural were detected. The presence of, yet unknown, compounds in the hydrolysate could have resulted in the inhibition of *Caldicellulosiruptor*. It was also noted throughout this study that higher concentrations of sugar intensified the occurrence of Maillard reactions. A concentration of 80 g/L glucose led to significant browning of the cultivation media and resulted in failure of growth when arising before inoculation and was presumably responsible for inconsistencies during cultivation at 30 g/L. Maillard products are known to inhibit the growth of other thermophilic bacterial species such as *Thermotoga* and *Thermoanaerobacter* (de Vrije et al. 2009, Tomás et al. 2013). The presence of Maillard-based products will reduce the efficiency of any large-scale fermentation. The obvious choice for mitigating such reactions would be the omission of cysteine from the cultivation medium.

Additionally, the co-cultivation of *C. owensensis* CO80 and *C. saccharolyticus* G5 resulted in a predominantly *C. saccharolyticus* G5 population, with detection of only small quantities of *C. owensensis* CO80. Although, this could indicate cell mass washout of *C. owensensis* CO80, a large quantity of biofilm was observed in the bioreactors after termination of each cultivation. *C. owensensis* is known for its ability to form biofilm (Peintner et al. 2010) and could indicate that *C. owensensis* CO80 was present in the fermentations but was primarily located in the biofilm.

Conclusions

The adaptation of *Caldicellulosiruptor* by ALE to higher osmotic conditions permitted survival at higher sugar concentrations, however, the developed strain *C. owensensis* CO80 displayed lower Q_{H_2} when cultivated at 80 g/L. Implementation of co-cultures of *C. owensensis* CO80 and *C. saccharolyticus* G5 facilitated cultivation in higher hydrolysate concentrations than previously reported, although, with a reduction of Q_{H_2} compared to *C. saccharolyticus* on more dilute hydrolysate. The kinetic models developed herein, were able to predict the behaviour of growth of CO80 when exposed to 10 and 30 g/L of glucose respectively. At 80 g/L of glucose there was a slight overestimation in the models and the growth kinetics used, this could merit from further development.

Although possible with *C. saccharolyticus* (Pawar et al. 2013), *C. owensensis* cannot be cultivated without cysteine, as this species lacks the sulfur assimilation pathway (Pawar & van Niel 2014). Therefore, co-cultivations of these two species in the absence of cysteine, but with sulfate as the sole sulfur source, could be of interest. In addition, co-cultivation of wild-type strains of *C. saccharolyticus* and *C. owensensis* could also stimulate biofilm formation (Pawar et al. 2015). However, in this study it was demonstrated that *C. saccharolyticus* G5 strain completely overtook the *C. owensensis* CO80 strain in the co-cultivations. Although this observation can be considered discouraging, large quantities of biofilm occurred indicating the presence of *C. owensensis* CO80. Therefore, alternative reactor systems could be implemented to enhance biofilm formation, hence, improving cell mass retention.

Material and Methods

Strains and cultivation medium

The wild-type strains of *Caldicellulosiruptor owensensis* DSM 13100, *Caldicellulosiruptor kronotskyensis* DSM 18902, *Caldicellulosiruptor bescii*

DSM 6725, *Caldicellulosiruptor acetigenus* DSM 7040 and *Caldicellulosiruptor kristjanssonii* DSM 12137 were obtained from the Deutsche Sammlung von Mikroorganismen und Zellkulturen (DSMZ; Braunschweig, Germany). Subcultivations were conducted in 250 mL serum flasks with 50 mL modified DSM 640 media (Willquist et al. 2009) with the addition of 50 mM HEPES and 10 g/L glucose, unless otherwise state. A 1000x vitamin solution was prepared as Zeidan and van Niel (2010) and a modified SL-10 solution was prepared described previously (Pawar & van Niel 2014).

Adaptation of species to higher osmolarity

Adaptation of *C. owensensis*, *C. kronotsyensis*, *C. bescii*, *C. acetigenus* and *C. kristjanssonii* to higher osmolarity was performed through adaptive laboratory evolution that initially involved repeated sub-cultivation of each strain in a modified DSM 640 medium containing 10 g/L of glucose. The glucose concentration was increased with 10 g/L increments when generation time for each strain was less than 0.4 h⁻¹ and OD was above 0.3. This sequential increase of glucose concentration was continued until no growth in higher glucose concentrations was observed (Pawar 2014). The current status is that an osmotolerant strain of *C. owensensis* has been achieved capable of growing at a glucose concentration of 100 g/L.

Fermentor set up

Batch cultivations were performed in a jacketed, 3-L fermentor equipped with an ADI 1025 Bio-Console and ADI 1010 Bio-Controller (Applikon, Schiedam, The Netherlands). A working volume of 1L was used in all batch cultivations and the pH was maintained at 6.5 ± 0.1 by automatic titration with 4 M NaOH. The temperature was thermostatically kept at 70 ± 1 °C. Stirring was maintained at 250 rpm and nitrogen was sparged through the medium at a rate of 6 L/h. A water-cooled condenser was utilised (4°C) to prevent the evaporation of the medium. During each cultivation, samples were collected at regular intervals to monitor of the optical density and HPLC. The supernatant from each sample was collected and stored at -20°C for further quantification of sugars, organic acids, furfural and HMF. Gas samples were collected from the fermentor's headspace to quantify H₂ and CO₂. Analysis of osmotolerant *C. owensensis* CO80 was performed using both batch cultivations with the addition of 10, 30 and 80 g/L of glucose. Each of the batch cultivation was conducted in duplicate except for 30 g/L which was performed in triplicate.

Analytical methods

Optical density was determined using an Ultraspec 2100 pro spectrophotometer (Amersham Biosciences) at 620 nm.

Sugars and organic acids were detected using HPLC (Waters, Milford, MA, USA). For the quantification of organic acids, HMF and furfural, a HPLC equipped with an Aminex HPX-87H ion exchange column (Bio-Rad, Hercules, USA) at 60°C and 5 mM H₂SO₄ as mobile phase was used at a flow rate of 0.6 mL/min. Glucose, xylose and arabinose quantification was conducted using a HPLC with two Shodex SP-0810 Columns (Shodex Japan) in series with water as a mobile phase at a flow rate of 0.6 mL/min.

H₂ and CO₂ concentrations were quantified with an Agilent 7890B Series GC (Agilent GC 7890, Santa Clara, CA) equipped with a TCD detector and a ShinCarbon ST 50/80 UM (2m x 1/16 x 1mm) column. He carrier gas was employed, at a flow rate of 10 mL/min. During operation, an initial oven temperature of 80°C was maintained for 1 min followed by a temperature ramp of 20°C/min for 4 min with a subsequent by a 2 min hold time.

Determination of population dynamics

DNA extraction from 2 mL of frozen cell pellets from the fermentations, were carried out as per protocol given with the Genejet kit (Thermofisher). qPCR was carried out by amplification of genomic DNA with primers (Table 5) amplifying single copy non-homogenous regions of *C. saccharolyticus* and *C. owensensis* obtained by multiple sequence alignment (Darling et al. 2004). PCR reactions were set up with DreamTaq DNA polymerase (Thermofisher) and EvaGreen (Biotium, Fremont, CA). The PCR conditions were as follows: Initial denaturation at 95°C for 7 min followed by 32 cycles of denaturation at 95°C for 30 sec, annealing at 54°C and 56°C for *C. owensensis* and *C. saccharolyticus*, respectively for 30 sec and extension at 70°C for 20 sec with plate read at the end of each cycle. A melt curve profile was also obtained for each PCR run. All qPCR's were carried out in a BioRad CFX96 Realtime PCR machine with copy numbers obtained in relation to defined standard concentrations obtained from Genomic DNA of pure cultures. The sum of calculated copy number values was used to determine the relative population of the different species.

Table 5: PCR primers for *C. saccharolyticus* and *C. owensensis* differentiation

| Species | Primer | Sequence |
|---------------------------|----------|--------------------------------|
| <i>C. owensensis</i> | Cowen_F1 | 5' - GGCAAGTGGGAAGAAGATGA - 3' |
| <i>C. owensensis</i> | Cowen_R1 | 5' - CTCCGCAAGACTTGAACACA - 3' |
| <i>C. saccharolyticus</i> | Csacc_F1 | 5' - TATTATGGGGATTGGGACGA - 3' |
| <i>C. saccharolyticus</i> | Csacc_R1 | 5' - CTGGGCGACCAAAGATAAAT - 3' |

Mathematical modelling

To quantify and evaluate the effect of the osmotolerant strains, a kinetic mathematical model was adapted from Ljunggren et al. (2011) and run in MATLAB R2017a (Mathworks, USA). The model was set up on a molar basis containing mathematical expressions for microbial growth, substrate consumption, product formation and gas to liquid mass transfer. The model was used with a few alterations to the mass balance equations. The mass balances of the gaseous compounds hydrogen and carbon dioxide are expressed as a change in concentration [M] over time instead of a change in flow over time. This is similar to what has been described in (Björkmalm et al. 2018) and given as Eq. 3-4:

$$\frac{dH_{2,g}}{dt} = \frac{V_{liq}}{V_{gas}} * \rho_{t,H_2} + (-H_{2,g} \cdot \frac{q_{gas}}{V_{gas}}) \quad (3)$$

$$\frac{dCO_{2,g}}{dt} = \frac{V_{liq}}{V_{gas}} * \rho_{t,CO_2} + (-CO_{2,g} \cdot \frac{q_{gas}}{V_{gas}}) \quad (4)$$

where V_{liq} and V_{gas} are the liquid and the gas volumes respectively (L), q_{gas} is the total gas flow (L/h), $H_{2,g}$ is gaseous hydrogen (M), CO_2 is gaseous carbon dioxide (M), ρ_{t,H_2} and ρ_{t,CO_2} are the mass transfer rate of hydrogen and carbon dioxide respectively (mol/L/h).

The osmolarity expression (Eq. 5), is calculated in the same way as in Ljunggren et al. (2011), except that $CO_{2,sol}$, i.e. the CO_2 ionic species (bicarbonate and carbonate), is excluded since it was not measured experimentally. This is further motivated by the fact that, according to model calculations in the current study, $CO_{2,sol}$ constituted to less than 2% of the total osmolarity.

$$OSM = Glu + 2 \cdot Ac + 2 \cdot Lac + 0.08 \quad (5)$$

where Glu, Ac and Lac are the molar concentrations of glucose, acetate and lactate, respectively. 0.08 is the estimated background osmolarity in the medium and it is adjusted slightly in comparison to the benchmark value from Ljunggren et al. (2011). The background osmolarity has not been experimentally measured in this case. The stoichiometric factor 2 implies that for each mole of acid produced, one mole of NaOH is included that was added to maintain the pH.

The inhibition due to osmolarity and dissolved hydrogen concentration is expressed as Eq. 6-7 (Ljunggren et al. 2011):

$$I_{osm} = 1 - \left(\frac{OSM}{OSM_{crit}} \right)^{n_{\mu}} \quad (6)$$

$$I_{H_2,aq} = 1 - \left(\frac{H_{2,aq}}{H_{2,aq,crit}} \right)^{n_{H_2}} \quad (7)$$

which are implemented in the growth kinetic expression (Eq. 8):

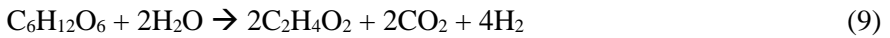
$$\mu = \mu_{max} \cdot \frac{S}{S+K_s} \cdot I_{osm} \cdot I_{H_2,aq} \quad (8)$$

where n_{μ} and n_{H_2} are exponential parameters describing the degree of inhibition and OSM_{crit} (M) and $H_{2,aq,crit}$ (M) are the critical osmolarity and critical dissolved hydrogen concentration, respectively. OSM_{crit} is central in this context where a high value of OSM_{crit} indicates a high tolerance for osmolarity. μ (h^{-1}) is the specific growth rate, μ_{max} (h^{-1}) is the maximum specific growth rate, K_s (M) is the affinity constant for glucose and S (M) is the concentration of glucose.

The model was evaluated against different batch experimental data. To fit the model to experimental data a parameter calibration was conducted using the function *lsqcurvefit* in MATLAB. This function solves the nonlinear curve-fitting problem using the least-square method. The parameters considered to be of greatest importance were μ_{max} , OSM_{crit} , r_{cd} (cell death rate, h^{-1}), Y_{S,H_2} (H_2 yield coefficient, mol H_2 /mol sugar), n_{μ} and n_{H_2} . The MATLAB function *nlparci* was used to calculate the 95% confidence interval for the calibrated parameters to assess their uncertainties.

To assess the accuracy of the model in relation to the experimental data, R^2 values and curve slope values were calculated. This was done by plotting the simulated values against the experimental values followed by a linear regression which gave the R^2 value as well as the linear equation $y = k \cdot x$, where k is the curve slope value. Both the R^2 value and the curve slope value are of importance when evaluating the accuracy of the model.

The biomass yield coefficient Y_{SX} (cmol biomass/mol sugar) was calculated using the experimental data but altered in the 80 g/L model to fit the experimental data. The other yields used in the model, $Y_{S,Ac}$, $Y_{S,Lac}$ and Y_{S,CO_2} , were based on stoichiometry according to Eq. 9-10:



Declarations

Not applicable

Ethics approval and consent to participate

Not applicable

Consent for publication

Not applicable.

Availability of data and materials

All data generated or analyzed during this study are included in this article. If additional information is needed, please contact the corresponding author.

Competing interests

The authors declare that they have no competing interests.

Funding

This study was funded by the Swedish Energy Agency (Metanova, 31090-2), Formas (HighQH2, 2017-00795) and Vinnova - Sweden's Innovation Agency (Multibio, 2017-03286) of which neither participated in the execution of the study or in the manuscript writing.

Authors' contributions

EB: design, operation and supervision fermentation processes, metabolite analysis and manuscript writing.

JB: data analysis, calculations, model development and manuscript writing.

JPB: fermentation processes, metabolite analysis and manuscript review

KS: development of genetic protocol and manuscript review.

KW: supervision of modelling, analysis and fermentation and manuscript writing.

EvN: supervision of fermentation processes, modelling, analysis and manuscript writing.

References

- Azimian, L., Bassi, A., Mercer, S.M. 2019. Investigation of growth kinetics of *Debaryomyces hansenii* (LAF-3 10 U) in petroleum refinery desalter effluent. *The Canadian Journal of Chemical Engineering*, **97**(1), 27-31.
- Azwar, M.Y., Hussain, M.A., Abdul-Wahab, A.K. 2014. Development of biohydrogen production by photobiological, fermentation and electrochemical processes: A review. *Renewable and Sustainable Energy Reviews*, **31**, 158-173.
- Björkmalm, J., Byrne, E., van Niel, E.W.J., Willquist, K. 2018. A non-linear model of hydrogen production by *Caldicellulosiruptor saccharolyticus* for diauxic-like consumption of lignocellulosic sugar mixtures. *Biotechnology for Biofuels*, **11**(1), 175.
- Byrne, E., Kovacs, K., van Niel, E.W.J., Willquist, K., Svensson, S.-E., Kreuger, E. 2018. Reduced use of phosphorus and water in sequential dark fermentation and anaerobic digestion of wheat straw and the application of ensiled steam-pretreated lucerne as a macronutrient provider in anaerobic digestion. *Biotechnology for Biofuels*, **11**(1), 281.
- Ciranna, A., Ferrari, R., Santala, V., Karp, M. 2014. Inhibitory effects of substrate and soluble end products on biohydrogen production of the alkalithermophile *Caloramator celer*: Kinetic, metabolic and transcription analyses. *International Journal of Hydrogen Energy*, **39**(12), 6391-6401.
- Claassen, P.A.M., van Lier, J.B., Lopez Contreras, A.M., van Niel, E.W.J., Sijtsma, L., Stams, A.J.M., de Vries, S.S., Weusthuis, R.A. 1999. Utilisation of biomass for the supply of energy carriers. *Applied Microbiology and Biotechnology*, **52**(6), 741-755.
- Darling, A.C.E., Mau, B., Blattner, F.R., Perna, N.T. 2004. Mauve: multiple alignment of conserved genomic sequence with rearrangements. *Genome research*, **14**(7), 1394-1403.
- de Vrije, T., Bakker, R.R., Budde, M.A., Lai, M.H., Mars, A.E., Claassen, P.A. 2009. Efficient hydrogen production from the lignocellulosic energy crop *Miscanthus* by the extreme thermophilic bacteria *Caldicellulosiruptor saccharolyticus* and *Thermotoga neapolitana*. *Biotechnology for Biofuels*, **2**(1), 12.
- de Vrije, T., Budde, M.A.W., Lips, S.J., Bakker, R.R., Mars, A.E., Claassen, P.A.M. 2010. Hydrogen production from carrot pulp by the extreme thermophiles *Caldicellulosiruptor saccharolyticus* and *Thermotoga neapolitana*. *International Journal of Hydrogen Energy*, **35**(24), 13206-13213.
- de Vrije, T., Mars, A.E., Budde, M.A.W., Lai, M.H., Dijkema, C., de Waard, P., Claassen, P.A.M. 2007. Glycolytic pathway and hydrogen yield studies of the extreme thermophile *Caldicellulosiruptor saccharolyticus*. *Applied Microbiology and Biotechnology*, **74**(6), 1358.
- Dragosits, M., Mattanovich, D. 2013. Adaptive laboratory evolution – principles and applications for biotechnology. *Microbial Cell Factories*, **12**(1), 64.
- Dötsch, A., Severin, J., Alt, W., Galinski, E.A., Kreft, J.-U. 2008. A mathematical model for growth and osmoregulation in halophilic bacteria. *Microbiology*, **154**(10), 2956-2969.

- European Parliament and Council. 2015. Directive (EU) 2015/1513 of the European parliament and of the council of 9 September 2015 amending Directive 98/70/EC relating to the quality of petrol and diesel fuels and amending Directive 2009/28/EC on the promotion of the use of energy from renewable sources, Official Journal of the European Union.
- Foglia, D., Ljunggren, M., Wukovits, W., Friedl, A., Zacchi, G., Urbaniec, K., Markowski, M. 2010. Integration studies on a two-stage fermentation process for the production of biohydrogen. *Journal of Cleaner Production*, **18**, S72-S80.
- Gonçalves, L.G., Borges, N., Serra, F., Fernandes, P.L., Dopazo, H., Santos, H. 2012. Evolution of the biosynthesis of di-myo-inositol phosphate, a marker of adaptation to hot marine environments. *Environmental Microbiology*, **14**(3), 691-701.
- Ljunggren, M., Willquist, K., Zacchi, G., van Niel, E.W. 2011. A kinetic model for quantitative evaluation of the effect of hydrogen and osmolarity on hydrogen production by *Caldicellulosiruptor saccharolyticus*. *Biotechnology for Biofuels*, **4**(1), 31.
- Ljunggren, M., Zacchi, G. 2010. Techno-economic analysis of a two-step biological process producing hydrogen and methane. *Bioresource Technology*, **101**(20), 7780-7788.
- Martins, L.O., Santos, H. 1995. Accumulation of Mannosylglycerate and Di-myo-Inositol-Phosphate by *Pyrococcus furiosus* in Response to Salinity and Temperature. *Applied and Environmental Microbiology*, **61**(9), 3299-3303.
- Nunes, O.C., Manaia, C.M., Da Costa, M.S., Santos, H. 1995. Compatible Solutes in the Thermophilic Bacteria *Rhodothermus marinus* and "*Thermus thermophilus*". *Applied and Environmental Microbiology*, **61**(6), 2351-2357.
- Panagiotopoulos, I.A., Bakker, R.R., de Vrije, T., Koukios, E.G., Claassen, P.A.M. 2010. Pretreatment of sweet sorghum bagasse for hydrogen production by *Caldicellulosiruptor saccharolyticus*. *International Journal of Hydrogen Energy*, **35**(15), 7738-7747.
- Pawar, S.S. 2014. *Caldicellulosiruptor saccharolyticus*: an Ideal Hydrogen Producer? *Faculty of Engineering, LTH, PhD Thesis*
- Pawar, S.S., Nkemka, V.N., Zeidan, A.A., Murto, M., van Niel, E.W.J. 2013. Biohydrogen production from wheat straw hydrolysate using *Caldicellulosiruptor saccharolyticus* followed by biogas production in a two-step uncoupled process. *International Journal of Hydrogen Energy*, **38**(22), 9121-9130.
- Pawar, S.S., van Niel, E.W.J. 2014. Evaluation of assimilatory sulphur metabolism in *Caldicellulosiruptor saccharolyticus*. *Bioresource Technology*, **169**, 677-685.
- Pawar, S.S., Vongkumpeang, T., Grey, C., van Niel, E.W. 2015. Biofilm formation by designed co-cultures of *Caldicellulosiruptor* species as a means to improve hydrogen productivity. *Biotechnology for Biofuels*, **8**(1), 19.
- Peabody, G., Winkler, J., Fountain, W., Castro, D.A., Leiva-Aravena, E., Kao, K.C. 2016. Benefits of a Recombination-Proficient *Escherichia coli* System for Adaptive Laboratory Evolution. *Applied and environmental microbiology*, **82**(22), 6736-6747.
- Peintner, C., Zeidan, A.A., Schnitzhofer, W. 2010. Bioreactor systems for thermophilic fermentative hydrogen production: evaluation and comparison of appropriate systems. *Journal of Cleaner Production*, **18**, S15-S22.

- Rainey, F.A., Donnison, A.M., Janssen, P.H., Saul, D., Rodrigo, A., Bergquist, P.L., Daniel, R.M., Stackebrandt, E., Morgan, H.W. 1994. Description of *Caldicellulosiruptor saccharolyticus* gen. nov., sp. nov: An obligately anaerobic, extremely thermophilic, cellulolytic bacterium. *FEMS Microbiology Letters*, **120**(3), 263-266.
- Rodrigues, M.V., Borges, N., Almeida, C.P., Lamosa, P., Santos, H. 2009. A Unique β -1,2-Mannosyltransferase of *Thermotoga maritima* That Uses Di-myo-Inositol Phosphate as the Mannosyl Acceptor. *Journal of Bacteriology*, **191**(19), 6105-6115.
- Sanderson, K. 2011. Lignocellulose: A chewy problem. *Nature*, **474**, S12.
- Schleifer, K.-H. 2009. Phylum XIII. Firmicutes Gibbons and Murray 1978, 5 (Firmacutes [sic] Gibbons and Murray 1978, 5). in: *Bergey's Manual® of Systematic Bacteriology*, Springer, pp. 19-1317.
- Sims, R., Taylor, M., Saddler, J., Mabee, W. 2008. From 1st-to 2nd-generation biofuel technologies. *Paris: International Energy Agency (IEA) and Organisation for Economic Co-Operation and Development*.
- Sivakumar, A., Srinivasaraghavan, T., Swaminathan, T., Baradarajan, A. 1994. Extended monod kinetics for substrate inhibited systems. *Bioprocess Engineering*, **11**(5), 185-188.
- Tomás, A.F., Karakashev, D., Angelidaki, I. 2013. *Thermoanaerobacter pentosaceus* sp. nov., an anaerobic, extremely thermophilic, high ethanol-yielding bacterium isolated from household waste. *International Journal of Systematic and Evolutionary Microbiology*, **63**(7), 2396-2404.
- van Niel, E.W.J., Claassen, P.A.M., Stams, A.J.M. 2003. Substrate and product inhibition of hydrogen production by the extreme thermophile, *Caldicellulosiruptor saccharolyticus*. *Biotechnol Bioeng*, **81**.
- VanFossen, A.L., Verhaart, M.R.A., Kengen, S.M.W., Kelly, R.M. 2009. Carbohydrate Utilization Patterns for the Extremely Thermophilic Bacterium *Caldicellulosiruptor saccharolyticus* Reveal Broad Growth Substrate Preferences. *Applied and Environmental Microbiology*, **75**(24), 7718-7724.
- Willquist, K., Claassen, P.A.M., van Niel, E.W.J. 2009. Evaluation of the influence of CO₂ on hydrogen production by *Caldicellulosiruptor saccharolyticus*. *International Journal of Hydrogen Energy*, **34**(11), 4718-4726.
- Zeidan, A.A., van Niel, E.W.J. 2010. A quantitative analysis of hydrogen production efficiency of the extreme thermophile *Caldicellulosiruptor owensensis* OLT. *International Journal of Hydrogen Energy*, **35**(3), 1128-1137.

